



UNIVERSITY OF
CAMBRIDGE

The role of modularity and integration in shaping primate pelvic girdle evolution

by Katrien Gwennola R. Janin
Wolfson College

This thesis is submitted for the degree of Doctor of Philosophy

May 2021

Declaration

This thesis the result of my own work and includes nothing which is the outcome of work done in collaboration except as declared in the Preface and as specified in the text. I further state that no substantial part of my thesis has already been submitted, or, is being concurrently submitted for any such degree, diploma or other qualification at the University of Cambridge or any other University or similar institution except as declared in the Preface and specified in the text.

The submitted thesis does not exceed the prescribed word limit (80.000 words) for the Archaeology and Anthropology Degree Committee. The word count of this thesis is 41.175, excluding supplementary information and references.

The role of modularity and integration in shaping primate pelvic girdle evolution

by *Katrien Gwennola R. Janin*
Wolfson College, University of Cambridge

Thesis Abstract

This thesis represents, to date, the most comprehensive investigation into the influence of integration (covariation) and modularity (the organisation of integrated units) on the morphological evolution of the primate pelvis. The concepts of integration and modularity are core tenets of evolutionary biology, yet their evolutionary role remains poorly understood. In this thesis, I quantified primate pelvis morphological variation across 4 clades encompassing the main primate locomotory specialisations. Shape was captured in detail, using a surface-based geometric morphometric approach, to test five alternative models of pelvis organisation, calculate integration levels, and reconstruct pelvis evolution.

In this thesis, I demonstrate that the primate pelvis is dominantly modulated by developmental pathways, with ilium, ischium, pubis, acetabulum, and sacrum having the capacity to vary and evolve in a relative independent manner (Chapter 2). This main modular pattern of primates is different to that of carnivores where in the latter group the ischium and pubis covary more closely together. The pubis-ischium parcellation is present in all examined primate phylogenetic groups (Lemuroidea, Ceboidea, Cercopithecoidea, and Hominoidea – humans excluded), suggesting that this parcellation was present in basal primates. Notably, a significant modular signal is also present for the functional hypothesis (locomotion-obstetrics). This suggests that the bony birth canal may vary and evolve relatively independently from the rest of the pelvis shape, alleviating the obstetric dilemma. Overall, this study demonstrates that the modularity pattern of the primate pelvic girdle is not simply limited to its developmental units. Instead, I find modular patterns acting in a complex multi-layered way, with developmental processes synergistically meeting functional needs.

Few studies have tried to explicitly clarify the role of integration plays in morphological variability and the evolutionary consequences this entails. In Chapter 3, I calculated the integration levels and tested whether integration may constrain or facilitate evolutionary

flexibility and diversity. I found an inverse relationship between integration magnitudes and disparity levels, indicating that the impact of primate pelvis integration is best supported by the hypothesis of constraint across the primate order, its phylogenetic and locomotory groups. My findings highlight the need to consider the impact of integration when modelling shape changes and reconstructing evolutionary pelvic trajectories.

In Chapter 4, I examined the role of integration in the morphological divergence of the human pelvis. Human integration levels are marked by a reduction across its developmental and functional pelvic constituents compared to the other sampled primates (*Gorilla beringei*, *Hylobates lar*, *Pan paniscus* and *Macaca mulatta*). The reduction of inherent human constraint is paired with elevated levels of disparity, indicative of inherent high levels of evolvability present within the human pelvis. Particularly of interest is the low integration signal between the human pubis and ischium, yet the integration levels within these elements are remarkably high. In the case of the pubis, this translates into limited evolutionary possibilities and reduced disparity. Conversely, the high ischium integration acts as a facilitator to morphological disparity, aiding evolutionary responsiveness. The increased evolutionary flexibility of the human ischium played a pivotal role in both bipedal efficiency and increased levels of sexual dimorphism, whereby ischium disparity is also an important aspect in easing parturition. The reduced integration levels between the human developmental and functional pelvis modules provide its pelvic bauplan with increased flexibility to respond to multiple selective pressures, facilitating the complex morphological modifications and divergence of the human pelvis along an evolutionary trajectory that may have otherwise been difficult or even impossible to achieve.

This thesis represents a significant advance in the study of pelvic modularity and morphological evolution. Chapters 2 and 3 form a comprehensive baseline for primate pelvis structuration and integration magnitudes, providing an in-depth exploration of hypotheses of modularity and the impact of integration on macroevolutionary patterns. The thesis is also novel in that it investigates developmental and functional integration patterns, and does so across and within species. This provides a multi-layered view on the role of modularity and integration of the primate pelvic girdle.

Acknowledgements

Many people played a part within this project, and I feel very grateful to have been able to draw on such wide support and kindness making my time at Cambridge a wonderful experience. Much thanks go to my supervisor Prof. Marta Mirazón Lahr and advisors Dr. Jason Head, Dr. Aurélien Mounier, and Prof. Rob Foley for their insights, guidance and patience. Equally I like to thank to Dr. Emmanuel Glissen (Royal Africa Museum, Brussels), Dr. Marcia Ponce de León and Dr. Christoph Zollikofer (University of Zurich), Dr. Trish Biers (Duckworth Collection, University of Cambridge), and Dr. Oliver Pauwels (Natural Science museum, Brussels) for generously granting me access to the skeletal collections of their respective institutes. My thanks also go to Prof. Chris Klingenberg (University of Manchester), Dr. Philip Guntz (Max Planck Institute for Evolutionary Anthropology Leipzig), Dr. Anne Le Maître (University of Vienna), and Dr. Laura Buck (Liverpool John Moores University) for allowing me to talk through the employed framework and complexities surrounding geometrical morphometric analyses to ensure the project's feasibility and robustness. My gratitude also goes to Dr. Aurélien Mounier (Centre National de la Recherche Scientifique, and University of Cambridge), Dr. Tom O'Mahoney (Angela Ruskin University, Cambridge), and Fabio Lahr (University of Cambridge) for their constructive input on how to navigate the technical challenges related to generating 3D models and the landmarking process. I am also indebted to Dr. Aurélien Mounier for keeping me sane during the pandemic.

Many people within Biological Anthropology, Archaeology and Zoology departments have helped throughout my PhD and life at Cambridge. Thank you, Fabio Lahr, for finding spare computer parts, helping me with my IT related problems, and the many hilarious chats. Next time we can meet, the drinks are on me. Another huge thank you goes to Silvia Hogg, sadly now deceased, who was our custodian of the Henry Wellcome Building. She looked after all of us, and none of us can properly function without her. I dearly miss our morning chats and your wise council. A big thank you must also go to my fellow PhD cohort, for your moral support, the array of ridiculous drawings on our white board, and the copious amount of handcrafted animals we made. To be surrounded by such a vibrant group of PhD students, studying varying subjects within our fields, has been a wonderful enriching experience. I am also hugely indebted to numerous post-docs, particularly the In-Africa working group, for fully adopting me into your circle and making sure I knew all the good pubs (and gin!) in Cambridge. To the members of the Cambridge University yacht club, and particularly my fellow crew members on our epic

Southampton – Bergen (Sweden) journey, I thank you. Night sailing with you into *that* North Sea thunderstorm will be an adventure I will never forget, nor will I forget the sight of the dolphins catching a free ride in our wake. The friendships we have formed will remain for life.

I also want to thank Dr. Appleby and Dr. Richard Thomas (both University of Leicester) for recognising and encouraging my love for bone morphologies and geometric morphometrics. The experiences I had working at your labs shaped much of my current research. To my family, I know you worried greatly when I decided to pursue this academic path. Yet you still supported me in my choice and, in typical Belgian fashion, you made sure there were plenty of chocolates, biscuits, and waffles stuffed in my suitcase whenever I travelled back to Cambridge.

My final thanks go to the Cambridge Trust and Wolfson College, for enabling and supporting my studies through the Vice Chancellor's scholarship. Without this funding, I would not have been able to undertake the PhD studies. Furthermore, financial support associated with the research cost were provided by Wolfson College, the department of Archaeology at the University of Cambridge, and the Santander Mobility grant. Without these none of this would have been possible.

Table of Contents

Declaration	2
Thesis Abstract	3
Acknowledgements	5
Table of Contents	7
Table of Figures	10
Table of Tables	12
Chapter 1: Introduction	14
1.1 <i>Context of study</i>	14
1.2 <i>Morphological modularity and integration</i>	16
1.2.1 Historical overview	16
1.2.2 Conceptual aspects and theoretical models	18
1.2.2.1 The functional mapping model	19
1.2.2.2 The developmental mapping model	20
1.2.2.3 The adjacent model	21
1.2.2.4 Relationship between the different types of modularity and integration	22
1.3 <i>Evolvability</i>	23
1.4 <i>Quantifying morphology</i>	25
1.5 <i>Overview of the primate pelvis</i>	27
1.5.1 Ilium	28
1.5.2 Ischium	29
1.5.3 Pubis	29
1.5.4 Acetabulum	29
1.5.5 Sacrum	30
1.6 <i>Research questions</i>	30
1.6.1 What is the inner modular structure of the pelvic girdle, and which processes underlie its structuring?	31
1.6.2 How may integration constrain or facilitate the ability of the pelvic girdle to respond to natural selection?	32
1.6.3 What is the role of integration in the morphological divergence of the human pelvis?	33
1.7 <i>Thesis organisation and significance</i>	33
Chapter 2: Patterns of Evolutionary Modularity in the Bony Pelvis of the Order Primates, Mammalia.	35
2.1 <i>Abstract</i>	35
2.2 <i>Introduction</i>	36
2.3 <i>Data and Analyses</i>	41
2.3.1 Osteological sample	41
2.3.2 Generating digital models	43
2.3.3 Geometric morphometrics: generalised Procrustes analysis	44

2.3.4	Repeatability Error	47
2.3.5	Influence of phylogeny and allometry	47
2.3.6	Detecting modular organisation	50
2.4	<i>Results</i>	53
	<i>Primate order</i>	53
2.4.1	Influence of phylogeny and evolutionary allometry on primate girdle shape	53
2.4.2	Modularity pattern for the primate order	53
2.4.3	Pairwise bone modularity within the primate order	54
	<i>Primate Groups</i>	58
2.4.4	Influence of allometry on the pelvis girdle shape of primate groups	58
2.4.5	Modularity test for separate groups of primates	59
2.5	<i>Discussion</i>	61
2.6	<i>Conclusion</i>	66
2.7	<i>Supplementary information</i>	67
	S1: Supplementary Information Primate Locomotion	67
	S2: Supplementary Information Landmarks	69
	S3: Supplementary Information Curve Semi-Landmarks	71
	S4: Supplementary Information Data Landmark Error Test	73
 Chapter 3: The Impact of Integration on Primate Pelvic Girdle Evolution.		75
3.1	<i>Abstract</i>	75
3.2	<i>Context of study</i>	75
3.3	<i>Data</i>	80
3.3.1	Osteological sample	80
3.3.2	Primate locomotion	80
3.3.3	Phylogeny	83
3.3.4	Geometric Data	83
3.4	<i>Analyses</i>	83
3.4.1	Generalised Procrustes analysis	83
3.4.2	Exploratory analyses	84
3.4.3	Module Integration analyses	85
3.4.4	Module morphological disparity analyses	86
3.4.5	Relationship between integration and morphological disparity	87
3.5	<i>Results</i>	88
3.5.1	Morphological variation and influencing factors.	88
3.5.2	Module Integration	95
3.5.3	Morphological disparity	103
3.5.4	Relationship between integration and morphological disparity	113
3.6	<i>Discussion</i>	119
3.7	<i>Conclusion</i>	121
3.8	<i>Supplementary Information</i>	123
	S1: Supplementary Information Primate Specimen	123
	S2: Primate Phylogenetic hypothesis	124
	S3: Size differences of phylogenetic and locomotory groups	125
	S4: Integration between modules	126
 Chapter 4: Divergence of the Human Pelvis Integration and Morphological Disparity		128
4.1	<i>Abstract</i>	128
4.2	<i>Introduction</i>	129

4.3	<i>Data</i>	132
4.3.1	Osteological sample	132
4.3.2	Geometric morphometric data	134
4.4	<i>Analyses</i>	134
4.4.1	Integration analyses	134
4.4.2	Morphological disparity analyses	135
4.4.3	Relationship of integration and disparity	136
4.5	<i>Results</i>	137
	<i>Developmental partition</i>	137
4.5.1	Integration	137
4.5.2	Morphological Disparity	139
4.5.3	Relationship developmental integration and disparity	143
	<i>Functional partition</i>	145
4.5.4	Integration of the functional partition	145
4.5.6	Disparity of the functional partition	146
4.6	<i>Discussion</i>	149
4.7	<i>Conclusion</i>	154
4.8	<i>Supplementary Information</i>	156
	S1: Morphospace of species	156
	S2: Size differences of species	157
	S3: Developmental modules: pairwise differences of species disparity	158
	S4: Functional modules: pairwise differences of species disparity	160
Chapter 5:	Conclusion and Future Directions	162
5.1	<i>What is the inner modular structure of the pelvic girdle, and which processes underlie its structuring?</i>	163
5.2	<i>How may integration constrain or facilitate the ability of the pelvic girdle to respond to natural selection?</i>	164
5.3	<i>What is the role of integration in the morphological divergence of the human pelvis?</i>	166
5.4	<i>The role of modularity and integration in shaping the primate pelvic girdle evolution</i>	168
	References	170
	Appendix: primate pelvis shapes	189

Table of Figures

Figure 1.1	Diagram functional integration and modularity	19
Figure 1.2	Diagram developmental integration and modularity	21
Figure 1.3	Relationships between the different types of modularity	23
Figure 1.4	False and true pelvis, and the birth canal planes	28
Figure 2.1	Illustration of the five tested hypotheses of primate pelvic girdle modularity patterns	40
Figure 2.2	Reconstruction process of a pelvic girdle	43
Figure 2.3	A 3D model of <i>Hylobates lar carpenteri</i> female pelvic girdle created using photogrammetry	44
Figure 2.4	Fixed landmark placement	45
Figure 2.5	Curve semi-landmark placement	46
Figure 2.6	Phylogenetic hypothesis of primates used in this study	49
Figure 2.7	CR coefficients and Z-CR effects obtained for connected bone constituents	57
Figure 3.1	Phylomorphospace of <i>shape data</i> variation along the PC1- PC2- time axes	89
Figure 3.2	Phylomorphospace of <i>shape data</i> variation along the PC1- PC3- time axes	90
Figure 3.3	Morphospace of <i>shape data</i> variation along the PC1- PC3 axes by clade	91
Figure 3.4	Morphospace of <i>shape data</i> variation along the PC1- PC3 axes by locomotion	92
Figure 3.5	Primate module integration	99
Figure 3.6	Primate module integration: R <i>MaxL</i> ρ – VE_{SD} method comparison	100
Figure 3.7	Clade module integration	101
Figure 3.8	Locomotion module integration	102
Figure 3.9	Primate module disparity	106
Figure 3.10	Clade module disparity	107
Figure 3.11	Locomotion module disparity	110

Figure 3.12	Primate integration and morphological disparity distribution patterns	114
Figure 3.13	Clade integration and morphological disparity distribution patterns	115
Figure 3.14	Locomotion integration and morphological disparity distribution patterns	116
Figure 3.15	Primate evolutionary rates of modules	118
Figure 4.1	Pelvic inlet relative to neonate dimensions of the sampled species	133
Figure 4.2	Developmental module integration	139
Figure 4.3	Developmental module disparity	142
Figure 4.4	Integration and disparity distribution of the developmental partition	144
Figure 4.5	Functional module integration	146
Figure 4.6	Functional module disparity	147

Table of Tables

Table 2.1	Primate species included in this study	42
Table 2.2	Summary of tested hypotheses	50
Table 2.3	Primate order: evolutionary allometry	53
Table 2.4	CR values for each proposed hypothesis	53
Table 2.5	Z-CR values for each proposed hypothesis	54
Table 2.6	<i>Shape data</i> : modular pairwise pelvic bone constituents' analyses	55
Table 2.7	<i>PIC data</i> : modular pairwise pelvic bone constituents' analyses	55
Table 2.8	<i>Allo data</i> : modular pairwise pelvic bone constituents' analyses	55
Table 2.9	Primate groups: allometry	58
Table 2.10	<i>Shape data</i> : modularity results for each primate group	59
Table 2.11	<i>Allo data</i> : modularity results for each primate group	60
Table 3.1	Primate Locomotion	82
Table 3.2	Overview analyses influencing factors	94
Table 3.3	Overview influence phylogenetic signal	94
Table 3.4	Primate integration magnitudes: $MaxL \rho - VE_{SD}$	98
Table 3.5	Clade integration magnitudes	98
Table 3.6	Locomotion integration magnitudes	98
Table 3.7	Primate module disparity: Pv values	105
Table 3.8	Clade module disparity: Pv values	105
Table 3.9	Locomotion module disparity: Pv values	105
Table 3.10	<i>Shape data</i> : pairwise absolute differences of clade disparity and p-values	108
Table 3.11	<i>Allo data</i> : pairwise absolute differences of clade disparity and p-values.	109
Table 3.12	<i>Shape data</i> : pairwise absolute differences of locomotory group disparity and p-values	111
Table 3.13	<i>Allo data</i> : pairwise absolute differences of locomotory group disparity and p-values	112

Table 3.14	Correlation coefficient between integration ($MaxL \rho$) and morphological disparity (Pv)	117
Table 4.1	Integration of the developmental modules	138
Table 4.2	Integration between the developmental modules	138
Table 4.3	Developmental module disparity	141
Table 4.4	Correlation coefficient between integration ($MaxL \rho$) and morphological disparity (Pv).	144
Table 4.5	Integration within and between functional modules	145
Table 4.6	Disparity within and between the functional modules	148

Chapter 1:

Introduction

1.1 Context of study

Evolutionary biology is a multi-disciplinary field seeking to understand the origins and evolutionary processes of complex organisms, and how changes to these processes influence the disparity of biodiversity at macro evolutionary level (Rolian 2014). Multiple methods can be employed to investigate evolutionary processes. Generally, these can be divided into two broad categories: bottom-up and top-down approaches. The bottom-up approach investigates the genetic and developmental mechanics and processes to understand the formation of phenotypic characteristics of any given species, and how differences in these mechanisms may lead to species divergence. In contrast, top-down approaches utilise the phenotype's characteristics to infer the causal factors controlling those characteristics, and what the differences between the phenotypic expression of species may reveal about the underlying mechanistic changes. The two approaches form the basis of two complementary research agendas within the field of evolutionary biology; the presented study falls within the second category, placing the morphological characteristics of the primate pelvic girdle at the core of the investigation.

The theoretical groundings of the presented thesis are those of modularity and integration that have been recognized as a core framework within evolutionary biology. The synthesis of modularity and integration is ongoing, yet empirical evidence has since come abundant, challenging fields that assume biological trait independence such as cladistics (Klingenberg 2008, Shirai and Marroig 2010, Melo *et al.* 2016). The concepts of modularity and integration are similar to those used in systems theory and network analysis, conceptualizing biological organisms as a network system of interconnected parts. These parts work together through networks with the interrelated parts having varying degrees of interconnectedness among them. Integration refers to the level of connectedness, the magnitude for parts to be interlinked, and consequently represents the level of coordinated variation. Measurements of trait variation and covariation have demonstrated that some traits correlate more strongly than others (Goswami and Polly 2010a). This heterogeneous pattern in organismal organisation is termed modularity, where modules are integrated by internal interaction but are relatively autonomous from other such modules (Eble 2004). In other words, integration modulates biological

organisms, and modularity (also termed integration pattern or parcellation) encompasses integration. As such, these two concepts are intimately connected. Both modularity and integration are identified through the examination of patterns of covariance.

Modularity and integration span across multiple levels of biology and are identifiable at every unit of biological organisation. The source of the phenotype covariation may be due to pleiotropy - when one gene influences multiple phenotypic traits, shared developmental pathways, and/or the need for coordinated functionality. Studying the inherent structuration of phenotypes is important since the relationships among traits influence their capability of variation and affects the biological organism's ability to respond to selection. This in turn biases the morphological diversity (disparity) on a macro evolutionary scale. As such, phenotypic modularity and integration are critical to our understanding of morphological evolution and biological diversity (Klingenberg 2005, Wagner and Zhang 2011, Klingenberg 2013, Felice *et al.* 2018, Goswami *et al.* 2014, 2015).

The primate pelvis structure represents an interesting model system for the study of modularity and integration, not least since it is within this context that the human obligatory bipedalism and rotational childbirth emerged. The pelvis is composed of several developmental units representing separate chondrification/ossification regions (Scheuer and Black 2004, Wall-Sheffler *et al.* 2020). These elements fuse during ontogeny, requiring developmental coordination. On the other hand, pelvic morphology serves a diversity of functional needs, including locomotion and parturition, also requiring coordination. Taken together, this leaves us with questions regarding the presence and strength of developmental and functional modularity in the pelvis, and the potential role of modularity and integration in biasing evolutionary trajectories including the divergent human pelvis morphology.

Previous works on the evolutionary role of morphological modularity and integration in primates predominantly have focused on patterns within the skull (e.g. see Cheverud 1995, 1996b, Ackermann and Cheverud 2004, Ackermann 2005, Mitteroecker and Bookstein 2008, Lieberman *et al.* 2010, Klingenberg 2013, Singh *et al.* 2013). These studies have revealed the presence of basicranium and face modules, and that primates broadly share a similar pattern of cranial modularity across taxa. Since the parts of the cranium are highly integrated, when one part changes this leads to other parts to co-evolve, which may explain the convergent evolution of short faces in hylobates (gibbons) and humans co-varying with changes to the basicranium

(Neaux 2017, Neaux *et al.* 2018). In sharp contrast, almost no research has been undertaken to investigate the pelvic area. Consequently, there is little understanding about the patterning within the primate pelvic girdle, and its potential role in primate pelvis diversity. The presented research seeks to address this knowledge gap by using primate pelvic morphology to investigate its modularity, magnitudes of integration, and evolutionary flexibility (i.e. the capacity to respond to selection).

In this introductory chapter, the concepts of morphological modularity and integration are examined through a brief historical overview, followed by an outline of the different theoretical models, and the relationship between the different kinds of modularity. Then evolvability and its relationship to modularity and integration will be discussed, before progressing to the topic of morphology quantification and landmark based geometric morphometrics, followed by a brief overview of the primate pelvis morphology. Next, the research questions and their contexts are presented. The last section of this introduction describes the thesis organisation and its significance.

1.2 Morphological modularity and integration

1.2.1 Historical overview

The recognition of the relationship of modularity and integration with the evolutionary process can be traced back as far as the publication of the 'Origin of Species'. Darwin (1859) recognised the importance of correlated variation (i.e. integration) and noted how slight evolutionary variations in one part of an organism result in other parts also being modified. He identified how certain traits are interconnected and highlighted its evolutionary importance. The concept of modularity also lies at the heart of comparative anatomy, which relies on the rationale that phenotypic wholes are decomposable into its anatomical parts, whilst natural historians map similarities/differences of those parts to infer species relatedness (Eble 2004).

The idea of modularity was also implicitly present at the founding of experimental embryology. Roux (1894)'s attempts to gain insights into the mechanics of development rested upon the expectation that if one part of the developmental process undergoes perturbations, the other parts of the embryo would continue to develop along their normal path. Roux thus assumed the presence of partitioned parts (i.e. modules) within the developmental processes whereby induced changes to one such a module would have minimal impact on another. Yet, it was not

until 1933 when this implicit thinking was made more explicit: Joseph Needham (1933) wrote that the embryo constitutes of developmental processes that can be disassociated from one another yet these very same processes coordinate to form an overall whole. He recognised, albeit in deferent terminology, that relatively autonomous modules exist within the overall integrated biological entity.

Despite these early recognitions of the tension between the phenotype as a whole and its relative separate parts within, the ideas received little further explicit attention until the seminal publication of Olsen and Miller (1958). Focusing on integration of morphological traits and body parts, Olsen and Miller hypothesised and demonstrated through a series of case studies that genetic, developmental and functional interactions are important sources of covariation. Equally important, Olsen and Miller developed a series of methods – mainly based upon correlation and regression statistics – permitting the identification and quantification of phenotypic trait and body part covariation. Not long after, Clausen and Hiesey (1960), using his botanical research, conceptualised and identified the presence of what they termed ‘character coherence’ (i.e. integration). The existence of morphological integration as conceptually outlined by Olsen and Miller (1958) and Clausen and Hiesey (1960) were soon independently verified when (Berg 1960) demonstrated that the vegetative and reproductive traits of angiosperm morphology significantly covary and coevolve.

Another important set of advances occurred during the 1990’s, when Wagner and colleagues provided a coherent evolutionary framework for the study of integration and the importance of its role within the evolution of biological bauplans (Wagner 1995, 1996, Wagner and Altenberg 1996, Wagner and Schenk 2000). An explicit distinction was made between phenotypic and evolutionary integration, and the recognition that modularity and integration magnitudes themselves are not static. Instead, modulation can change through the increase/decrease of integration levels or through the re-organisation of modules by partitioning previously integrated traits or integrating previously separate modules. They then proceeded to provide a comprehensive analysis of the role of integration and modularity in terms of facilitating or constraining adaptation, thus linking integration and modularity with evolvability and morphological diversity (Wagner 1995, Wagner and Altenberg 1996, Wagner and Schenk 2000). Further theoretical and empirical advances were made by linking genetic and morphological modularity and integration (e.g. see Lande 1979, Cheverud 1984, 1988, Polly 2016, Wagner and

Altenberg 1996, Arnold 1992) and explicitly including developmental modularity and integration (Klingenberg 2008).

1.2.2 Conceptual aspects and theoretical models

Attempts to precisely define complex concepts often hinder rather than aid scientific research (Pigliucci 2003), and this is also the case for integration and modularity. At its most minimal, morphological integration is defined as the cohesion among traits resulting as a consequence of interactions, regardless of the nature of these interactions or what their source may be (Eble 2004). A morphological module is a unit however that unit may be defined (e.g. morphological trait, anatomical element, genes, etc.) that are more integrated among themselves than they are compared to other such units. Modularity refers to the relative degrees of integration within the biological system (Klingenberg 2008, Esteve-Altava 2017). The definitions are intentionally kept vague to be as inclusive as possible. Because these make no reference to causal factors that determine how or why integration amongst units originates and varies, these definitions are applicable to a wide range of biological systems, and even non-biological networks.

What is important about the above definitions are the recognisable properties of integration and modules, and it is these that are examinable through a range of statistical analyses. The analyses are used as vehicles to infer the causal factors that structure the organismal pattern and changes those patterns (Klingenberg 2009). In practice, the causal factors are inferred through the use of *a priori* hypothesis-driven testing. The hypotheses are formulated based on available genetic, developmental and functional biological information to evaluate the structuring effects of these processes and mechanisms within the investigated biological system, in this case: the primate pelvis (Cheverud 1996a, Klingenberg 2009). It must be said that causal factors are not mutually exclusive, quite the contrary, and the different types of modulation interact as described in more detail below in section 1.2.2.4. Research along these different lines, however, do provide a way forward to gain insights into the extent by which each process forms and imparts structuration within and between phenotypic traits. In this way, studies of the patterns of modularity and integration inform about the processes and their strength involved in the modulation of phenotypes, enabling the study of their influence on phenotypic variation and evolvability.

Currently, two frameworks dominate integration and modularity studies: the functional and developmental mapping models. Both can be traced back to the seminal publication of Olson

and Miller (1958), but have been formalised and expanded upon by Wagner and Altenberg (1996) and Klingenberg (2008) respectively. To be complete, the adjacent model (Magwene 2001) is also included in this review, although not directly utilized within this thesis. Their respective theoretical bases are discussed in more detail below.

1.2.2.1 The functional mapping model

The functional mapping model, also referred to as the genotype-phenotype mapping model, is the classic model as set out in the seminal papers by Wagner, and Wagner and Altenberg, both published in 1996. Modules are defined as phenotypic traits that collectively serve a primary functional role, with different modules serving different functions. High level of integration and thus covariation exists within the modules due to pleiotropic effects whereas lower levels of pleiotropy occur between such modules (fig. 1.1.)

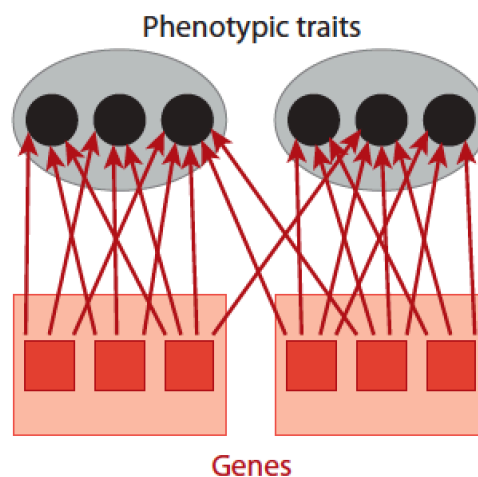


Fig. 1.1. Diagram functional integration and modularity

The phenotypic characters, represented by black circles, form two modular character complexes as depicted by the grey oval areas, serving different primary functions. This modulation is made possible by genetic restriction of pleiotropic effects (integration is illustrated by the red arrows with red squares representing the individual genes) between the modules.

Source: Klingenberg 2008

In this framework, phenotypic character traits may operate relatively independently because the pleiotropic effects are largely restricted to functional subsets within an organism. Conversely, functional traits with a common genetic basis are inherited jointly and will be

phenotypically expressed to a greater extent in a coordinated manner (Lande 1979, Cheverud 1996b). Importantly, Wagner and Altenberg (1996) describe the modular organisation in terms of genotype-phenotype connections, incorporating how the genotype modulation largely corresponds with phenotype modulation. Subsequent studies investigating patterns of covariance have since empirically confirmed these similarities between genetic and phenotypic covariation (e.g see Cheverud 1988, 1996b, Roff 1995, 1996, Cheverud *et al.* 1997, Klingenberg and Leamy 2001, Klingenberg *et al.* 2004, Wagner *et al.* 2007, Kenney-Hunt *et al.* 2008, Marroig *et al.* 2009, Porto *et al.* 2009), including studies that demonstrate significant correlation between the genetic and morphological covariance pattern of the rodent pelvis (Kohn and Atchley 1988, Roseman *et al.* 2020). Morphological data thus offers insights into the underlying genetic basis, and contains the potential to infer genetic information from the fossil record.

The functional genotype-phenotype mapping model is, however, very much genotype and function orientated. The explicit role of development in modularity and integration was largely left out. Yet parallel studies within the fields of embryology and evolutionary development demonstrate that phenotypic variation also relates to and is structured by development (Smith *et al.* 1985, Hendrikse *et al.* 2007, Muller 2007). It would take another decade for development to be formally incorporated into the modularity-integration framework: the developmental mapping model (Klingenberg 2008).

1.2.2.2 The developmental mapping model

The developmental mapping model, as advanced by Klingenberg (2008), broadened the functional genotype-phenotype model by including the role of genetic factors in structuring the developmental system which in turn affect phenotypic covariation (fig. 1.2). Adding the developmental pathways carries important implications, making it feasible to investigate similar/different developmental origins of phenotypic covariation and their influence on the possibilities of evolutionary trajectories. In the developmental context, covariation amongst traits can result from the direct interaction along pathways through precursor partition or inductive signalling. In both cases, upstream variation is transmitted in the pathways, leading to covariation between the affected traits (Klingenberg 2010). However, covariation may also arise without direct developmental input when separate developmental pathways respond in the same way to an external stimulus termed parallel variation by Klingenberg (2008, 2010).

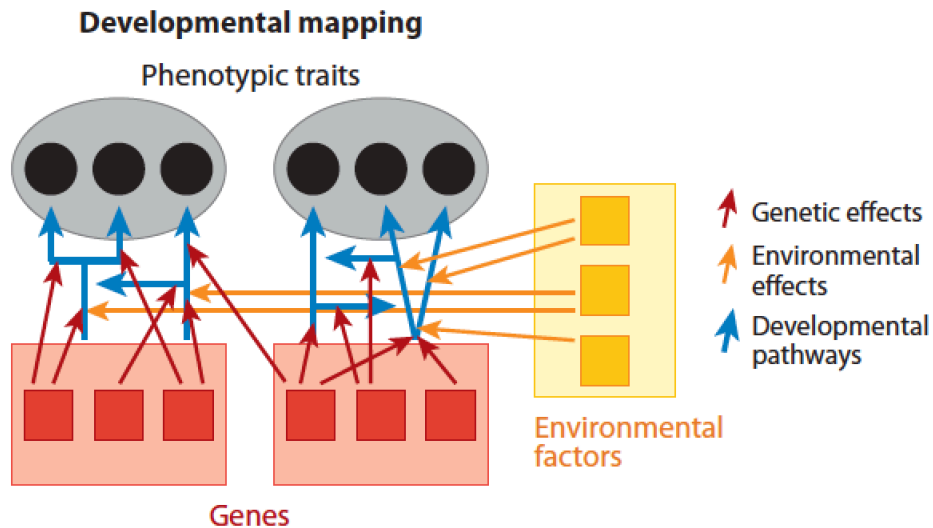


Fig. 1.2. Diagram developmental integration and modularity

The genetic (red lines) and environmental (yellow lines) impact the developmental pathways, with the developmental pathways forming the individual phenotypic traits (black circles). The grey ovals depict developmental modules that results from these processes.

Source: Klingenberg 2008

1.2.2.3 The adjacent model

The adjacent model provides a different theoretical perspective to predict the pattern of morphological covariation and coevolution. This model, as advanced by Magwene (2001), posits that anatomically adjacent bones in close spatial proximity will covary to a stronger degree than bones separated by greater spatial proximity, even if no obvious shared genetic or developmental underlying mechanisms are known (e.g see Gomez-Robles *et al.* 2014). Although this model has received considerably less attention, it may be relevant for the pelvis. The pelvis is a composite structure comprised of the hip bones and the sacrum. The sacrum is genetically and developmentally more closely aligned to the vertebrae than to the other pelvic components. Yet the sacrum connects directly with the ilia, and sacrum shape and position influence the overall pelvic morphology (Scheuer and Black 2004, White *et al.* 2012). In this thesis, the adjacent model is not used to formulate hypotheses and thus not directly investigated. Yet it serves as a reminder that certain covariation aspects, outside the two main frameworks, often remain unexplored and that covariation due to element proximity (Magwene 2001) and

allometry (Gould 1966, Klingenberg 2008, Felice *et al.* 2018) may also influence morphological covariation.

1.2.2.4 Relationship between the different types of modularity and integration

Modularity and integration are key concepts to many different domains of biology and can be examined at multiple biological levels such as at genetic, functional, developmental and evolutionary level. How these different levels of biological structuration interact with each other represents another complex interacting network as illustrated in figure 1.3.

Genetic, developmental, and functional modularity and integration occur within biological phenotypes (Klingenberg 2008). Developmental modularity interrelates with genetics and functionality since the developmental modulation effectuates the possibilities of actualised phenotypic variation. Genetic modularity influences developmental modularity through the genetic control of development, whereas developmental modularity may influence genetic modularity when specific developmental covariations provide a fitness advantage become genetically encoded. Another two-way interaction exists between genetic and functional modularity whereby pleiotropy coordinates functional traits, and traits that perform a joint function can become genetically encoded through pleiotropy. Functional modularity, in turn, effects development through plasticity and/or mechanical load influencing variability and the morphological direction during developmental growth (West-Eberhard 2005). In the other direction, the developmental processes shape the structures that perform functions. Development modularity thus may influence the functional modulation although admittedly many questions remain on how and the strength of this relationship, particularly when developmental and functional modulation appear to be incongruent (Breuker *et al.* 2006).

Evolutionary modularity, in turn, is the result of these phenotypic trait associations as accumulated within lineages through time (Klingenberg 2008, 2014). Evolutionary modularity describes the trait relationships across taxa, providing insights into macro evolutionary patterns in organismal form.

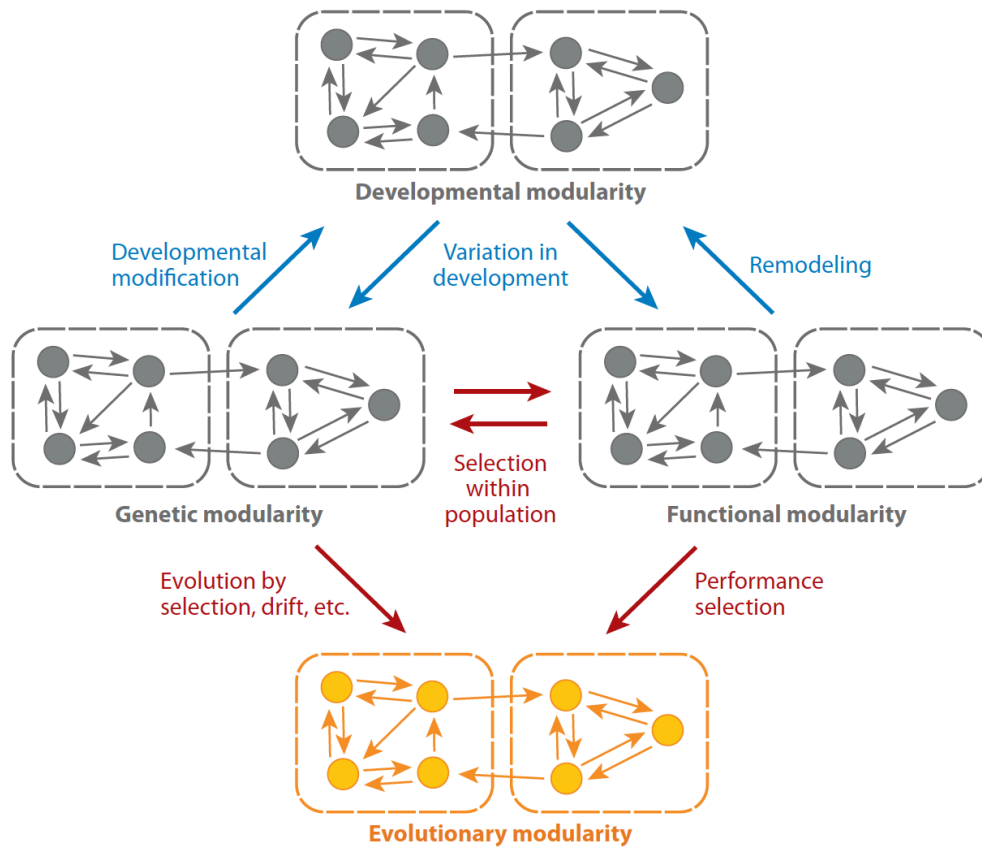


Fig. 1.3. Relationships between the different types of modularity

Genetic, developmental, and functional modularity occur at phenotypic level whereas evolutionary patterning is the results of the divergence histories across clades. The different types of modularity influence one another at individual level (blue arrows), and population level (red arrows).

Source: Klingenberg 2008

1.3 Evolvability

Studies of morphological modularity and integration have also stimulated an interest in the question of evolvability (also termed evolutionary flexibility). Evolvability denotes the capacity of a system for adaptive evolution. Despite the enormous diversity of primates, indeed of all living and extinct biological forms, it is quite clear that not all imaginable forms have come into existence. In the past, this 'restriction' of feasible life forms has been interpreted as the result of inbuilt constraints and natural selection. A particular phenotype may not exist because of

inherent constraints and/or because its selective advantage never outweighed that of an alternative form. In principle, given enough variation and enough time, biological organisms are capable to adapt to a variety of environments yet they will also be constrained in their morphological possibilities by their own inbuilt evolutionary history and intrinsic constraints (Merila and Bjorklund 2004, Zelditch *et al.* 2012, Melo and Marroig 2015).

Studying the integration and modularity pattern across species sheds light on the intrinsic constraints which biases the possible evolutionary trajectory possibilities of biological systems. Traditionally, integration has been predominately conceptualised as a constraint. High levels of integrations were equated with high levels of inherent constraint at the cost of evolutionary flexibility by reducing the available response directions (e.g. Maynard Smith *et al.* 1985). Conversely, low magnitudes of integration were associated with low levels of constraints, facilitating phenotypic variation in multiple directions thus increasing evolutionary flexibility (Hansen 2003, Wagner *et al.* 2007, Hansen and Houle 2008).

Contrary to the above theoretical conceptualisation that equates integration to constraint, Gould (1989, 2002) warned that high magnitudes of covariation (i.e. integration) may not necessarily be a limiting force constraining evolvability; instead high integration could potentially enhance evolvability by channelling evolutionary variation in a particular direction. Recent simulations confirmed Gould's thinking by demonstrating that that high levels of integration can generate new morphological possibilities by aligning the covariate response along the preferred direction of selection (Goswami *et al.* 2014, 2015). In such cases, the response follows a path of least resistance in phenotype morphospace, facilitating evolutionary shifts along these preferred directions but limiting disparity into the different subspaces of morphospace. This phenomenon can lead to extremely varied morphologies. In summary, the responses to selection dependent on an organism's modularity pattern and integration levels since the intrinsic modulation biases the feasibility of the different evolutionary options open to any biological organism (Zelditch *et al.* 2012). The influence of integration on an organism's ability to respond to selection depends on integration magnitude and the direction of selection (Goswami *et al.* 2014, Felice *et al.* 2018). Importantly, high integration magnitudes can no longer be understood as limiting the evolvability of traits, since high integration may also facilitate new avenues for evolutionary change. The potential effect of integration magnitudes on trait evolvability and diversity thus cannot be assumed but must be investigated.

The modular system and its integration levels not only affects the response to selection, but is moulded by selection itself (Pigliucci 2008). Computational evolutionary experiments reveal that networks respond and change when directional selection pressure is applied by minimizing connection costs whilst maximizing its network performance compared to the control experiments which were not subjected to those selective forces (Clune *et al.* 2013, Melo and Marroig 2015). Minimizing connections cost occurs, by the formations of smaller relative independent units within previously integrated units (i.e parcellation), or by reducing integration magnitudes within and/or between biological units. Changes to the modular system, be it through parcellation or changing integration magnitudes are by-products of past selection which in turn alters the possible responses to subsequent selections. Conversely, stabilizing selection maintains established organisational pattern.

1.4 Quantifying morphology

For centuries, biologists have been fascinated by the complexity and diversity of biological lifeforms. From the simple observation that organisms differ, naturalists have long sought to document these differences and strived to explain how these differences came to be (Darwin 1859). The ability to accurately quantify form is crucial to this endeavour. Traditionally, morphometric analyses were accomplished by applying univariate and multivariate statistics to sets of metrical measurements that included linear distances, ratios, and angles (i.e., traditional morphometrics) (Adams *et al.* 2013). Yet the geometrical relationship among the measured variables is often lost with this approach, limiting the biological interpretations. In the early 90's, a radically different approach emerged: geometric morphometrics (GMM) (Rohlf and Slice 1990, Bookstein 1991). With this method, the geometry of the biological shape is captured through a series of landmarks representing discrete biological points, and the relationship between these points is retained throughout its analysis. Furthermore, the incorporated Procrustes paradigm (Kendall 1984) provides an efficient way to remove non-shape variation, facilitating the effective quantification of the shape of the biological structure under investigation (Adams *et al.* 2013). Advances in shape theory combined with technological advances in the GMM tool box and 3D imaging have considerably expanded our capabilities to accurately quantify morphology (Bookstein 1991, Rohlf and Marcus 1993, Dryden and Mardia 1998, Adams *et al.* 2004, Gunz *et al.* 2005, Slice 2005, Mitteroecker and Gunz 2009, Lawing and Polly 2010, Zelditch *et al.* 2012, Gunz and Mitteroecker 2013).

In the past, biological structures were typically characterised by biologically homologous Type I landmarks and geometrical Type II landmarks (*sensu* Bookstein 1991). However, this approach limited the morphological description of complex irregular morphologies where few Type I and II landmarks are present, as is the case for the pelvis structure. Recent years, however, have brought a refinement in the development and expansions of geometric morphometric toolkit, including the use of semi-landmarks (i.e. curve and surface landmarks) which alleviate such problems (Gunz and Mitteroecker 2013). Detailed descriptions and empirical comparisons demonstrate the merits of employing semi-landmarks, resulting in more precise and nuanced quantification of the studied morphologies (Gunz *et al.* 2005, Gunz and Mitteroecker 2013, Wantanabe 2018, Bardua *et al.* 2019a, Goswami *et al.* 2019).

The high-density geometric morphometric approach provides a powerful way to quantify the pelvis shape and examine the covariation of those shapes. Many studies have employed semi-landmarks when examining phenotypic modularity and integration magnitudes, including Gunz *et al.* 2009, Huseynov *et al.* 2017, Felice *et al.* 2018, Bardua *et al.* 2019b, Marshall *et al.* 2019, Bon *et al.* 2020, Fabre *et al.* 2020). Yet recently some questions have surfaced over the appropriateness regarding the use of semi-landmarks in the study of covariation (Cardini 2019). First, there is the question whether the use of semi-landmarks increase the spread of variance during the Procrustes superimposition, which Cardini (2019) proposes may hamper the ability to detect biological modularity in data. Secondly, Cardini (2019) also suggests that the use of semi-landmarks may inflate the modularity signal as their position is dependent on their neighbouring landmark.

Whilst it must be recognised that each method has its advantages and inherent limitation, the above concerns, however, have since been addressed by Goswami *et al.* 2019. They demonstrated through a series of simulations and empirical biological examples that: 1) semi-landmarks provide far more comprehensive and nuanced characterizations of morphological variation than analysis of landmarks alone, and 2) produced broadly congruent modularity results between landmark only and semi-landmark included data sets based on empirical samples, although in some instances modules could not be detected in the landmark only data set due to insufficient landmark coverage. It thus appears that more nuanced morphological characterisation of shape yields better insights into the modular structure under investigation. Their studies further illustrate how high-dimensional data may be less impacted by module

boundary and allometric effects bias. What remains, however, difficult to resolve is a hierarchical approach to investigate morphological relationship across and within traits, for which no appropriate statically tool yet exists. Full description of the pelvis landmarks and semi-landmarks used within this thesis are provided in Chapter 2.

1.5 Overview of the primate pelvis

The pelvis comprises three bones – the right and left hip bone (also termed the *os coxae* or innominate bone) and the sacrum. The hip bone is divided into three regions, the ilium, ischium and pubis (pubic bone). Each region develops from separate growth centres and the three elements fuse together at the acetabulum, the hip joint. The latter forms a socket for the femoral head (Scheuer and Black 2000). The *ossa coxae* articulate with each other anteriorly at the pubic symphysis and posteriorly with the sacrum at the sacroiliac joint to form the pelvis.

The cranial part of the pelvis is also referred to as the greater or false pelvis, while the caudal part - comprising the bony birth canal - is termed the lesser or true pelvis (White *et al.* 2015, Wall-Scheffler *et al.* 2020). The birth canal or obstetric canal is divided into three planes: the inlet, mid-plane, and the outlet (fig 1.4). The inlet or pelvic brim forms the boundary between the false and true pelvis as demarked by the linea terminalis; the mid-plane is formed by the transverse space between the ischial spines and the sagittal dimension between the fusion point of the penultimate and last sacral bodies with the dorsomedial inferior pubis; and the outlet is the space demarked in a transverse direction by the space between the inner margins of the ischial tuberosities and in a sagittal direction between the dorsomedial inferior pubis and the last sacral body. The shape of the primate birth canal is traditionally measured through a series of transverse and sagittal linear measurement of each plane, as described in numerous osteological manuals (Martin 1928, White *et al.* 2015).

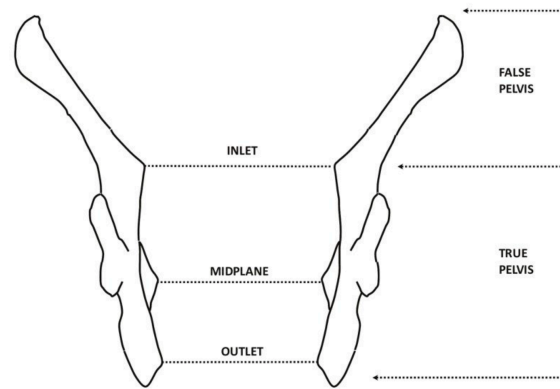


Fig 1.4. False and true pelvis, and the birth canal planes

Source: Betti et al. 2013

The general differences in pelvic shape among primates are discussed below, and for convenience grouped per bone of the pelvis. Past studies focused on isolated morphological traits or linear measurement, and the locomotory implications of these differences. This approach is reflected in the provided brief overview. The comparative morphological differences of humans with other primates are detailed in Chapter 4.

1.5.1 Ilium

The ilium forms the superior portion of the hip bone. In most primates, it is blade-shaped except for most non-anthropoid primates, which instead have long narrow rod-like ilia (Jouffroy 1975, Lewton 2010, Gebo 2014). The length and orientation of the blade considerably varies among species. The length of the primate ilia affects the mechanics of the hip joint, whilst the ilia width relates to the iliac plane which determines the surface area of the gluteal and iliacus musculature (Gebo 2014). The ilium of primates is generally long in quadrupeds, though shorter in terrestrial than arboreal taxa, and shortened in suspensory taxa and bipeds (Lewton 2010). A tall and wide ilium, as often seen in anthropoids, allows for long moment arm and larger *gluteus medius* muscle attachment site. Leapers are also characterized by long ilia, proposed to facilitate the lengthening of the *tensor fascia lata* moment arm, needed to flex the femur during the recovery stroke (Gebo 2014). The iliac plane is ventrally oriented in all quadrupeds, suspensory taxa, and large-bodied vertical clinging and leapers (VLC), but more laterally orientated in small-bodied VCL (Lewton 2010). The anterior inferior iliac spine is small or absent in quadrupeds (Straus 1929), yet prominent in VCL (Jouffroy 1975) and bipeds (e.g. White et al. 2015).

1.5.2 Ischium

The ischium forms the posterior-caudal aspect of the hip bone. The ischial tuberosity is the attachment site of the hamstring muscles. Cranial-medial to the ischial tuberosity lies the ischial spine. The ischial spine is the origin of the sacrospinous ligament which attaches to the sacrum at the other end (Wall-Sheffler *et al.* 2020). In general, quadrupeds have longer ischia than non-quadrupeds, with terrestrial quadrupeds having the longest (Waterman 1929). Conversely, VLC and bipeds have shorter ischia and often these are dorsally bent, proposed to facilitate hip extensor leverage during hindlimb extension (Fleagle and Anapol 1992). VCL and bipeds have prominent ischial spines while these are small or absent in other primates (Waterman 1929, Abitol 1988, Lewton 2010). Old world monkeys and gibbons show ischial callosities, although still little is known about their purpose (Gebo 2014).

1.5.3 Pubis

The pubis, or pubic bone, forms the anterior part of the pelvis. The left and right pubic bone articulates medially at the pubic symphysis. Two rami connect the pubic body to the ilium and ischium: the ilio-pubic (superior) and the ischio-pubic (inferior) ramus. Several adductor muscles of the hip originate from the anterior surface of the pubic body and ischio-pubic ramus including the adductor brevis, longus, magnus, and gracilis (Wall-Sheffler *et al.* 2020). Little is known about pubic morphology variation amongst primates (Lewton 2010). Generally, the cranial-caudal length of the pubic symphysis is longer in prosimians compared to other primates. Differences may relate to cursorial animals relying less on hip adductor musculature, although no functional study has yet tried to relate pubic length with a specific locomotory adaptation (Anemone 1993, Gebo 2014, Lewton 2010).

1.5.4 Acetabulum

The acetabulum forms the lateral aspect of the hip bone, where ilium, ischium and pubis meet. It is a cup-shaped socket, which articulates with the femoral head to form the hip joint. The acetabulum is pivotal in transmitting load from the hindlimb to the pelvis and trunk (Wall-Sheffler *et al.* 2020). Primate acetabulum morphology can be broadly categorized in two types: the dorsally and ventrally buttressed joint (Gebo 2014). These differences predominantly relate to the differing load transmission between pronograde (horizontal) and orthograde (upright) postures of primate taxa. For the dorsally buttressed joint, the dorsal part of the acetabular facet is larger than its ventral part. It is associated with pronograde posture such as primates

performing quadrupedal locomotory behaviour. Conversely, the second type of hip joint comprises a larger ventral facet, associated with orthograde postures.

1.5.5 Sacrum

The sacrum forms part of the pelvis (posterior-cranial aspect) and the spinal column. It transmits upper body weight to the lower limb via the sacroiliac joints (Wall-Sheffler *et al.* 2020). The sacrum consists of sacral vertebrae and the left and right alae wings which fuse together into one bone during adulthood. The number of sacral vertebrae varies greatly among primates from two in some small-bodied strepsirrhines and platyrrhines species to seven in Lorisidae (Schultz 1969). Sacrum width and curvature are less variable, with most primates having long, narrow, and relatively straight sacra (Schultz 1930). Humans are unique in this respect because they have short, ventrally curved, and wide sacra (Schultz 1930, Leutenegger 1977, Gruss and Schmitt 2015). The sacroiliac joint is small in quadrupeds and VCL, and large in suspensory primate taxa and bipeds (Ankel Simons 2000). The greater sacroiliac surface helps relieve tension from the trunk on pelvic girdle and hindlimb. Moreover, a recent study by Showalter (2018) demonstrated that the use of prehensile tails also affects sacrum morphology, with different types of tail prehensility corresponding with morphological differences in relative size and transverse sacrum expansion, and relative size of articular surfaces of sacral vertebrae.

1.6 Research questions

The overarching aim of the proposed research is to answer the following question: what is the role of modularity and integration in shaping the primate pelvic girdle evolution? To answer this question, the following three sub questions are posed:

- 1) what is the inner modular structure of the pelvic girdle, and which processes underlie its structuring?
- 2) how may integration constrain or facilitate the ability of the pelvic girdle to respond to natural selection?
- 3) what is the role of integration in the morphological divergence of the human pelvis?

1.6.1 What is the inner modular structure of the pelvic girdle, and which processes underlie its structuring?

Chapter 2 focuses on the modular structure of the primate pelvic girdle. Whilst in principle computerised random models can be used to explore and find the optimised pattern of modularity within any given structure, Mitteroecker and Bookstein (2007) warn against such practice since these may make little biological sense. I investigate whether and the extent to which development and/or functional modulation is present within the primate pelvis. Based on available genetic and developmental information, four *a priori* developmental hypotheses (H_1 - H_4) are formulated, designed to resolve outstanding questions around whether the pubis, ischium, and acetabulum act as separate units within the primate pelvis bauplan. The fifth hypothesis (H_5) proposes a modular structure along the two main functions of the pelvis: obstetric and locomotion. The functional subdivision is based upon previous observations and the functional hypothesis as proposed by Lovejoy (2005), Hirata *et al.* (2011), Grabowski (2012), and Huseynov *et al.* (2017). The investigation of the functional division has great potential to contribute to the 'the obstetric dilemma (OD)' debate (Washburn 1960). The dilemma, as proposed by Washburn, incorporates the difficulty of reconciling two different selective forces enacting upon the human pelvic girdle: selection for biomechanical efficiency, which is hypothesised to favour narrow pelvises, versus selection for large-brained/big-bodied neonates, requiring an obstetrically efficient wide female pelvis structure (Rosenberg 1992). The OD is often framed in a human-centric way, yet the question is equally applicable to primates. Compared to other mammals, primates as a group are generally characterised by high encephalization quotient (i.e. relative large head compared to body size) (Schultz 1949, Rosenberg and Trevathan 1996, Trevathan 2015). For most primates, this translates into a close fit between neonate and maternal birth canal size. The exception to this pattern is the large-bodied apes who do not share such a close correspondence. In this sense, humans are the exception to the exception since humans are large-bodied apes that birth neonates with a high cephalisation quotient (Schultz 1949, Rosenberg and Trevathan 1996, Trevathan 2015).

Huseynov and colleagues (2017) found both a developmental and functional modularity pattern present within the chimpanzee pelvis. It is currently unclear whether this result can be translated across primates at a macroevolutionary level, and what the comparative modulation strengths may be. Moreover, if a functional modulation signal can be detected, it would provide empirical evidence of functional modularity relatively dividing locomotion and obstetrics across primates. This would signify that the functional demands placed upon the pelvis can relatively

independently vary and evolve, alleviating primate OD (Washburn 1960). The developmental and functional hypotheses are tested upon the primate order, and four primate clades: Lemuroidea, New and Old World Monkeys, and Hominoidea (excluding humans) in order to investigate whether the modular pattern evolved or is conserved across primates.

1.6.2 How may integration constrain or facilitate the ability of the pelvic girdle to respond to natural selection?

To date, no study has examined the macroevolutionary role of developmental integration within the pelvis structure, not for primates nor for any other vertebrate groups. Two studies (Grabowski 2012, Lewton 2012) did investigate the impact of the overall integration of the hipbone. They found low magnitudes of integration and high evolutionary flexibility. These studies may serve as an initial indication of expectation. However, questions remain on how developmental integration magnitudes differ across the pelvis structure and their impact in terms of constraining or facilitating the response for each element. Chapter 3 addresses this gap in our understanding and hopefully may serve as an initial reference for future studies.

I partition the pelvis according to the strongest modular signal obtained in Chapter 2 (H_1 which indicates that ilium, ischium, pubis, acetabulum, and sacrum are modular components within the pelvis structure) and focus on the integration magnitudes of those modules to investigate if integration constrains or facilitates adaptation. To do so, I largely follow methodology as employed by Randau and Goswami 2017 and Bardua *et al.* 2019b, 2020. I calculate integration magnitude and morphological disparity, a measure of evolutionary flexibility, to assess the constraining/facilitating influence of integration on the pelvic constituents' evolutionary trajectories. Within this section, I investigate the primate order, the above-mentioned clades, and the two main locomotory categories: specialists and quadrupeds.

Allometry is often theorized to act as a constraining factor within biological organisms (Klingenberg 2008, Felice *et al.* 2018), yet surprisingly, till date no empirical assessment examining the relationship of allometry, integration, and evolutionary constraint/facilitation has taken place. As above, to address this gap in our understanding, I include the impact of allometry within this chapter to provide an empirical example to the theoretical discussion. Last, but not least, within this chapter I test two different types of integration calculation - the Spearman's coefficient and relative eigenvalue dispersal method - to gain clarity on the equivalence of these methods.

1.6.3 What is the role of integration in the morphological divergence of the human pelvis?

Chapter 4 investigates the possible role of integration in the morphological divergence of the human pelvis. The human pelvis is morphologically distinct from other primates, leading to the question of whether this divergence is underpinned by integration changes within its inherent bauplan. To answer this question, I compare the integration and disparity values for the developmental and functional pelvis modules of humans to those of other primate species. Past research by Grabowski (2012) in relation to obstetric module suggests that the human integration magnitudes diverge from other apes. Specifically, Grabowski found that whilst integration magnitudes of the obstetric traits retrain similar magnitude levels, the lower integration between obstetric and non-obstetric pelvic components is what contributes to the evolutionary flexibility of the human bony birth canal.

The study by Grabowski (2012) provides a direct comparable study for the functional partition. However, our employed methods differ. Grabowski's employed univariate measurements and Lande (1979)'s breeder equations as a measure of evolutionary flexibility, whereas I use GMM data in combination with morphological disparity. Using very different methods, it will be of interest to see whether a similar signal is obtained. Moreover, I also investigate the impact of developmental integration within this comparative framework. As mentioned above, currently no such developmental studies exists. The focus within this chapter is on humans. Results are discussed in relation to hominid evolution, and the obstetric dilemma.

1.7 Thesis organisation and significance

This thesis is formatted as a series of studies addressing the above sub questions, bookended by the current chapter (Chapter 1) and the concluding chapter (Chapter 5). Chapters 2-4 are written as intended for publication and consequently can be read relatively independently. The combination of these chapters represents a unified thesis following the overall aim to explore the role of modularity and integration in shaping primate pelvic girdle morphologies and their influence on evolutionary trajectories.

Before I progress, a few clarifications are in order. Since chapter 2-4 are being planned for publication, within these chapters I have substituted the pronoun 'I' by 'we'. Detailed

descriptions of the GMM landmarks and data collection are provided in Chapter 2, however only shortly summarized in Chapter 3 and 4 in adherence to the degree committee rules. In Chapter 3 and 4 modules are the base unit of investigation. As such, the morphologies of modules are treated and termed as traits. Chapter 2 and 3 focus on primate modularity and integration. Humans are not included in these chapters, as the magnitude of the shape divergence of their pelvis and the singular nature of their locomotion among primates greatly impacts the analyses. Furthermore, in Chapter 4 the term *humans* and *Homo sapiens* refer to modern humans unless differently specified within text.

The study of modularity and integration at macro evolutionary level remains relatively rare, nonetheless the importance and ability to provide novel insights of such studies are well understood (Fleagle 2013). Currently, much emphasis is placed on how integration and modularity contribute to cranial shape diversity, with relatively few studies investigating the other elements of the body plan (Esteve-Altava 2017). The findings of this thesis will thus help address this imbalance and contribute generally to our wider understanding of organismal body patterning, and specifically to primate organismal structuring. The study is also novel in the sense that it investigates developmental and functional integration pattern, and does so across and within species, another rarity within the current literature (Esteve-Altava 2017). This provides a multi-layered view on the role of modularity and integration of the primate pelvic girdle.

The presented study is timely, given the recent increased interest into understanding the evolution of the pelvic area (Rosenberg and Desilva 2017). Furthermore, whilst my study uses skeletal material of extant primates, it may form an important baseline to (re-)evaluate fossil finds. The recent expansion of fossil pelvic finds, combined with an increasing rate of computerised reconstructions, means that these strands of evidence can be incorporated into future studies.

Chapter 2:

Patterns of Evolutionary Modularity in the Bony Pelvis of the Order Primates, Mammalia.

2.1 Abstract

Understanding patterns of morphological modular organisation can provide important information into phenotypic evolution. To gain insights into the modular organisational structure within the primate pelvic girdle, we employed three-dimensional geometric morphometrics to test four different developmental and one functional modular hypotheses. These hypotheses were tested upon the primate order, and four phylogenetic groups: Lemuroidea, Ceboidea (New World monkeys), Cercopithecoidea (Old World monkeys), and Hominoidea. The results indicate: 1) that overall modularity within the primate pelvic girdle is high, 2) that the modular organisational structure best matches a developmental partition along all the main structural elements of the pelvis - the sacrum, ilium, ischium, pubis, and acetabulum, and 3) that this pattern is ancestrally shared across primates apart from possibly Lemuroidea, among whom the acetabulum appears less modular than the other hip bone elements compared to the other primate groups. This main modular pattern of primates is different to that of carnivores where in the latter group the ischium and pubis covary more closely together. The pubis-ischium parcellation is present in all examined primate groups, suggesting that this parcellation was present in basal primates. Notably, our study also revealed a significant modular signal for the functional hypothesis, namely a partition between locomotion and obstetric pelvic elements. This suggests that the bony birth canal may vary and evolve relatively independently from the rest of the pelvis shape *contra* the obstetric dilemma theory. Overall, this study demonstrates that the modularity pattern of the primate pelvic girdle is not simply limited to its main developmental units. Instead, we find modular patterns acting in a complex multi-layered way, with developmental processes meeting functional needs in a synergistical manner.

2.2 Introduction

Integration and modularity conceptualise biological organisms as a network system of parts which have varying degrees of interconnectedness among them. Phenotypic integration refers to the level of cohesion, the tendency for phenotypic parts to be correlated and consequently to vary in a coordinated manner. This can be due to different factors, such as pleiotropy (when one gene, genetic pathway, or genetic regulatory system influences multiple phenotypic traits), shared developmental pathways, and/or the need for coordinated functionality (*sensu* Olson and Miller 1958). Phenotypic modularity refers to the structural organisation within an organism, whereby groups of organs and tissues, or their parts, are internally strongly integrated but are relatively autonomous from other such modules (Eble 2004).

From an evolutionary perspective, these concepts may offer important insights into how the organisational pattern influences morphological evolutionary trajectories. Theoretically, organisms with a low level of modular structure have a structural limit to their possible variation, and thus constraints to adaptation as integrated traits must evolve together, whilst a more modular organisation may be more amenable to adaptive evolution since selection can act relatively independently on each module (Hansen 2003, Mittenroecker and Bookstein 2007, Wagner *et al.* 2007, Hansen and Houle 2008, Goswami *et al.* 2014, 2015). Modularity itself is also open to the forces of evolution and may evolve over time. This can occur through altered levels of cohesion (i.e., integration) between sets of modules, resulting in a higher/lower magnitude of coordination, or new modules may be formed through the compartmentalisation of traits into new smaller units that release previously held constraints (Wagner 1995, 1996). The processes involved in the compartmentalisation of previously integrated traits may be an important mechanism in the evolutionary toolkit to counterbalance the effects of genetic pleiotropy and developmental canalisation, which otherwise could continuously increase over evolutionary time and potentially lead to reduced phenotypic variation (Wagner and Schenk 2000, Hansen and Houle 2004, Wagner *et al.* 2007, Goswami and Polly 2010b). Alternatively, previously disassociated modules may be re-absorbed into one cohesive covariate unit, particularly under novel functional selective pressures (Wagner 1996, Wagner and Altenberg 1996). It is generally held that trait integration represents the plesiomorphic state of biological organisms and enhances evolutionary stasis, while selection drives increased modularity through time, allowing for the formation of new morphological expressions, evolutionary divergence, and increased biodiversity along an evolutionary trajectory (Wagner 1996, Shirai and Marroig 2010). By investigating the evolutionary integration and modularity (i.a. the

correlated evolutionary changes and independent evolutionary changes) (Zelditch and Goswami 2021), the evolutionary relationship among traits can be identified and its magnitude quantified.

The primate pelvis represents an interesting model system for the study of modularity. Composite structures, such as the pelvis and skull, represent complex modular networks due to the embedded duality between the developmental processes of the discrete constituent bone elements requiring a level of coordination during the fusing process to form a larger integrated whole, while interplaying with the multiple functional demands placed on these structures. The morphological modularity of the skull has been the topic of multiple investigations in amphibians (Bardua *et al.* 2019b), lizards (Sanger *et al.* 2012), birds (Felice and Goswami 2018), mammals in general (Goswami 2006, Drake and Klingenberg 2010, Goswami and Polly 2010b, Porto *et al.* 2013, Machado *et al.* 2018), and primates (Cheverud 1995, Ackermann and Cheverud 2004, Ackermann 2005, Bastir and Rosas 2005, Singh *et al.* 2013). In contrast, the modular organisation of the pelvic girdle has received comparatively little attention. Studies by Martin-Serra *et al.* 2018 and Lewton 2012 investigating carnivores and primates respectively, focused on the individual hipbone. So far, only Huseynov *et al.* 2017 studied the full pelvic girdle, focusing on the development of the modular pattern within chimpanzees. The identification of modularity within the adult primate pelvis has yet to be the topic of a comprehensive investigation.

The primate bony pelvis consists of the left and right os coxae (hip bone or innominate bone) and the sacrum. Much of our current knowledge about the genetic networks (i.e., the collection of genes that interact to govern gene expression) and developmental processes of the pelvic girdle derives from research in mouse and chick (Malashichev *et al.* 2005, Malashichev *et al.* 2008, Pomikal and Streicher 2008, Pomikal *et al.* 2011, Capellini *et al.* 2011, Sears *et al.* 2015, Young *et al.* 2019). Developmental studies demonstrate that the three bones of the os coxae (ilium, ischium and pubis) originate from mesenchymal cells from the somatopleure, whereas the sacrum arises from somite-derived sclerotome (Young *et al.* 2019). The sacrum follows the developmental pathways noted in the vertebral column; ablation of lumbar-sacral somites do not affect the developmental processes of the os coxae but do result in absence of sacrum (Malashichev *et al.* 2008). However, ablation of the hindlimb somatopleure results in the os coxae not being formed (Malashichev *et al.* 2008). Within the os coxae, each bone undergoes separate chondrification and ossification at different centres at different times; in the avian hip

bone the sequence is ilium, followed by the pubis, and lastly by the ischium (Malashichev *et al.* 2005), although for humans this order is slightly different: ilium, then ischium, followed closely by the pubis (Scheurer and Black 2004). Each pelvic element is differentially controlled by one or more genes - *Pixt1*, *Emx2* and *Sox9* (ilium), *Alx1/4*, *Prrx1/2* and *Twist1* (pubis), and *Pax1* (ischium) whilst upstream the *Pbx 1/2/3* genes hierarchically control these effectors of pelvic girdle morphogenesis (Capellini *et al.* 2011, Young *et al.* 2019).

Furthermore, upstream genes appear to divide the os coxae into cranial/superior (ilium) and caudal/inferior (pubis and ischium) components. Ilium loss is observed when *Pbx1* is not expressed, while the ischium and pubis continue their normal developmental pathways (Pomikal and Streicher 2010). Conversely, several genes play a specific role in the caudal/inferior os coxae development: *Islet1* operates in parallel with the *Pbx* genes but only impacts the regulation of the ischium and pubis. The absence of *Islet1* expression leads to reduction/loss of ischium and pubis during mouse development (Itou *et al.* 2012, Sears *et al.* 2015), as is also the case when *Pbx2* and *Pbx3* are simultaneously lost. This suggests that the ischium and pubis are genetically more closely linked to one another than to the ilium, giving rise to the question whether the ischium and pubis are more closely integrated despite being also controlled by unique genes and their individual developmental pathways. Conceptually, the ischium and pubis could thus potentially act as one or two modules. Martin-Serra *et al.* (2018) found the ischium and pubis to covary relatively closely in the carnivore innominate bone. Unfortunately, the two studies on the primate pelves published are not informative in this respect - Huseynov *et al.* 2017 did not address this question, whilst Lewton's research (2012) was hampered by a lack of sufficient landmarks to capture the ischium and pubis shape (three and two respectively).

When considering pelvis modularity from a developmental perspective, the morphogenesis of the acetabulum is another element to consider. The acetabulum forms in conjunction with the development of the hind limb bud (the femoral head); without this contact the acetabulum cannot develop along its normal path (Pomikal and Streicher 2010). The formation of the acetabulum is not directly tied into the underlying genetic architecture of the os coxae but instead is the result of an epigenetic process. Furthermore, the ischium and pubis interact closely with the hind limb throughout ontogeny (Pomikal and Streicher 2010), and in its absence (e.g., in limb ablation experiments), the ischio-pubis does not develop normally (Malashichev *et al.* 2005). *Tbx4* and *Pitx1*, needed for the normal development of the pelvis, also play a role in the initial growth and patterning of the hind limb, including the femoral head (Sears *et al.* 2015),

which in turn impacts the relative position and form of the acetabulum. For this reason, within the present study, the acetabulum is considered as a possible separate module, a hypothesis not tested in the two previous studies of the primate pelvis mentioned above (Huseynov *et al.* 2017, Lewton 2012).

Modular patterns can also be influenced by shared functionality. Whilst functional and developmental modularity are often thought to be congruent (i.e., matching hypothesis of Wagner and Altenberg 1996), the pelvic girdle has two main functional demands - obstetrics and locomotion - that are incongruent with the developmental pathways (Lovejoy 2005, Grabowski *et al.* 2011, Hirata *et al.* 2011, Grabowski 2012, Lewton 2012, Huseynov *et al.* 2017). Huseynov *et al.* (2017) found that the adult chimpanzee pelvis contains both an obstetric and locomotion functional modular signal. Whether this modular signal is present across primates remains currently unknown.

This study aims to explore the evolutionary modular pattern of the primate pelvic girdle. To do so, five alternative hypotheses were developed based on phenotypic developmental and functional partitioning (fig.2.1, table 2.2): hypothesis 1 (H_1) contains five modules and tests for developmental based partition to determine if all 5 pelvic bones constituents act in a relative independent manner (ilium, ischium, pubis, acetabulum, sacrum); hypothesis 2 (H_2) removes the acetabulum as a possible unit, to examine the modular signal of partitioning along ilium, ischium, pubis and sacrum; hypothesis 3 (H_3) tests the pleiotropic influence on the ischium and pubis by combining these two bone constituents into one partition whilst keeping the acetabulum and ilium as possible separate modules; hypothesis 4 (H_4) mirrors H_3 but removes the acetabulum as a possible independent unit. H_1 - H_4 are based on available genetic and developmental information, and are designed to resolve outstanding questions around whether the pubis, ischium, and acetabulum act as separate units within the primate pelvis bauplan architecture. Hypotheses 5 (H_5), on the other hand, tests functional modularity. H_5 tests whether the primate pelvic structure contains a functional signal that is incongruent with developmental hypotheses by exploring two subsets of data - one representing bone morphology hypothesised to be mainly involved in obstetrics (the pelvic inlet region), and one in locomotion of the primate pelvic girdle.

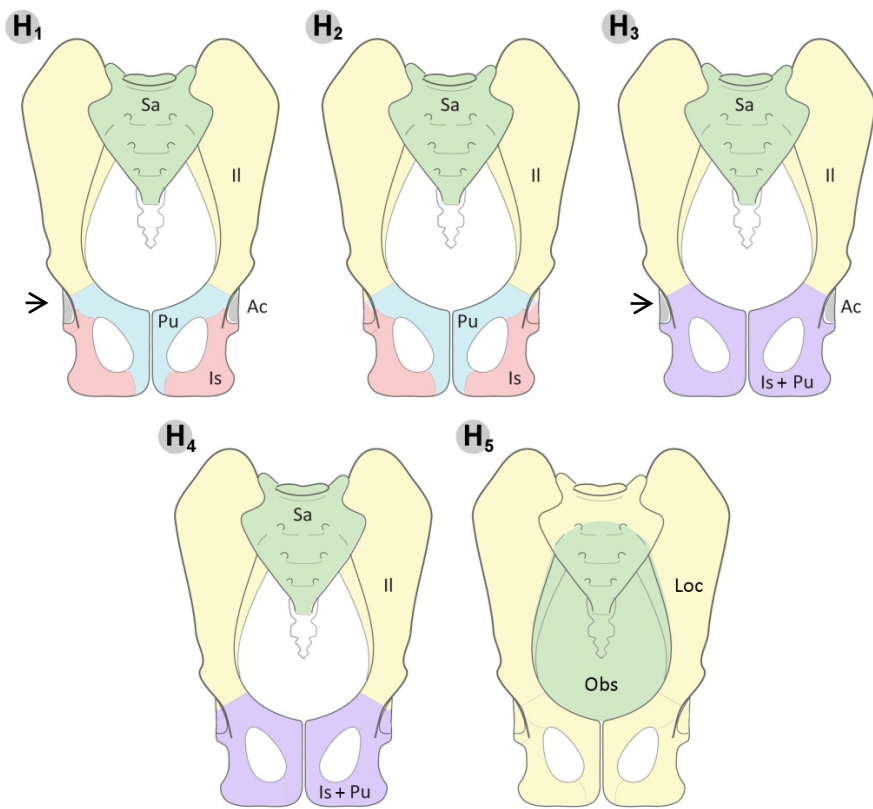


Fig 2.1. Illustration of the five tested hypotheses of primate pelvic girdle modularity patterns

Key to illustration: Il= ilium (yellow), is= ischium (pink), pu= pubis (blue), ac=acetabulum (grey), sa=sacrum (green), pu+is = ischio-pubis (purple), obs= obstetrics (green), and loc = locomotion (yellow)

2.3 Data and Analyses

2.3.1 Osteological sample

The data used in this study were obtained from articulated primate pelvic structures of 176 individuals drawn from collections housed at the Duckworth Laboratory (University of Cambridge), Anthropological Institute and Museum (University of Zurich), Royal Museum of Central Africa (Tervuren, Belgium) and Museum of Natural Sciences (Royal Belgian Institute of Natural Science). Only well-preserved pelvic girdles were utilised. All specimens are adult individuals as indicated by complete fusion of the iliac crest and complete femoral epiphyseal fusion. In instances where the bony pelvic girdle was no longer articulated, these were re-articulated using casting putty following procedures set out by Hammond *et al.* 2016 and Ward *et al.* 2018. This was only needed for the large bodied Hominoidea.

The sample includes 49 species across 10 primate families (table 2.1), and represents all primate locomotory specialisations except obligate bipedalism (table S1). Humans are not included in the present study, as the magnitude of the shape divergence of their pelvis and the singular nature of their locomotion among primates greatly impacts the covariance patterns. Additionally, the species chosen for this study also encompass a wide range of body mass, ranging from 800 g, *Nycticebus coucang*, to over 170 kg, male *Gorilla beringei* and *Gorilla gorilla* (Petter and Desbordes 2010).

Parvorder	Clade	Family	Species	N _F	N _M	N	
Strepsirrhini	Lemuroidea	Daubentoniidae	<i>Daubentonia madagascariensis</i>	1	1	2	
		Indridae	<i>Indris indris</i>	1	1	2	
		Lemuridae	<i>Eulemur fulvus rufus</i>	1	2	3	
			<i>Lemur catta</i>	1	1	2	
			<i>Varecia variegata</i>	1	1	2	
	5	6	11				
	Lorisoidae	Galagidae	<i>Otolemur crassicaudatus</i>	1	1	2	
		Lorisidae	<i>Nycticebus coucang</i>	1	1	2	
	2	2	4				
	Platyrrhini	Ceboidea (NWM)	Atelidae	<i>Alouatta semniculus</i>	0	1	1
<i>Ateles geoffroy</i>				1	0	1	
<i>Ateles pansicus</i>				0	1	1	
<i>Lagothrix Lagothricha</i>				3	2	5	
Cebidae			<i>Cebus apella</i>	0	2	2	
			<i>Cebus capucinus</i>	1	1	2	
5	7	12					
Catarrhini	Cercopithecoidea (OWM)	Cercopithecidae	<i>Cercocebus galeritus</i>	1	1	2	
			<i>Cercopithecus ascanius</i>	2	2	4	
			<i>Cercopithecus cephus</i>	2	0	2	
			<i>Cercopithecus hamlyni</i>	2	1	3	
			<i>Cercopithecus lhoesti</i>	2	2	4	
			<i>Cercopithecus mitis</i>	2	2	4	
			<i>Cercopithecus mona</i>	2	2	4	
			<i>Cercopithecus neglectus</i>	2	2	4	
			<i>Cercopithecus nictitans</i>	2	2	4	
			<i>Cercopithecus petaurista</i>	0	1	1	
			<i>Cercopithecus pogonias</i>	0	1	1	
			<i>Chlorocebus aetiops</i>	4	6	10	
			<i>Colobus guereza</i>	2	2	4	
			<i>Colobus polykomas</i>	3	3	6	
			<i>Erythrocebus patas</i>	2	2	4	
			<i>Lophocebus albigena</i>	4	4	8	
			<i>Lophocebus aterrimus</i>	1	0	1	
			<i>Macaca fascicularis</i>	2	3	5	
			<i>Macaca maura</i>	2	2	4	
			<i>Macaca mulatta</i>	1	1	2	
			<i>Macaca nemestrina</i>	1	1	2	
			<i>Mandrillus sphinx</i>	1	1	2	
			<i>Papio anubis</i>	2	2	4	
			<i>Papio cynocephalus</i>	2	2	4	
			<i>Papio hamadryas</i>	5	5	10	
			<i>Piliocolobus badius</i>	2	2	4	
			<i>Piliocolobus kirkii</i>	2	0	2	
			<i>Presbytis comata</i>	1	1	2	
			<i>Pygathrix nemaus</i>	0	1	1	
			<i>Semnopithecus entellus</i>	1	1	2	
			<i>Theropithecus gelada</i>	1	1	2	
			56	56	112		
				Hominoidea	Hominidae	<i>Gorilla beringei graueri</i>	4
<i>Gorilla gorilla</i>	1	0				1	
<i>Pan paniscus</i>	3	5				8	
<i>Pan troglodytes</i>	2	2				4	
<i>Pongo pygmaeus</i>	1	2				3	
Hylobatidae	<i>Hylobates lar</i>	5				5	10
	<i>Symphalangus syndactylus</i>	1				1	2
17	20	37					
Overall total						176	

Table 2.1. Primate species included in this study

N_F = Number of female specimens, N_M = Number of male specimens, N = Number of specimens per species

2.3.2 Generating digital models

Three dimensional (3D) models of all specimens were constructed using photogrammetry. Photogrammetry allows the creation of 3D models by taking multiple overlapping photographs recording the full surface of an object (figure 2.2). Using the position of the camera as it moves around an object, photogrammetry software Agisoft Photoscan (version 1.3.3) utilises these images to calculate and calibrate X, Y and Z coordinates for each pixel of the original image and derive measurements to create a highly accurate 3D model (Katz and Friess 2014) (figure 2.3). All images were photographed on a white background, with bones lighted using two soft diffuse light boxes to minimize shadow interference during the point detection process. All images were taken on a Leica D-Lux 6 digital camera with the equivalent of a 50 mm lens to create images with minimal photographic distortion (Mullin and Taylor 2002).

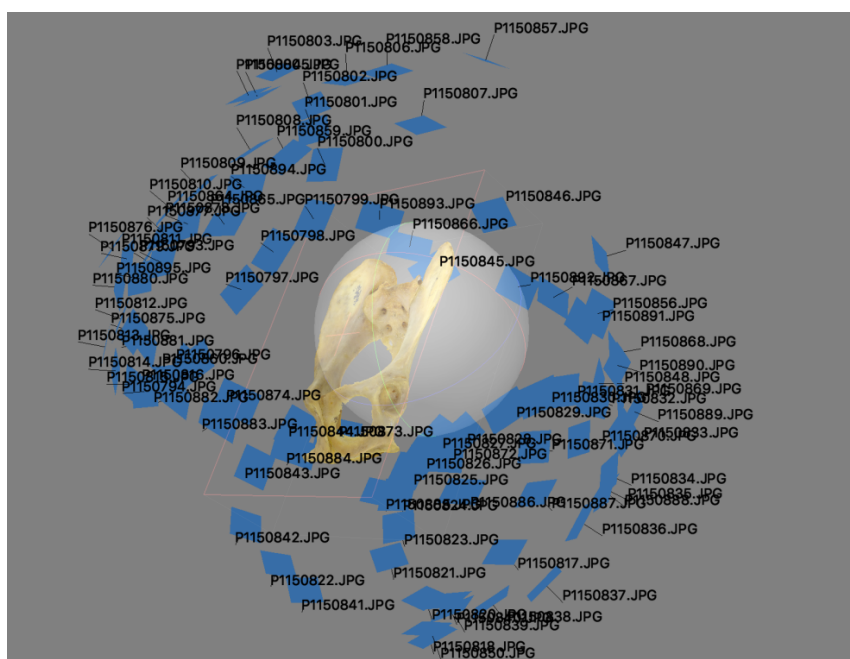


Fig. 2.2. Reconstruction process of a pelvic girdle.

Each blue rectangle represents one photographic image.

To generate each model, the following workflow was undertaken: 1) import the full stack of overlapping images into the software; 2) mask all non-bone pixels; 3) align images; 4) build dense point cloud; 5) remove points with 0.5 or more projection uncertainty; 6) build mesh; 7) render the surface texture; and 8) export .ply file and import into MeshLab (version 2016.12), an open source mesh processing tool, to set the scale where the scale is set according to collected

metrical data (i.e., actual object size). Subsequent mesh cleaning was also performed in MeshLab. To investigate digitisation error, a paired t-test was performed on corresponding measurements taken both on the digital model and on the physical specimen. There were no significant differences in the results for digital ($M = 61.83$, $SD = 30.16$) and physical measurements ($M = 60.45$, $SD = 30.48$) of the same specimens; $t = 0.441$, $p = 0.658$.

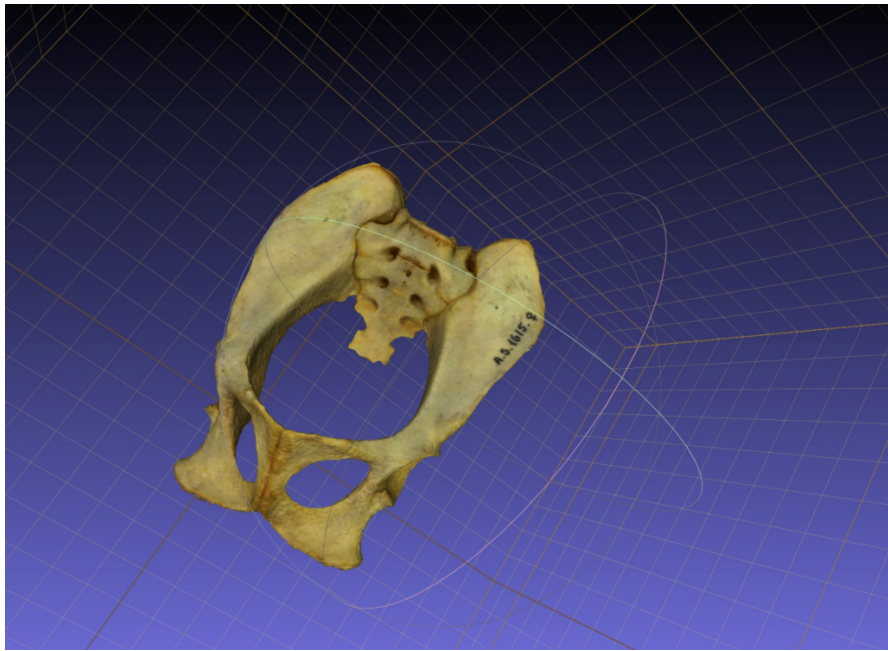


Fig. 2.3. A 3D model of a *Hylobates lar carpenteri* female pelvic girdle created using photogrammetry

2.3.3 Geometric morphometrics: generalised Procrustes analysis

The pelvic girdle has a complex shape which is not readily amenable to traditional biometric techniques (McHenry and Corruccini 1978, Lycett and von Cramon-Taubel 2013). To address the concerns of linear measurements not adequately capturing pelvic morphology, the study adopted a 3D geometric morphometric (GMM) and landmarking approach to obtain shape data. GMM provides several advantages compared to traditional multivariate morphometric metrical analysis of linear and/or angle measurements: 1) GMM quantifies morphology using a Cartesian 3D-coordinate system that represents biological and/or geometric homology points of the specimens in the dataset, 2) GMM effectively separates (isometric) size from shape (geometry), and 3) GMM enables visual inspection of morphological changes throughout statistical analyses as it maintains the relative position of the variables throughout. Making use of the Cartesian geometric coordinates, GMM allows for the identification and quantification of subtle shape

variations/covariations, underpinned by shape theories and a robust mathematical framework (Dryden and Mardia 1998, Bookstein 1991, Bookstein 1997, Rohlf and Marcus 1993, Rolph 2000, Adams *et al.* 2004, Slice 2007, Zelditch *et al.* 2012, Klingenberg 2013).

Using the Landmark software package from the Institute of Data Analysis and Visualisation (Wiley *et al.* 2005), we characterised the pelvis shape through 153 landmarks comprised of 63 fixed landmarks and 90 semi-landmarks. The fixed landmark configuration consists of 29 landmark pairs and 5 midline landmarks, representing topological discrete pelvis points as fully described in **S2** and illustrated in figure 2.4. Unlike the cranium, few pelvis landmarks exist. To alleviate this problem and to capture more fully the complexity of the pelvis shape, semi-landmarks were added along pelvis margins and ridges. Their description and placements are listed in **S3** and depicted in figure 2.6. To ensure homology of the semi-landmarks, these were slid in an iterative process along their corresponding meshes using minimum bending energy (Gunz *et al.* 2005). This procedure was performed in R package *Morpho*, version 2.3.1.1. (Schlager 2016).

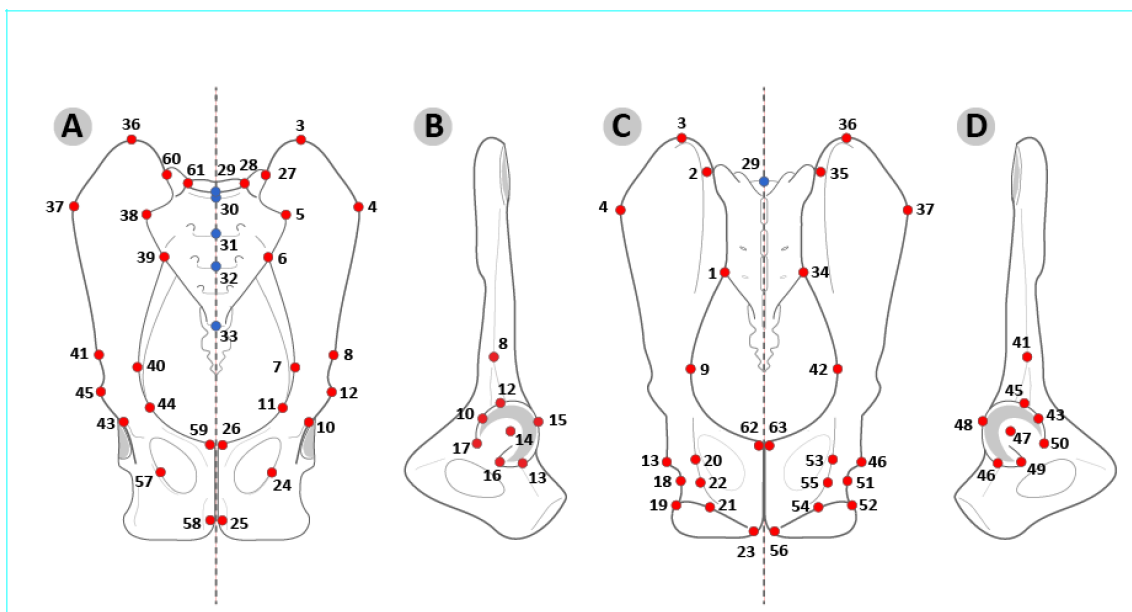


Fig 2.4. Fixed landmark placement

A: anterior view, B: left lateral, C: posterior view, D right lateral

Red circles: fixed paired landmarks, blue circles: fixed midline landmarks

Landmark descriptions in supplementary information S2 table

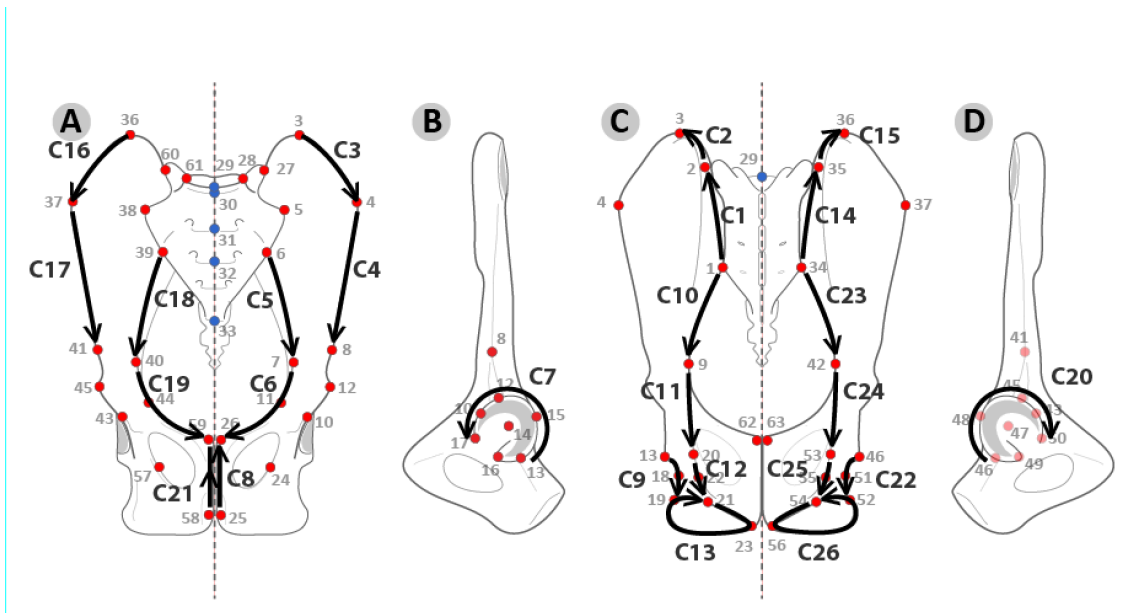


Fig 2.5. Curve semi-landmark placement

A: anterior view, B: left lateral, C: posterior view, D right lateral

Curve semi-landmark descriptions in supplementary information S3 table

After digitizing landmarks and sliding of the semi-landmarks, we performed a general Procrustes analysis (GPA). GPA superimposes the landmark configurations and removes variance due to position, rotation and isometric size. The GPA process performs the following steps: 1) it translates all specimens to a common location by superimposing their centroids, 2) calculates the common centroid, 3) scales each configuration according to that common centroid, and 4) standardizes orientation through the rotation of all configurations until the landmarks are as close together as possible (Gower 1975, Rohlf and Slice 1990, Bookstein 1991, Goodhall 1991, Rohlf and Marcus 1993, Dryden and Marcia 1998, Kendall *et al.* 1999, Adams *et al.* 2004, Slice 2005, 2007, Lawing and Polly 2010, Zelditch *et al.* 2012, Adams *et al.* 2013, Srivastava and Klassen 2016, Klingenberg 2020). The GPA brings all landmark configurations into a common morphospace (i.e. Kendall's shape space) (Kendall 1984). However, this morphospace is curved and non-linear, whilst most statistical tools assume linear Euclidian space. To obtain the Procrustes shape variables needed for statistical analysis, the superimposed configurations was projected into its shape tangent space (Kendall 1984, Small 1996).

Using the above outlined GPA procedure, we created five data sets: primate order ($n=49$), Lemuroidea ($n=10$), Hominoidea ($n=38$), New World monkeys (Ceboidea) ($n=11$), and Old World

monkeys (Cercopithecoidea) ($n=110$). For the primate order data set, we averaged the Procrustes coordinates and centroid size per species as to enable analyses in a phylogenetic context. The primate groups, on the other hand, represent data of the individual specimens rather than species averages to maximise sample size. The Lorisoidea primate group was not investigated due to the insufficient sample size (table 2.2). The GPA procedure was performed using the *geomorph* package in R (Adams and Otárola-Castillo 2013) and the resulting shape variables are hereafter referred to as *shape data*.

2.3.4 Repeatability Error

Following Arnqvist and Martensson (1998), we quantified the error inherent to the landmarking procedure (i.e. the repeatability error) with a Procrustes analysis of variance (ANOVA). This method is based on the intra class correlation coefficient (Fisher 1958), the ratio among individual variance versus within individual variance in relation to total variance, whereby landmarking repeatability is calculated in the following manner:

$$R = S^2_A / S^2_W + S^2_A$$

R is the repeatability error, S^2_A is the among individual variance, and S^2_W is the within individual variance component. The among variance (S^2_A) is obtained by adding the ANOVA sum of squares (MS) of the among and within groups, divided by the amount of repeat observations. The within individual variance (S^2_W) equates to the obtained ANOVA MS of the within individual variance. The error dataset included 10 specimens. These specimens represent the 10 primate family groups used within this study (S4.1: Specimen Overview Error test). We landmarked each specimen 3 times with a space of at least one month between the landmarking procedures, resulting in three error groups. The results of the Procrustes ANOVA indicate that variation between specimens was much greater (>99%) than between the replicated groups (<1%). The great correspondence between the repeat group is confirmed by the repeatability error value of $R = 0.99$, indicative that measurement error is very small (S4.2 Procrustes ANOVA Error Test Result).

2.3.5 Influence of phylogeny and allometry

To investigate the influence of phylogenetic histories amongst the sampled primate taxa, we tested the primate order *shape data* to detect the presence of a phylogenetic signal - the

tendency of related species to resemble each other due to shared ancestry (Blomberg *et al.* 2003). The phylogenetic hypothesis of primate relationships used in this study is a consensus tree from the 10KTrees Project, version 3, of the sampled species (Arnold *et al.* 2010). The consensus tree was pruned using Mesquite software (version 3.2) to contain only information relevant to the data used this study to contain only information relevant to the data used within this study (figure 2.6). We quantified phylogenetic signal in our primate *shape data* using the K_{mult} statistic, a multivariate version of the K -statistic (Blomberg *et al.* 2003), under a Brownian model of evolution (Adams 2014a, Adams and Collyer 2017). Statistical significance of the phylogenetic signal was assessed by permutation of the primate *shape data* across the tips of the phylogenetic tree for 1000 iterations (Adams and Collyer 2015). We calculated the K_{mult} statistic and its significance by using the function *physignal* (Adams 2014a, Adams and Collyer 2017) of the *geomorph* package (Adams and Otarola-Castillo 2013). To account for shared evolutionary history and presumed increased similarities between more closely related species, we computed phylogenetic independent contrasts (Felsenstein 1985) for our *shape data*, and refer to this data set as *PIC data* in our subsequent analyses.

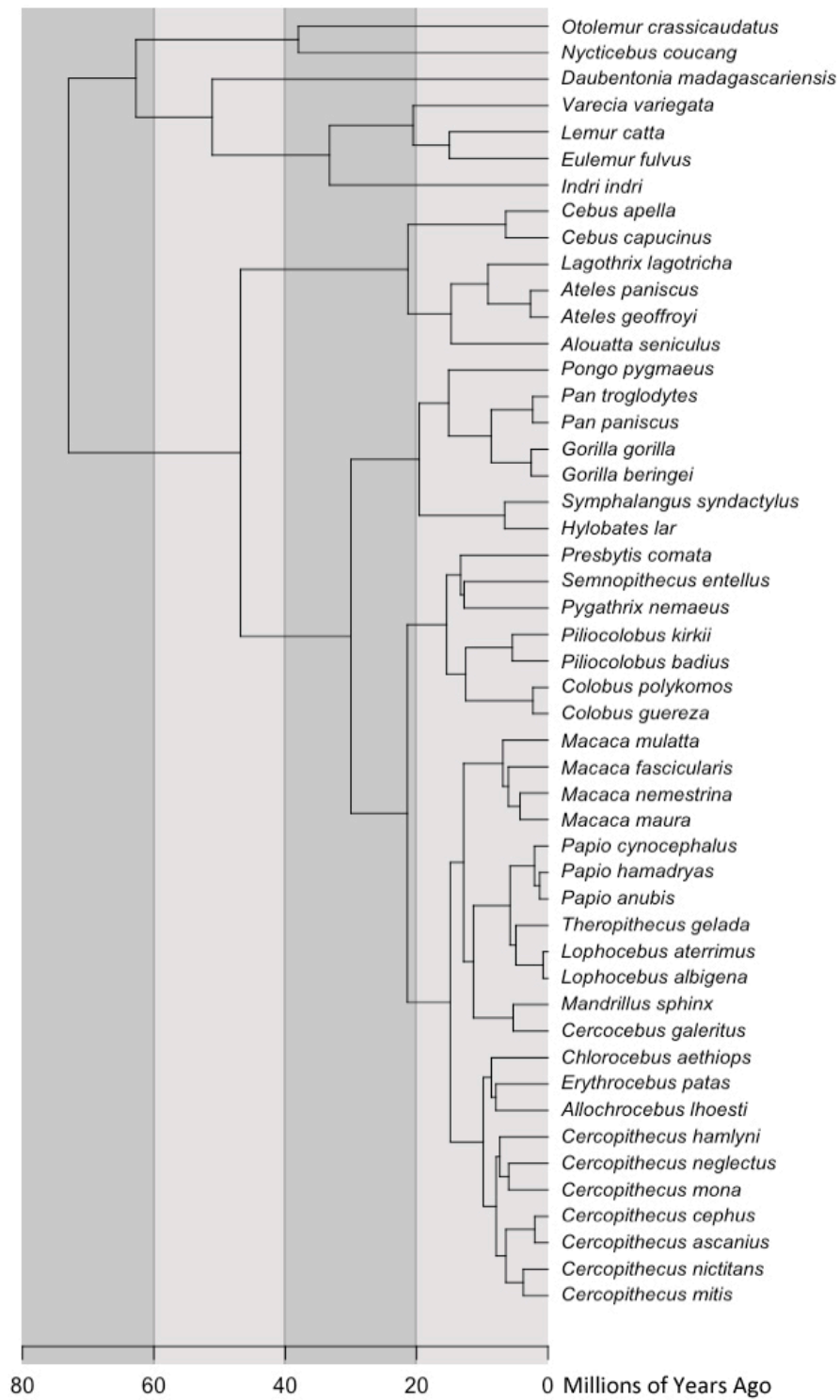


Fig. 2.6. Phylogenetic hypothesis of primates used in this study

Allometry is the concomitant change of shape variation with (isometric) size (Gould 1966). Whilst the process of Procrustes superimposition removes size, it does not remove the effects that size has upon shape. Yet allometry is an important factor to consider in the study of integration and modularity, as changes in body size often affect entire shapes, be it across the entire pelvis or the entire organism. Allometry can contribute to covariation of morphological traits and influence the modularity pattern (Klingenberg 2009, Goswami and Polly 2010a, Klingenberg and Marugan-Lobon 2013). We assessed the influence of evolutionary allometry (primate order) and allometry (primate groups) by employing regression, using the functions *procD.pgls* and *procD.lm* respectively (Adams 2014b, Adams and Collyer 2015, Adams and Otárola-Castillo 2013), where *shape data* are the dependent variables and the log-transformed pelvic centroid size is the independent variable. Residuals of these regression are taken forward as allometric-corrected data, hereafter referred to as *allo data*. We did not apply allometric correction to primate *PIC data*, due to a strong phylogenetic signal present in log centroid size data ($K=1.396$, $p=0.001$, effect size= 8.251), making the data prone to overcorrection.

2.3.6 Detecting modular organisation

To investigate patterns of modularity in the primate pelvis girdle, we attributed the landmarks to subsets according to the proposed modules for each hypothesis (table 2.2, figure 2.1).

<i>Hypothesis</i>	<i>Modules</i>	<i>Modules Partition</i>
H ₁	5 modules	il/is/pu/ac/sa
H ₂	4 modules	il/is/pu/sa
H ₃	4 modules	il/is+pu/ac/sa
H ₄	3 modules	il/is+pu/sa
H ₅	2 modules	obs/loc

Table 2.2. Summary of tested hypotheses

il= ilium, is= ischum, pu= pubis, ac=acetabulum, sa=sacrum, obs= obstetrics, loc = locomotion

Next, we calculated the modular signal for each hypothesis using the covariance ratio (CR) coefficient method. To do so, we employed the *modularity.test* function (Adams 2016) of the *geomorph* package (Adams and Otárola-Castillo 2013). The CR coefficient is a robust statistical tool shown to be independent of sample size and dimensionality of the multivariate data. It uses the pairwise covariance within and between variables (here represented by the modules tested in each hypothesis) to quantify its modular structure. The CR of modules Y_1 and Y_2 is calculated as follows:

$$CR = \text{tr}(S_{12}S_{21}) / [\text{tr}(S_{11}S_{11})\text{tr}(S_{22}S_{22})]^{1/2}$$

where *tr* is the trace (i.e., the sum of the diagonal elements of the squared matrix representing the total covariance between the two sets of variables), S_{11} and S_{22} are the matrices of within-module covariance of two modules Y_1 and Y_2 ; S_{12} is the between-module covariance matrix of the two modules Y_1 and Y_2 , and S_{21} is its transpose (Adams 2016). In this way, CR describes covariation between modules relative to covariation within modules. Obtained CR values ~ 1 signify equal amounts of within and between module covariation (i.e., no modular signal), whereas $CR < 1$ indicates smaller between-module than within-module covariation (i.e., modular signal). To test the statistical significance of each CR value, a randomized residual permutation procedure (RRPP) was applied, where 999 permutations of random modular partitioning were generated to compare the proportions of random partitions with CR coefficients smaller or equal to the observed CR coefficient of the tested hypothesis. Confidence level was set at $\alpha = 0.001$.

We also calculated the CR effect sizes across hypotheses and datasets to be able to compare the strength of the modular signal across the alternative hypotheses and data sets. The effect size of the CR (i.e. Z-CR) is obtained as:

$$Z\text{-CR} = \frac{CR_{\text{obs}} - \mu_r}{\sigma_r}$$

where CR_{obs} is the observed covariance ratio (CR) for the dataset as calculated above, μ_r is the expected value of the CR under a null hypothesis of no modularity (the empirical sampling distribution obtained from the RRPP for each hypothesis in each data set is here

re-used, and the mean of the empirical sampling distribution set as the null hypothesis of no modularity), and σ_r is the standard error (SE) of the mean for which the standard deviation (SD) of the obtained sampling distribution was used (Adams and Collyer 2019). Values from these distributions are log-transformed prior to effect size estimation to ensure normally distributed data.

The Z-CR represents a stable analytic tool to compare CR coefficients across alternative hypotheses and different datasets, and it is used here used to determine whether the strength of a modular signal is greater in one hypothesis and/or one dataset compared to another. When a modular signal is present, the observed Z-CR value will be negative as the obtained value will be less than the mean of the re-sampling, with more negative values signifying the presence of a greater modular signal (for a comprehensive overview of Z-CR see Adams and Collyer 2019). The Z-CR were calculated using the *compare.CR* function (Adams and Collyer 2019) of the *geomorph* package (Adams and Otárola-Castillo 2013).

We calculated the modularity signal (CR) and its effect (Z-CR) for the five outlined hypotheses within primate *shape*, *PIC* and *allo data* sets. As well as exploring modularity in the pelvis across the primate order, we also analysed the patterns of modularity for the following groups: Lemuroidea (LEM), New World monkeys (NWM), Old World monkeys (OWM), and Hominoidea (HOM). To preserve the relative position of the bone elements (Baab 2013, Klingenberg 2009, Zelditch *et al.* 2012), no new GPA is performed and the modules are a subset from the overall landmark configuration. Results obtained in the right-side pairs were used as control and validation of the left.

2.4 Results

Primate order

2.4.1 Influence of phylogeny and evolutionary allometry on primate girdle shape
 A phylogenetic signal is present (observed $K_{mult} = 0.4002$, $p = 0.001$, effect size = 9.4763) in the primate pelvic *shape data* and evolutionary allometry predicts 11.10% ($p = 0.001$) of the observed shape variation (table 2.3).

	<i>Df</i>	<i>SS</i>	<i>MS</i>	<i>Rsq</i>	<i>F</i>	<i>Z</i>	<i>Pr(>F)</i>
Allometry	1	0.5044	0.50442	0.111	6.104	4.5497	0.001
Residuals	47	3.8839	0.08264	0.889			
Total	48	4.3883					

Table 2.3. Primate order: evolutionary allometry

2.4.2 Modularity pattern for the primate order

Significance testing indicates that all the hypothesised modularity patterns within the primate pelvic girdle are statistically significant ($p = 0.001$) compared to 1.000 random modulations. In primate *shape*, *PIC* and *allo data*, the H_1 partitioning of the pelvic girdle obtains the strongest modular signal (table 2.4). When applying z-scoring to ensure the null hypothesis of no modularity is set equally across all datasets, H_1 represents the highest modular signal indicative that of the proposed hypotheses H_1 matches best the modular signal present in the primate pelvis. Furthermore, Z-CR values demonstrate the magnitude of the phylogenetic and allometric effect: the modular signal strength within the *PIC* and *allo data* is stronger compared to *shape data*; this trend is present across all the tested modular partitions (table 2.5).

<i>CR values</i>	H_1	H_2	H_3	H_4	H_5
<i>Shape data</i>	0.7357	0.7550	0.7679	0.7804	0.7901
<i>PIC data</i>	0.6826	0.7183	0.7512	0.7444	0.7474
<i>Allo data</i>	0.7198	0.7503	0.7466	0.787	0.8687

Table 2.4. CR values for each proposed hypothesis

Note: lower CR coefficient value denotes stronger modular signal

Z-CR	H_1	H_2	H_3	H_4	H_5
<i>Shape data</i>	-8.402	-8.045	-7.406	-7.670	-5.339
<i>PIC data</i>	-12.214	-11.146	-10.126	-11.029	-9.034
<i>Allo data</i>	-13.801	-12.774	-12.631	-11.934	-6.158

Table 2.5. Z-CR values for each proposed hypothesis

Note: more negative Z-CR effects represent stronger modular signal

2.4.3 Pairwise bone modularity within the primate order

As H_1 best explains the modularity pattern within the primate pelvic girdle, we calculated the CR and Z-CR values of each possible bone pair, for *shape*, *PIC* and *allo data* (tables 2.6 - 2.8). All pairwise CR coefficients are statistically significant ($p= 0.001$). The results show that the strengths of the modular signal within the H_1 configuration differs in *shape*, *PIC* and *allo data*. Compared to *shape data*, a greater modular signal across all bone pairs is detected in the *PIC data* as indicated by the increased Z-CR values. Particularly noticeable is the increased pubis-ischium modular signal, revealing the species relatedness effects on the co-evolution of these bones. Yet despite the difference in modular sign strength, overall a similar pattern can be observed (fig. 2.7).

Compared to *shape* and *PIC data*, the pattern of modular signal strength differs in the *allo data*. This indicates that the different bone constituents do not have a uniform response to allometric effects. The main difference, as indicated by the Z-CR values, centres around the ilium and ischium. Specifically, in the *shape* and *PIC data* the high modular zone is concentrated around the ischium (ilium - ischium, ischium - pubis, ischium - acetabulum), whereas this shifts to bone pairs containing the ilium (ilium - ischium, ilium - acetabulum, ilium - sacrum) in the *allo data*. Furthermore, it is notable that the caudal positioned pairs (ischium-acetabulum, ischium-pubis, and pubis-acetabulum) express comparatively more modularity in *shape* and *PIC data* than in the *allo data* set, suggesting that in this part of the pelvis allometry does not reduce but potentially enhances the modular signal. Conversely, the modular signal associated with the cranial positioned bone pairs appears to be reduced by allometric influences (fig. 2.7).

In line with expectations (Magwene 2001), bone constituents which are not immediately connected to each other show a higher modular signal, as seen in the sacrum paired with the ischium or with the acetabulum. The co-ordination effect between connecting bones is exemplified by the sacrum and ilium pair. Despite the sacrum and ilium being formed by very different developmental pathways, the sacrum-ilium pairing does not contain a particularly high modular signal, indicative that relative position and bone fusing (the formation of the sacroiliac joint) require coordination even if the mechanisms that facilitate the observed covariation are not yet fully understood.

<i>Shape</i>	<i>ilium</i>	<i>ischium</i>	<i>pubis</i>	<i>acetabulum</i>	<i>sacrum</i>
ilium		-6.040	-4.168	-4.028	-4.865
ischium	0.730		-6.749	-7.014	-10.213
pubis	0.668	0.676		-5.164	-8.970
acetabulum	0.715	0.813	0.713		-11.351
sacrum	0.615	0.582	0.695	0.552	

Table 2.6. Shape data: modular pairwise pelvic bone constituents' analyses*

<i>PIC</i>	<i>ilium</i>	<i>ischium</i>	<i>pubis</i>	<i>acetabulum</i>	<i>sacrum</i>
ilium		-6.919	-5.607	-4.676	-6.023
ischium	0.679		-11.828	-7.764	-11.571
pubis	0.508	0.533		-6.949	-10.813
acetabulum	0.684	0.862	0.650		-10.563
sacrum	0.569	0.536	0.534	0.644	

Table 2.7. *PIC Data*: modular pairwise pelvic bone constituents' analyses*

<i>Allo</i>	<i>ilium</i>	<i>ischium</i>	<i>pubis</i>	<i>acetabulum</i>	<i>sacrum</i>
ilium		-9.518	-6.476	-7.307	-7.419
ischium	0.662		-5.410	-6.562	-11.102
pubis	0.647	0.695		-3.967	-10.137
acetabulum	0.625	0.742	0.752		-14.601
sacrum	0.738	0.573	0.656	0.578	

Table 2.8. *Allo Data*: modular pairwise pelvic bone constituents' analyses*

**Tables 2.6 -2.8: Below the diagonal cells show the CR while above diagonal values display z-effect. All results are statistically significant (p= 0.001)*

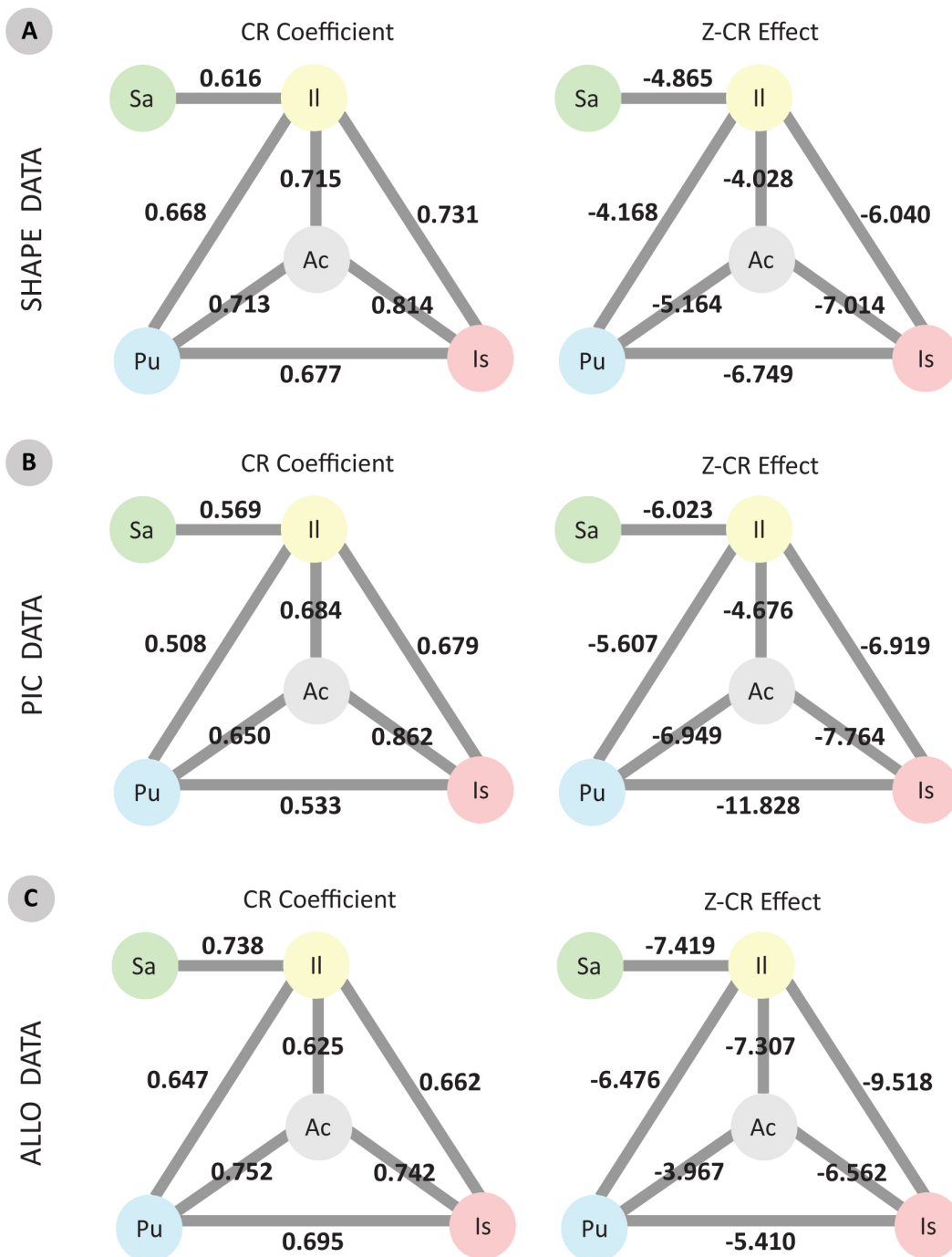


Fig. 2.7. CR coefficients and Z-CR effects for the connected bone constituents.

Each circle indicates a pelvic girdle bone constituent: Sa = sacrum, Il = ilium, Ac = acetabulum, Pu = pubis, and Is = ischium. Each value represents the calculated CR and Z-CR for each paired element and each pair is indicated by the connecting grey line. These values were calculated from the primate order shape data (see A), PIC data (see B), and allo data (see C).

Primate Groups

2.4.4 Influence of allometry on the pelvis girdle shape of primate groups

The results of the allometric ANOVA performed for each primate super family are presented in table 2.8. The influence of allometry on shape is variable across the primate groups: Hominoidea 46.6%, Lemuroidea 22.4%, New World monkeys 23.3% and Old World monkeys 14.6% (table 2.9).

Hominoidea (HOM)							
	<i>Df</i>	<i>SS</i>	<i>MS</i>	<i>Rsq</i>	<i>F</i>	<i>Z</i>	<i>Pr(>F)</i>
Allometry	1	0.169	0.1685	0.466	30.6	5.63	0.001
Residuals	36	0.193	0.0055	0.534			
Total	37	0.361					
Lemuroidea (LEM)							
	<i>Df</i>	<i>SS</i>	<i>MS</i>	<i>Rsq</i>	<i>F</i>	<i>Z</i>	<i>Pr(>F)</i>
Allometry	1	0.0118	0.01184	0.224	2.3	1.79	0.050
Residuals	10	0.0411	0.00514	0.776			
Total	11	0.0529					
New World Monkeys (NMW)							
	<i>Df</i>	<i>SS</i>	<i>MS</i>	<i>Rsq</i>	<i>F</i>	<i>Z</i>	<i>Pr(>F)</i>
Allometry	1	0.0192	0.01924	0.233	2.73	2.73	0.017
Residuals	11	0.0634	0.00704	0.767			
Total	12	0.0826					
Old World Monkeys (OMW)							
	<i>Df</i>	<i>SS</i>	<i>MS</i>	<i>Rsq</i>	<i>F</i>	<i>Z</i>	<i>Pr(>F)</i>
Allometry	1	0.086	0.0865	0.125	14.6	6.55	0.001
Residuals	111	0.604	0.0059	0.875			
Total	112	0.690					

Table 2.9. Primate groups: allometry

2.4.5 Modularity test for separate groups of primates

The modularity tests conducted on the primate groups *shape data* (table 2.10) reveal that New and Old World monkeys largely follow the same modular pattern as the primates, with H₁ obtaining the highest modular signal within these two groups. This is the case for both the CR coefficient values as the Z-CR values. Examining the Z-CR data, the Lemuroidea and Hominoidea pelvic girdles, however, appear to be differently structured. For Lemuroidea, hypotheses that exclude the acetabulum as a separate unit obtain higher modularity values than when the acetabulum is included. H₂ (ilium, ischium, pubis, sacrum) best explains the modular pattern, followed by H₄, the modularity pattern that partitions the ilium, ischio-pubis, and sacrum. Furthermore, in the hominoid *shape data* H₄ carries the highest modular signal and the Z-CR effect values reveal that, except for H₅, Hominoidea contain a lower modular signal compared to the other primate groups. When the *allo data* is examined, a rather different picture emerges: the results for Hominoidea now follow those of New and Old World monkeys, and the detected modular pattern is best represented by H₁ (table 2.11ps).

<i>Shape data</i>	<i>HOM</i>	<i>LEM</i>	<i>NWM</i>	<i>OWM</i>
<i>CR values</i>				
H ₁	0.8857	0.8176	0.7792	0.6509
H ₂	0.8900	0.8140	0.8239	0.6685
H ₃	0.8956	0.8281	0.7894	0.7286
H ₄	0.8854	0.8354	0.8504	0.7395
H ₅	0.9189*	0.9006	0.9541*	0.7256
<i>Shape data</i>	<i>HOM</i>	<i>LEM</i>	<i>NWM</i>	<i>OWM</i>
<i>Z-CR</i>				
H ₁	-6.603	-12.953	-11.630	-13.202
H ₂	-6.412	-13.746	-10.007	-12.961
H ₃	-5.951	-12.590	-11.207	-10.869
H ₄	-6.899	-13.103	-9.261	-11.287
H ₅	-3.897	-7.112	-3.233	-9.656

Table 2.10. *Shape data*: modularity for primate groups

*HOM = Hominoidea, LEM = Lemuroidea, NWM = New World monkeys (Ceboidea), and OWM = Old World monkeys (Cercopithecoidea). Note: lower CR coefficient value denotes stronger modular signal whilst in the comparative analysis the more negative Z-CR effects represent stronger modular signal. All results were statically significant at $p=0.001$, unless the obtained value is denoted by * which indicates $p = 0.01$*

<i>Allo data</i>	<i>HOM</i>	<i>LEM</i>	<i>NWM</i>	<i>OWM</i>
<i>CR values</i>				
H ₁	0.6942	0.8156	0.7836	0.6133
H ₂	0.7209	0.7964	0.7902	0.6283
H ₃	0.7351	0.8323	0.7981	0.6652
H ₄	0.7344	0.8150	0.8146	0.6796
H ₅	0.8281	0.9287	0.9124	0.7179
<i>Allo data</i>	<i>HOM</i>	<i>LEM</i>	<i>NWM</i>	<i>OWM</i>
<i>Z-CR</i>				
H ₁	-11.706	-14.077	-13.327	-13.890
H ₂	-10.570	-15.631	-13.179	-13.699
H ₃	-10.065	-13.593	-12.878	-12.477
H ₄	-10.880	-15.695	-12.590	-12.810
H ₅	-5.879	-5.811	-5.075	-9.421

Table 2.11. *Allo data*: modularity primate groups

HOM = Hominoidea, LEM = Lemuroidea, NWM = New World monkeys (Ceboidea), and OWM = Old World monkeys (Cercopithecoidea). As above, lower CR coefficient value denotes stronger modular signal whilst in the comparative analysis the more negative Z-CR effects represent stronger modular signal. All results were statically significant with $p = 0.001$.

2.5 Discussion

This study represents the first comprehensive attempt to quantify developmental and functional modularity of the adult primate pelvis. As in any study, the study of modularity rests upon certain assumptions and has its inbuilt limitations. These are discussed first.

Phenotypic modularity is a pervasive characteristic of biological entities (Goswami *et al.* 2014). Although morphological modular organisational patterns can be observed through the analysis of variance-covariance matrices, the underlying mechanisms and processes that structure such organisational pattern are not directly observed (Klingenberg 2003). In line with Cheverud (1988), this study assumes broad similarity between genetic, the **G** matrix, and phenotypic morphological covariance patterns, the **P** matrix, yet this assumption cannot be empirically validated among primates since large scale primate breeding and experimental gene modifications projects are not ethically and practically feasible (Rolian 2014).

Equally, the adult pelvic girdle morphology is the outcome of multiple processes that generate variance and covariance, where genetic, developmental, functional, environmental and evolutionary influences all may play a part with greater or lesser impact. These processes overlap - in some morphological regions amplifying each other, whilst in others cancelling each other out (Hallgrimson *et al.* 2009, Zeldich *et al.* 2012). The proposed developmental and functional hypothesised models provide a statistical means to separate the potential causal processes involved in modular patterning, and rely on the assumption that the quantified modular signal strengths detectable within the bony adult primate pelvis represents a measure of strength of the underlying processes shaping its modular organisation. Whether this inference is correct, and its quantified correlate in terms of degree is accurate, cannot be tested for the same reasons outlined above.

Keeping these caveats in mind, the results shown here suggest that, overall, the non-human primate pelvis is highly modular, implying that its ability to respond to natural selection is high (Marroig *et al.* 2009, Porto *et al.* 2009). Our results complement findings by Grabowski *et al.* (2011) and Lewton (2012), who found generally low signals of

integration and high levels of evolvability in the primate hip bone when using metrical measurement without taking modularity into account. The modular pattern revealed by this study is statistically best supported by H_1 , identifying the ilium, ischium, pubis, acetabulum and sacrum as relatively independent modules, and implying that the modular organisation of the non-human primate pelvic girdle is predominantly influenced by developmental processes. The need of these modules to covary is limited, facilitating divergent morphological forms to rise in response to evolutionary selective pressures since separate modules can evolve relatively independently from one another (Wagner *et al.* 2007).

An interesting aspect of our study is the identification of the ischium and pubis as two separate modules despite the presence of genetic pleiotropy between those two elements as shown in mouse and chick models. Both H_1 and H_2 , which consider the ischium and pubis acting as separate modules, obtained higher modular signals compared to their counterparts, H_3 and H_4 , which projected an integrated ischiopubis. Strikingly, the ischium was even identified as the most independent module in the *shape data* analysis of the primate order, suggestive of an abundance of relatively independent different ischium morphologies (Miller 1945, Rose 1974, Ward *et al.* 2018). These findings contrast with the modular organisation of the carnivore hipbone, where ischium and pubis shapes do covary more closely (Martin-Serra *et al.* 2018). Compared to the carnivore organisational pattern, the dissociation of the primate ischium and pubis point to a reduction in the level of constraints placed on the concerted shape evolution of these bones, enhancing their independent evolvability, and thus possibly decreasing the amount of time needed to generate new adaptive variants that might have been previously difficult or impossible to arise (Altenberg 1994, 2005; Mitteroecker and Bookstein 2007).

What may have caused the need for such a relative increased parcellation of the ischium and pubis among primates? Unfortunately, not much is known about primate pubis morphological variation (Lewton 2010, Gebo 2014). We do know more, however, about the ischium. Primate species that utilize a dominant hind leg form of locomotion, such as vertical clingers and leapers, exhibit a shortened and dorsally bent ischium compared to quadrupeds. This ischium morphology facilitates the hip extensor leverage during

hindlimb extension (Fleagle and Anapol 1992). We hypothesize that this functional need may underpin an increase of ischium independence to facilitate ischium morphology, which in turn may have contributed to the observed ischium-pubis parcellation. Regardless of the possible cause, a modular ischium and pubis are present in each examined primate group, suggesting that this parcellation took place deep in time within primates. Thus the 'liberated' ischium is a key feature of the primate pelvic modular pattern as attested by its high modular signal across primates. As mentioned in the introduction, integration is hypothesised to be the basal state and, by theoretical extension, primates would have evolved a more modular pattern, undergoing a disassociation of two previously integrated traits in response to natural selection. To test this hypothesis, however, a broad comparative mammalian analyses with the inclusion of fossil data where possible is necessary to determine how the primate pelvic modularity pattern compares to other mammalian groups beyond carnivores, and the nature of their relationships to the ancestor mammalian modular organisation.

The identified modularity patterns within the primate groups provide some insights on how the modular organisation itself may have evolved within the primate order, and the influence of allometry on the modular signal. Both monkey groups displayed a modular pattern corresponding with H_1 whilst lemurs and hominoids (to the exclusion of humans) exhibited a different modular organisation, H^2 and H^4 respectively. For Hominoidea, the hypothesis that best fitted the pattern of modularity had fewer modules than among other primates, shaped by closer coordination between the ischium, pubis and acetabulum. The evolutionary processes behind this unique hominoid pattern are revealed by the analysis of the *allo data*, showing that once allometry is removed, the hominoid pelvis has a similar modular structure as the monkey groups. These results offer fascinating insights into the co-ordinating effects of allometry and the constraints imposed by increased body size on pelvis shape variation. In the case of hominoids, these constraints may be fabrication (Seilacher 1970), leading to less modularity of the caudal/inferior elements of the pelvic girdle and a consequently reduced degree of evolutionary flexibility.

The second group that shows a different modular structure of the pelvis shape was Lemuroidea. Lemuroidea differ from monkeys and apes in that their acetabulum is more

closely integrated to the three bony elements that form the os coxae than observed in the other primate groups. Two possible interpretations of these results exist. On the one hand, the results could reflect a step-wise evolutionary history of pelvic modularity from ancestral primate, to strepsirhines, to haplorrhines. This implies that the H_1 modular organisation would have evolved early in the emergence of the Haplorrhini group, with monkeys and apes sharing the same modular organisation. On the other hand, the smaller number of modules among Lemuroidea than among haplorrhines could reflect a derived adaptation of the Lemuroidea, possibly associated with their unique vertical clinging and leaping locomotory strategies. Interpreting Lemuroidea modularity as relatively derived is strengthened by a comparison with carnivores. Among Canidae, Felidae and Ursidae, the acetabulum also forms a separate module (Martin-Serra *et al.* 2018), as observed here in all haplorhine groups. If so, the modular pattern associated with H_1 would have been present early in the evolution of the primate order whereby a flexible one-to-many mapping configuration seems to enable modifications to the modular magnitude levels to suit specific primate group needs instigated by allometry or other evolutionary pressures. To resolve the above, whether a relatively independent acetabulum module forms part of a wider mammalian pattern or represents evolutionary convergence unique to these taxa (haplorhines and the above listed group of carnivores), possibly associated to their shared flexible quadrupedal walking and running, needs testing with larger comparative mammalian datasets.

Even if the results presented here suggest that the main pattern of evolutionary modularity of the primate pelvis is aligned with developmental partitioning of the pelvic girdle, the tested locomotory-obstetric functional partition (H^5) also contained a significant evolutionary modular signal. This could reflect the accumulated effect within primates across time of how at an individual level the developmental programmes interact with these functional regions, even if it remains unclear precisely how these processes interact (Klingenberg 2008, Ruff *et al.* 2006). The locomotory-obstetric partition has received attention before, particularly in terms of the obstetric dilemma framework. The obstetric dilemma, as formulated by Washburn (1960), describes the difficulty of reconciling two opposing selective forces enacting upon the human pelvis: selection for biomechanical efficiency, which is hypothesised to favour narrow pelvises, versus selection for large-brained/big-bodied neonates requiring an obstetrically efficient wide female

pelvis structure (Schultz 1949, Rosenberg 1992, Rosenberg and Threvathan 1996). Understanding the level by which the obstetric and locomotory modules must co-evolve or can relative independently respond to such evolutionary pressures is crucial to our understanding of the possible OD effects on not just humans but also the primate pelvic evolutionary restrictions, possibilities and outcomes. Grabowski (2012) addressed this question at a phenotypic (species) level utilising metrical measurement to calculate levels of evolvability and evolutionary flexibility of the locomotory-obstetric partition for *Homo*, *Pan*, *Gorilla*, *Pongo* and *Hylobates*. His results indicated that *Homo* underwent a significant divergence from the pattern observed in other apes, with humans displaying notable higher evolutionary potential within the birth canal and between obstetric and other pelvic traits. Furthermore, Huseynov *et al.* (2017), applying a methodology comparable to our study, found a significant modular signal of the locomotory-obstetric partition within the *Pan troglodytes* pelvis, suggesting that the structural organisation enabling divergence of *Homo* pelvis morphology was likely already present in the last common ancestor of humans and chimpanzees (Huseynov *et al.* 2017).

Our results at evolutionary level provide evidence that the locomotory-obstetrics partition is embedded deeply within primate evolutionary history as it is detectable as a significant signal across the primate order. The discovery of this shared functional partition, even if varying in strength across the primate branches, implies that such a functional modular organisation, key to ameliorating the obstetric dilemma, is present in the wider primate order. Our results suggest instead that this secondary modular structure contributes to the relative independent evolutionary outcomes of the obstetric and locomotory modules. Rather than being a human apomorphy, the locomotory-obstetrics partition is a shared primate trait, established before - perhaps even being the facilitator of - the evolution of the widely varying primate locomotory adaptations observed and the general primate characteristic of birthing large-headed neonates (Schultz 1949, Rosenberg and Trevathan 1996, Trevathan 2015). Furthermore, whilst sexual dimorphism was not directly investigated within this study, the existence of a functional partition may play a role in the evolution of pelvic sexual dimorphism.

2.6 Conclusion

Within this chapter, we have undertaken an empirical analysis of the primate pelvis evolutionary modular organisational pattern testing developmental and functional hypotheses. The findings demonstrate that the primate pelvic girdle is highly modular, identifying ilium, ischium, pubis, acetabulum and sacrum as developmentally-aligned modules able to act relatively independently from one another. This pattern is ancestrally shared across primates apart from possibly Lemuroidea, among whom the acetabulum appears less modular than in the other examined primate groups. Compared to the carnivore organisational pattern, the increased dissociation of the primate ischium and pubis is a key primate characteristic. This pubis-ischium parcellation is present in all examined primate groups, suggesting that this parcellation was present in basal primates. The modular ischium and pubis may represent one of the derived features that characterise the divergence of the primates from other mammals, and likely is a contributing factor to the great diversity of extant primate pelvic morphology and expanded locomotory repertoire. Further research involving a broad mammalian sample including early primate fossil data is needed to resolve the question of how the identified primate modular pattern relates to the underlying mammalian and examine early primate ancestral patterns.

Our results also suggest that the primate pelvic girdle is predominantly organised along developmental modules, whilst also providing functional modular support. Primates seem to have an inbuilt capacity to alleviate potential antagonistic selective pressures of locomotor and obstetric demands (Washburn 1960), as both partitions have the ability to respond in relative independence. Overall, our results demonstrate that the primate pelvis contains a complex modulation that is multi-layered and possibly hierarchical in architecture, underpinning the wide range of morphological disparity and locomotor behaviours attested within the primate order.

2.7 Supplementary information

S1: Supplementary Information Primate Locomotion

Locomotion	Sub-type locomotion	Activity description	Representative taxa included in this study
Vertical Clinging and Leaping		Leaping in trees and hopping on the ground	<i>Daubentonia madagascariensis</i> <i>Eulemur fulvus</i> <i>Indri indri</i> <i>Lemur catta</i> <i>Otolemur crassicaudatus</i> <i>Varecia variegata</i>
Quadrupedalism	Slow Climbing	Cautious climbing, no leaping or branching	<i>Nycticebus coucang</i>
	Arboreal Quadrupedalism	Climbing, springing, branch running and jumping	<i>Cercocebus galeritus</i> <i>Cercopithecus ascanius</i> <i>Cercopithecus cephus</i> <i>Cercopithecus hamlyni</i> <i>Cercopithecus lhoesti</i> <i>Cercopithecus mitis</i> <i>Cercopithecus mona</i> <i>Cercopithecus neglectus</i> <i>Cercopithecus nictitans</i>
	Terrestrial Quadrupedalism	Ground running	<i>Chlorocebus aethiops</i> <i>Erythrocebus patas</i> <i>Lophocebus albigena</i> <i>Lophocebus aterrimus</i> <i>Macaca fascicularis</i> <i>Macaca maura</i> <i>Macaca mulatta</i> <i>Macaca nemestrina</i> <i>Mandrillus sphinx</i> <i>Papio anubis</i> <i>Papio cynocephalus</i> <i>Papio hamadryas</i> <i>Semnopithecus entellus</i>
Suspension	New World Monkey Suspension	Arm-swinging with use of prehensile tail	<i>Alouatta seniculus</i> <i>Ateles geoffroyi</i> <i>Ateles paniscus</i> <i>Cebus apella</i> <i>Cebus capucinus</i> <i>Lagothrix lagotricha</i>
	Old World Monkey Suspension	Arm-swinging and leaping	<i>Colobus guereza</i> <i>Colobus polykomos</i> <i>Ptilocolobus badius</i> <i>Ptilocolobus kirkii</i> <i>Presbytis comata</i> <i>Pygathrix nemaus</i>
Brachiation	True	Arm-swinging and arm-hanging	<i>Hylobates lar capenteri</i>

		<i>Symphalangus syndactylus</i>
Modified	Knuckle walking and fist-walking	<i>Gorilla beringei</i> <i>Gorilla gorilla</i> <i>Pan paniscus</i> <i>Pan troglodytes</i> <i>Pongo pygmaeus</i>

Table S1. Primate Locomotion

S2: Supplementary Information Landmarks

<i>Landmark</i>	<i>Landmark description</i>	<i>Area</i>
<i>L/R</i>	<i>Bilateral:</i>	
1-34	Apex of the dorsal caudal iliac spine (homolog of posterior inferior iliac spine in humans - PIIS)	ilium
2-35	Apex of the dorsal cranial iliac spine (homolog of posterior superior iliac spine in humans – PSIS)	ilium
3-36	Most cranial point on the iliac crest	ilium
4- 37	Ventral cranial iliac spine (homolog of anterior superior iliac spine in humans - ASIS)	ilium
5- 38	Most cranial point along the ventral margin of the auricular surface	ilium
6- 39	Intersection point of sacro-iliac and pelvic brim (linear terminalis arcuate line)	ilium
7- 40	Point along the linea terminalis arcuate line at the minimum breadth of the ilium, corresponding with point used to measure maximum distance of pelvic inlet traverse.	ilium
8-41	Point along the lateral iliac margin at the minimum breadth of the ilium	ilium
9- 42	Point along the medial iliac margin at the minimum breadth of the ilium	ilium
10- 43	Most cranial point along the ventral part of the acetabular rim at minimum distance from the cranial pubic ramus	acetabulum
11 -44	Point along the cranial margin of the pubis at minimum distance to the acetabulum (opposite point 9)	pubis
12-45	Cranial acetabulum: most cranial point on the acetabular rim adjacent to the lateral iliac margin, as the extension of ASIS and AIIS)	acetabulum
13- 46	Caudal acetabulum: most caudal point on the acetabular rim along the axis of the ischium	acetabulum
14- 47	Centre acetabulum: Central point of acetabular fossa	acetabulum
15- 48	Dorsal acetabulum: Most dorsal point on the acetabular rim	acetabulum
16- 49	Most medial tip of the caudal portion of the lunate surface	acetabulum
17- 50	Most caudal tip of the medial portion of the lunate surface	acetabulum

18- 51	Most medial point on the lateral ischium margin	ischium
19- 52	Point at the intersection of the lateral ischium margin and ischial tuberosity, along the extension of S12 and S17	ischium
20- 53	tip of the ischial spine (see cranial part of the dorsal ischium margin)	ischium
21- 54	Point at the intersection of the dorsal ischium margin and ischial tuberosity	ischium
22- 55	Most ventral point along the dorsal ischium margin	ischium
23- 56	Most medial part of the ischial tuberosity margin	ischium
24- 57	Point on the obturator margin at the minimum breadth of the ischium	ischium
25- 58	Caudal margin pubic symphysis (anterior)	pubis
26- 59	Cranial margin pubic symphysis	pubis
27 - 60	Most cranial point on the lateral alar border of the sacrum	sacrum
28 - 61	Most lateral point on the cranial margin of the first sacral vertebral body	sacrum
62-63	Caudal margin pubic symphysis (posterior)	pubis
<i>Midline:</i>		
29	Midpoint of the ventral margin of the first sacral vertebral body	sacrum
30	Midpoint under the rim of first sacral vertebral body margin	sacrum
31	Midpoint of the caudal margin of the first sacral vertebral body	sacrum
32	Midpoint of the caudal margin of the second sacral vertebral body	sacrum
33	Midpoint of the caudal margin of the last sacral vertebral body	sacrum

Table S2. Landmark Placement Definitions

S3: Supplementary Information Curve Semi-Landmarks

<i>Curve</i>	<i>Descriptions</i>	<i>Placements</i>	<i>sLM</i>	<i>Area</i>
L: C1	Following Caudal iliac	<i>Left:</i> start LM1 - end LM2 with 4 subdivisions.	L: 64, 65, 66	ilium
R: C14	spine	<i>Right:</i> start LM34 - end LM35 with 4 subdivisions.	R: 109, 110, 111	
L: C2	iliac crest: following	<i>Left:</i> start LM2 - end LM3 with 5 subdivisions.	L: 67, 68, 69, 70,	ilium
R: C15	medial border	<i>Right:</i> start LM36 - end LM37 with 5 subdivisions.	R: 112, 113, 114, 115	
L: C3	iliac crest: following	<i>Left:</i> start LM2 - end LM3 with 5 subdivisions.	L: 71, 72, 73, 74,	ilium
R: C16	lateral border	<i>Right:</i> start LM37 - end LM38 with 5 subdivisions.	R: 116, 117, 118, 119	
L: C4	Following lateral ilium	<i>Left:</i> start LM3 - end LM7 with 5 subdivisions.	L: 75, 76, 77, 78,	ilium
R: C17	edge	<i>Right:</i> start LM38 - end LM42 with 5 subdivisions.	R: 120, 121, 122, 123,	
L: C5	pelvic brim: following	<i>Left:</i> start LM5 - end LM6 with 4 subdivisions.	L: 79, 80, 81,	ilium
R: C18	cranial margin	<i>Right:</i> start LM40 - end LM41 with 4 subdivisions.	R: 124, 125, 126,	
L: C6	pelvic brim: following	<i>Left:</i> start LM6 - end LM63 with 5 subdivisions.	L: 82, 83, 84, 85,	ilium/ pubis
R: C19	caudal margin	<i>Right:</i> start LM41 - end LM64 with 5 subdivisions.	R: 127, 128, 129, 130,	
L: C7	following acetabular margin	<i>Left:</i> start LM12 – LM14 with 2 subdivisions, LM14 – LM11 with 2 subdivisions, LM11 – LM9 with 2 subdivisions, LM9 – end LM16 with 2 subdivisions.	L: 86 87 88 89	acetabulum
R: C20		<i>Right:</i> start LM47 – LM 49 with 2 subdivisions, LM49 – LM46 with 2 subdivisions,	R: 131 132	

		LM46 – LM44 with 2 subdivisions,	133	
		LM44 – end LM51 with 2 subdivisions.	134	
L: C8	following pubic	<i>Left:</i> start LM24 – end LM25 with 4 subdivisions.	L: 90, 91, 92,	pubis
R: C21	symphysis	<i>Right:</i> start LM59 – end LM60 with 4 subdivisions.	R: 135, 136, 137,	
L: C9	following lateral ischium	<i>Left:</i> start LM12 - LM17 with 2 subdivisions, LM 17 – end LM 18 with 2 subdivisions.	L: 93, 94,	ischium
R: C22	margin	<i>Right:</i> start LM47 - LM52 with 2 subdivisions, LM 52 – end LM 53 with 2 subdivisions.	R: 138, 139,	
L: C10	following medial dorsal ilium margin	<i>Left:</i> start LM0 – LM8 with 4 subdivisions, LM8 – end LM19 with 4 subdivisions.	L: 95, 96, 97, 98, 99, 100,	ilium
R: C23		<i>Right:</i> start LM35 – LM43 with 4 subdivisions, LM43 – end LM54 with 4 subdivisions.	R: 140, 141, 142, 143, 144, 145,	
L: C11	following medial dorsal ischium	<i>Left:</i> start LM19 - LM21 with 2 subdivisions, LM21- end LM20 with 2 subdivisions.	L: 101, 102,	ischium
R: C24	margin	<i>Right:</i> start LM54 - end LM56 with 2 subdivisions, LM56 – end LM55 with 2 subdivisions.	R: 146, 147	
L: C12	following ischial tuberosity	<i>Left:</i> start LM20 – LM22 with 3 subdivisions, LM22 – LM18 with 3 subdivisions, LM18 – end LM20 with 3 subdivisions.	L: 103, 104, 105, 106, 107, 108,	ischium
R: C25		<i>Right:</i> LM255– LM57 with 3 subdivisions, LM57 – LM53with 3 subdivisions, LM53 – end LM55 with 3 subdivisions.	R: 148, 149, 150, 151, 152, 153	

Table S3. Curve Landmark Placement

S4: Supplementary Information Data Landmark Error Test

<i>ID</i>	<i>Group</i>	<i>Specimen ID</i>	<i>Family</i>	<i>Species</i>
Ceb1	1	CebApe07530M5NWM	Cebidae	<i>Cebus apella</i>
Ceb2	2	CebApe07530M5NWM	Cebidae	<i>Cebus apella</i>
Ceb3	3	CebApe07530M5NWM	Cebidae	<i>Cebus apella</i>
Ery1	1	EryPat17897M4OWM	Cercopithecidae	<i>Erythrocebus patas</i>
Ery2	2	EryPat17897M4OWM	Cercopithecidae	<i>Erythrocebus patas</i>
Ery3	3	EryPat17897M4OWM	Cercopithecidae	<i>Erythrocebus patas</i>
Eul1	1	EulRuf04005M1LEM	Lemuridae	<i>Eulemur fulvus rufus</i>
Eul2	2	EulRuf04005M1LEM	Lemuridae	<i>Eulemur fulvus rufus</i>
Eul3	3	EulRuf04005M1LEM	Lemuridae	<i>Eulemur fulvus rufus</i>
Hyl1	1	HylLar01579F7HOM	Hylobatidae	<i>Hylobates lar</i>
Hyl2	2	HylLar01579F7HOM	Hylobatidae	<i>Hylobates lar</i>
Hyl3	3	HylLar01579F7HOM	Hylobatidae	<i>Hylobates lar</i>
Ind1	1	IndInd00674M1LEM	Indriidae	<i>Indri indri</i>
Ind2	2	IndInd00674M1LEM	Indriidae	<i>Indri indri</i>
Ind3	3	IndInd00674M1LEM	Indriidae	<i>Indri indri</i>
Lag1	1	LagLag04024M5NWM	Atelidae	<i>Lagothrix lagotricha</i>
Lag2	2	LagLag04024M5NWM	Atelidae	<i>Lagothrix lagotricha</i>
Lag3	3	LagLag04024M5NWM	Atelidae	<i>Lagothrix lagotricha</i>
Nyc1	1	NycCou17351M2LEM	Lorsidae	<i>Nycticebus coucang</i>
Nyc2	1	NycCou17351M2LEM	Lorsidae	<i>Nycticebus coucang</i>
Nyc3	2	NycCou17351M2LEM	Lorsidae	<i>Nycticebus coucang</i>
Oto1	1	OtoCra27412M1LEM	Galagidea	<i>Otolemur crassicaudatus</i>
Oto2	2	OtoCra27412M1LEM	Galagidea	<i>Otolemur crassicaudatus</i>
Oto3	3	OtoCra27412M1LEM	Galagidea	<i>Otolemur crassicaudatus</i>
Pan1	1	PanPan13202M8HOM	Hominidae	<i>Pan paniscus</i>
Pan2	2	PanPan13202M8HOM	Hominidae	<i>Pan paniscus</i>
Pan3	3	PanPan13202M8HOM	Hominidae	<i>Pan paniscus</i>
Pap1	1	PapHam03040F4OWM	Cercopithecidae	<i>Papio hamadryas</i>
Pap2	2	PapHam03040F4OWM	Cercopithecidae	<i>Papio hamadryas</i>
Pap3	3	PapHam03040F4OWM	Cercopithecidae	<i>Papio hamadryas</i>

Table S4.1. Overview Specimen Used in Error Test

<i>Error</i>	<i>df</i>	<i>SS</i>	<i>MS</i>	<i>Rsq</i>	<i>F</i>	<i>Z</i>	<i>Pr(>F)</i>
Ind	9	0.82179	0.091310	0.99816	1209.413	19.4227	0.001**
Rep	2	0.00016	0.000080	0.00019	1.0572	0.3295	0.374
Residuals	18	0.00136	0.000075	0.00165			
Total	29	0.82331					

Table S4.2. Procrustes ANOVA Error Test Result

Ind = Individual Specimen, Rep = repeated measurement

Chapter 3:

The Impact of Integration on Primate Pelvic Girdle Evolution.

3.1 Abstract

Phenotypic integration and modularity are integral features of complex organismal systems. The modular pattern and integration magnitudes do not only describe the manner and strength of the relationships of biological parts but also raises question on how it may influence shape variability and bias evolutionary trajectories. Yet few studies have tried to explicitly clarify the role of morphological integration in variability and the evolutionary consequences this entails. Here, we investigate the link between magnitude of primate pelvis module integration and its impact on morphological disparity - the breadth of observed morphological variation across taxa. We test whether the primate pelvic girdle mainly adheres to a theoretical model of constraint or facilitation. Our results demonstrate that despite variation among primate groups, levels of integration are conserved across primates, and an inverse relationship exists between integration and morphological disparity. The inverse relationship suggests that the impact of primate pelvis integration is best supported by a hypothesis of constraint. Our findings highlight the need to consider integration when modelling trait changes and reconstructing evolutionary pelvic adaptation.

3.2 Context of study

Evolutionary researchers frequently use comparisons across biological organisms to infer behaviours, locomotion, phylogenetic relatedness, and the selective pressures that may have contributed to the differences observed across taxa. Yet the noted similarities and differences are the outcome of evolution. It is the interaction of natural selection and the inherent organismal ability to respond to selection that shapes its evolution trajectory. Natural selection has long been held as a mechanism of evolution, yet variation – the raw material for natural selection to act upon – is not limitless nor does it appear at random. Instead variation includes structured covariation whereby the covariation biases the

amount and direction of possible variation organisms can produce. Biological entities are complex systems composed of parts (modules) with varying degrees of interdependence and dependence within and between its system parts (integration) (Olson and Miller 1958, Cheverud 1982). This model system is formed by and results from the combined effects of genetic, developmental, functional, and environmental interactions. The structured variation and the correlated relationship of its parts as described by integration have direct consequences on the manner in which phenotypic variation can be realized, as well as the extent to which phenotypes can vary, and thus, by extension, influences its evolutionary potential.

How may integration magnitude affect the breadth of morphological variance? Theoretically, integration has traditionally been conceptualised as a constraining mechanism since trait correlations dictate that changes must occur in a co-varying fashion. Whilst this safeguards the cohesion of shared genetic, developmental pathways, and functionality of traits, it does come at the detriment of their flexibility to respond to selection (Marroig *et al.* 2009, Porto *et al.* 2009, Goswami *et al.* 2014). In this scenario, strong correlation of traits negatively affects the spectrum of available variation, and reduces the range of responses to selection (Wagner 1996, Lynch and Walsh 1998, Hansen *et al.* 2003, Hansen and Houle 2004, Hansen and Houle 2008). Conversely, low levels of integration enable selected traits to evolve in a more independent manner, promoting responsiveness to selection although this may come at the price of reduced cohesion of that trait. This has been associated with higher levels of morphological variability and increased availability of possible responses (Marroig *et al.* 2009, Porto *et al.* 2009). Patterns and magnitudes of integration thus bias the response to natural selection. Morphological disparity, the consequence of evolutionary flexibility, is the result of the interaction of selection and the intrinsic constraint levelled on variation, whereby the level of that constraint on variation is described by magnitudes of integration (Goswami *et al.* 2014, Felice *et al.* 2018).

In the above theoretical model, integration and disparity are characterised by an inverse relationship, whereby high levels of integration act as a constraint on morphological disparity and low levels of integration reduce the strength of constraints on morphological variation. Integration may also underpin preference for homoplasy and convergent

evolution since only a limited amount of forms can be realised. However, simulation models demonstrate that high levels of integration can also be associated with the facilitation of novel forms and increases disparity (Goswami *et al.* 2014, 2015). In this case, integration and disparity are characterised by a direct relationship. This occurs when the preferred direction of selection and the correlated response align, enabling organismal forms to shape along the lines of least resistance. The above-mentioned simulations demonstrate that such high phenotypic integration can produce both more and less disparate morphologies than expected under random walk models (Goswami *et al.* 2014). In other words, the relationship between integration and morphological disparity is more complex than initially theorised, with integration magnitude and preferred direction of selection combined playing a role in influencing the breadth of disparity.

Studies explicitly investigating the role of integration on variation are few and obtained varying results. Felice and Goswami (2018) found integration acting as a constraining influence on morphological disparity of avian cranial modules. Conversely, Navalon *et al.* (2020) detected strong integration acting in a facilitating manner when examining Darwin's finches and the Hawaiian honeycreeper, argued to have contributed to the adaptive radiation of those species. Research by Randau and Goswami (2017) also linked increased levels of integration with increased levels of morphological disparity within the felid vertebral column. Yet, no recoverable relationship could be found between cranial integration and disparity in the Fire salamander (*Salamander salamander*) and caecilian skull (Marschall *et al.* 2018, Bardua *et al.* 2019b, Bon *et al.* 2020). These studies show that no pattern in the relationship between integration and disparity can be assumed, even when similar structures are under investigation. An additional difficulty within this line of enquiry is that, whilst it has been proposed that genetic and developmental interactions involved in morphogenesis play an important role in realised integration, assigning integration magnitudes and changes to specific genetic, developmental or functional origins remains problematic (Felice *et al.* 2018). This leaves the specific drivers or combination of drivers involved in integration often unknown.

Studies pertaining to integration and the influence of integration on disparity of the pelvis are even more rare, and those that have been carried out tend to concentrate on the differences and similarities between *Homo sapiens* and other primate species. Using

linear measurements of the hip bone, Grabowski *et al.* (2011, 2015) and Lewton (2012) investigated integration levels and evolutionary flexibility of the overall hip bone. Whilst Grabowski found that humans display significant reduction of integration and increased evolutionary flexibility compared to other great apes, Lewton uncovered a different signal whereby the *Pan* hip bone, rather than that of *Homo*, contained the lowest levels of integration. Lewton also found high evolutionary flexibility to be present throughout her sampled data set which contained 35 primate taxa ranging from strepsirrhines to hominoids. Whilst these studies tentatively indicate that the primate hip bone is characterised by low levels of integration, the modules present within the articulated primate pelvis were not considered. As such, despite the pelvic girdle being an interesting model system, the relationship between integration and disparity of its constituent developmental modules remains unstudied and unknown.

To address this gap in our understanding, we partition the primate pelvis girdle along its developmental constituent modules (see previous chapter H₁ hypothesis) to explore the impact of integration on primate pelvic module morphological disparity. We contrast our results with the expectations of the theoretical models – integration acting as a constraining or facilitating factor in shaping the disparity in primate pelvic morphology. Specifically, the constraining model (M₁) posits that integration acts as a constraint on morphological disparity, and is characterised by an inverse relationship in the distribution of integration versus the distribution of disparity whereby high levels of integration are paired with low levels of disparity and low levels of disparity with high levels of integration. Conversely, the facilitating model (M₂) predicts a direct relationship between integration and disparity distribution whereby high levels of integration correspond to high levels of morphological disparity and vice versa. In this scenario, the direction of selection and the correlated response align, resulting in an enhanced adaptive response. However, a third possibility must be considered where no discernible pattern exists between integration and disparity distribution. This could be due to several factors, including mixed alignments of selection and response of the modules. If so, this should be detectable within the results. It may also be that the pattern may exist but is not apparent because of sample constitution due to either sampling or extinction. Other conditions in which a no clear pattern may be established is when other constraining factors disrupt the signal of integration and/or disparity, or simply no discernible relationship exists in

the sampled data. By necessity, these models represent simplifications of complex biological processes and mechanisms, and as such do not capture fine-tuned nuances of the interplay between integration and disparity. Nevertheless, they provide a framework to test for the interaction between these factors.

Here, we assess integration and disparity in the morphology of the pelvis in the primate order and its constituent clades (Hominoidea – excluding humans, Lemuroidea, New and Old World monkeys) to detect possible differences in distribution patterns related to phylogenetic histories. We also evaluate integration and disparity magnitudes between groups of different locomotory behaviours. Studies focusing on limb integration found that the dissociation of fore and hind limb proportions, as seen in specialist forms of locomotion, are characterised by decreasing levels of integration and increased disparity of limb size and morphology (i.e. reduced constraint) compared to generalized quadrupeds (Young and Hallgrimson 2005, Rolian 2009, Young *et al.* 2010, Rolian 2019). If such a similar signal exists within the pelvis structure which plays an integral role in hindlimb locomotion remains to be determined.

Whilst the impact of integration on primate pelvic morphology is the central focus of our research, the role of allometry in influencing levels of integration is also of interest. The effects of allometry are hypothesised to act as an integrating factor as scaling necessitates coordination across modules. The increase of biomechanical forces placed upon large bodied organisms may be another factor contributing to the need for inherent cohesion (Klingenberg 2008, Shirai and Marroig 2010). Given the wide variety of body mass within our sampled taxa, ranging from 2.5 kg in *Eulemur fulvus rufus* to over 170 kg in male *Gorilla beringei* and *Gorilla gorilla* (Petter and Desbordes 2010), the integrating effects of allometry and their impact may be particularly relevant to our analyses.

3.3 Data

3.3.1 Osteological sample

The osteological sample consists of articulated primate pelvic structures as described in more detail in Chapter 2. The Lorisoidea outgroup (*Nyctcebus* and *Otolemur*) were removed due to small sample size. The dataset used in this chapter consist of 172 specimens as detailed in the supplementary information S1.

3.3.2 Primate locomotion

Primates represent one of the most diverse mammalian orders when it comes to the variety of locomotor specialisations, with taxa ranging from arboreal to terrestrial quadrupedalism, dramatic leaping, arm-swinging, knuckle-walking and more (Lewton 2010, Fleagle 2013, Gebo 2014) (table 3.1). These different modes of locomotion enable primates to access different parts and various types of habitats where the both the density and the positioning of suitable supports may be quite different (Fleagle 2013). With as many as 74 locomotory modes having been described, a simplification of the diverse and multi-modal ways primates move across a wide range of substrates is needed as a mean to classify primate locomotion. Following Fleagle (2013), Napier and Napier (1967), and Schultz (1969), we classify primates according their main mode of locomotion: arboreal quadrupedalism, terrestrial quadrupedalism, vertical clinging and leaping, trail prehensile suspension, suspension, and brachiation (table 3.1). In the latter group, we combine the true and modified brachiation in our data due to the small sample size of the true brachiation group within our study.

Primates may be divided into two broad groups based on limb ecomorphology: 1) a group of generalized arboreal and terrestrial quadrupeds which use all four limbs for locomotion in which the fore- and hindlimbs are approximately equal in length, and 2) a phylogenetically diverse group in which the unequal proportioned limb are associated with various specialized modes of locomotion (Fleagle 2013, Fleagle and Lieberman 2015, Rolian 2019). Vertical clinging and leaping species (e.g., galagos and lemurs) have longer hindlimbs relative to forelimbs, associated with improved locomotor performance when leaping between substrates (Legreneur *et al.* 2010). Suspensory and brachiating species, on the other hand, have longer fore- than hindlimbs, proposed to facilitate arm hanging, swinging, and knuckle/fist walking. Specialist are characterised by greater joint mobility

compared to the generalist. When it comes to body position, generalist share the horizontal (pronograde) body position whereas the specialist hold their body in a more vertical, upright (orthograde) position resulting in very different pelvic loading transmission regimes (e.g. see Bezanson 2017, Jenkins and Camazine 1977, Lewton 2015, Lycett and von Cramon-Taubadel 2013, Middleton *et al.* 2017, Schultz 1936, Ward *et al.* 2018).

The contrast between the generalist and specialist locomotory behaviours has been the topic of past integration and evolvability studies. Young (2010) found that that limb proportions of specialist primate species are characterised by lower integration compared to those of generalists. Yet Rolian (2019) proposes that when a primate species commits to a such a specialized type of locomotion, this results in a loss of evolvability within those species resulting in reduced ability to evolve toward alternative ecomorphologies including locomotory adaptations. Thus, locomotory (over)specialisation increases the probability of those primate species to go extinct before they may evolve new adaptive strategies (Rolian 2019). It is of interested to examine the pelvis and investigate if a similar/different signal can be observed.

<i>Locomotion/ body position</i>	<i>Sub-type locomotion</i>	<i>Activity description</i>	<i>Representative taxa included in this study</i>
Generalist/ Pronograde	Terrestrial quadrupedalism (TER)	Ground running	<i>Chlorocebus aethiops</i> <i>Erythrocebus patas</i> <i>Lophocebus albigena</i> <i>Lophocebus aterrimus</i> <i>Macaca fascicularis</i> <i>Macaca maura</i> <i>Macaca mulatta</i> <i>Macaca nemestrina</i> <i>Mandrillus sphinx</i> <i>Papio anubis</i> <i>Papio cynocephalus</i> <i>Papio hamadryas</i> <i>Semnopithecus entellus</i>
	Arboreal quadrupedalism (ARB)	Climbing, springing, branch running and jumping	<i>Cercocebus galeritus</i> <i>Cercopithecus ascanius</i> <i>Cercopithecus cephus</i> <i>Cercopithecus hamlyni</i> <i>Cercopithecus lhoesti</i> <i>Cercopithecus mitis</i> <i>Cercopithecus mona</i> <i>Cercopithecus neglectus</i> <i>Cercopithecus nictitans</i>
Specialist/ Orthograde	Vertical Clingers & Leapers (LEAP)	Leaping in trees and hopping on the ground	<i>Daubentonia madagascariensis</i> <i>Eulemur fulvus</i> <i>Indri indri</i> <i>Lemur catta</i> <i>Otolemur crassicaudatus</i> <i>Varecia variegata</i>
	New World Monkey Suspension (TPR)	Arm-swinging with use of prehensile tail	<i>Alouatta seniculus</i> <i>Ateles geoffroyi</i> <i>Ateles paniscus</i> <i>Cebus apella</i> <i>Cebus capucinus</i> <i>Lagothrix lagotricha</i>
	Old World Monkey Suspension (SUSP)	Arm-swinging and leaping	<i>Colobus guereza</i> <i>Colobus polykomos</i> <i>Piliocolobus badius</i> <i>Piliocolobus kirkii</i> <i>Presbytis comata</i> <i>Pygathrix nemaeus</i>
	True Brachiation (BRA)	Arm-swinging	<i>Hylobates lar capenteri</i> <i>Symphalangus syndactylus</i>
	Modified Brachiation (BRA)	Knuckle-walking and fist-walking	<i>Gorilla beringei</i> <i>Gorilla gorilla</i> <i>Pan paniscus</i> <i>Pan troglodytes</i> <i>Pongo pygmaeus</i>

Table 3.1. Primate Locomotion

3.3.3 Phylogeny

Phylogenetic relationships are important considerations when investigating patterns of morphological variation. As in Chapter 2, we use the 10KTrees Project primate consensus tree, version 3, commonly used in primate comparative studies (Arnold *et al.* 2010). Using Mesquite software (version 3.2), the tree was pruned to contain only taxonomic information relevant to the present study (S2) without further modifications.

3.3.4 Geometric Data

Geometric data collection follows the methodology outlined in Chapter 2. In summary, we obtained 153 landmarks and semi-landmarks representing the left and right halves of the primate pelvic girdle using the Landmark software package from the Institute of Data Analysis and Visualisation (Wiley 2005). Landmarks were placed on three dimensional (3D) models of each specimen. Models were created using photogrammetry (Agisoft Photoscan, version 1.3.3).

3.4 Analyses

3.4.1 Generalised Procrustes analysis

A Generalised Procrustes Analysis (GPA) was employed to superimpose the landmark configurations and remove non-shape aspects of the data. Prior to performing the Procrustes fit, missing landmarks were estimated using their bilateral counterparts using the *fixLMmirror* function and paired landmarks were symmetrized using the *Symmetrize* function, both in the R *Morpho* package (Schlagen 2017). The left and right sides of the primate pelvis girdle were included in the Procrustes fit to improve the accuracy of the alignment (Cardini 2016, 2017). The resulting Procrustes variables were orthogonally projected into their linear tangent space to obtain variables amenable to statistical analysis (Dryden and Mardia 1998, Baab *et al.* 2012, Zelditch *et al.* 2012). After performing the GPA procedure, the Procrustes coordinates and centroid size were averaged per species. The GPA procedure was performed using the *geomorph* package in R (Adams and

Otarola-Castillo 2013), and the resulting shape variables is hereafter referred to as *shape data*.

3.4.2 Exploratory analyses

We used principal component analysis (PCA) to identify the major shape variation across primate pelvises. Shape variation associated with the minimum and maximum values of the PC axes were visualised by warping a 3D surface of *Hylobates* onto those PC values using the *tps3d* function of the *Morpho* package (Schlager 2017).

Next, in accordance with the results of the Chapter 2 on modularity, landmarks associated with the individual H^1 modules - ilium, ischium, pubis, acetabulum, sacrum - were partitioned from within the global pelvis morphospace (i.e. the within configuration approach), as to preserve biological variation information due to relative size, position, and orientation of the modules and to reflect the biological reality that these modules form part of a larger structure: the pelvic girdle. Performing separate GPAs per module would lose this information (Dryden and Mardia 1998, Klingenberg 2009, Baab *et al.* 2012, Zelditch *et al.* 2012). The subsequent analyses used the landmarks characterising the left ilium, ischium, pubis, and acetabulum. For the sacrum, we used the left side and midline landmarks of this module.

To investigate the influence of evolutionary histories amongst the primate taxa included in the analysis, the morphometric data were tested to detect the presence of a phylogenetic signal – the tendency of related species to resemble each other more than non-related species. We employ a multivariate version of the Blomberg's K (K_{mult}), giving its appropriateness and stability for assessing high-dimensional multivariate data (Blomberg *et al.* 2003, Adams 2014a). K_{mult} estimates the strength of the phylogenetic signal relative to the expectation that variation accumulates at a rate proportional to time (evolutionary model of Brownian Motion). The function *physignal* (Adams 2014a) of the R *geomorph* package (Adams and Otárola-Castillo 2013) was used to estimate the degree of phylogenetic signal present in both the pelvis and individual module *shape data*. The observed phylogenetic signal $K_{(obs)}$ was evaluated statistically via permutation, during which data at the tips of the phylogeny are randomized relative to the tree, and the values of those randomisations $K_{(rand)}$ are compared to $K_{(obs)}$ (Blomberg *et al.* 2003, Dean 2014).

The randomisations were also used to calculate effect sizes to compare magnitudes of the detected phylogenetic signals across the investigated modules.

Whilst the process of Procrustes superimposition removes isometric size, it does not remove the effects that size has upon shape: allometry (Gould 1966). The impact of allometry/evolutionary allometry on shape was assessed by regression using the functions *procD.lm* and *procD.pgls* respectively (Adams and Otárola-Castillo 2013, Adams 2014b, Adams and Collyer 2015, 2017). Logged pelvis centroid size was used as a proxy for size. Residuals of these regression were taken forward as allometric-corrected data, hereafter referred to as *allo data*, to assess the potential role allometry plays in expressed integration magnitudes and morphological disparity of the investigated primate species. Regressions were also used to analyse the potential impact of locomotion and clade association on pelvis shape, with and without taking the effects of allometry into account (i.e. we run the latter regressions both on *shape* and *allo data*).

3.4.3 Module Integration analyses

To calculate comparable magnitudes of integration of the modules, we first created a trait correlation matrix for each module and each data set (Goswami and Polly 2010a). We first used the *dotcorr* function of the *Paleomorph* package (Lucas and Goswami 2017) to calculate the 3D vector correlation matrix using the congruence coefficient. The congruence coefficient is a derivative of the product moment correlation coefficient and is designed to calculate correlations amongst multidimensional variables, thus appropriate for 3D geometric morphometric data (Goswami and Polly 2010a). The congruence coefficient is the sum of the covariances between all pairs of multidimensional variables over all the specimens in the dataset, divided by its pooled variance (Abdi 2007). We then employed the two most commonly used integration methods – estimated product-moment correlation coefficient (*MaxL ρ*) and relative eigenvalue dispersion (*VE_{SD}*), both implemented in R (R Core Team 2017).

Method 1: Estimated product-moment correlation coefficient (MaxL ρ)

The method of Pearson product-moment correlation was used to measure the degree of morphological integration within the pelvis and its modules: ilium, ischium, pubis, acetabulum, and sacrum. We employed the *EMMLi* function of the *EMMLi* (Evaluating

Modularity with Maximum likelihood) package (Goswami and Finarelli 2016) to estimate the product-moment correlation coefficient. Since the Pearson product-moment correlation method assumes normal data distribution, a Fisher Z- transformation is applied to the correlation matrix during this procedure to ensure normal distribution and Pearson product-moment correlation assumptions are met (Dytham 2011, Goswami and Finarelli 2016). This transformed correlation matrix is then treated as a set of realizations (the values of r) of a hypothesized true correlation coefficient (ρ). The maximum log-likelihood of the hypothesized value of ρ , given an observed value of r , is used as magnitude of integration indicator ($MaxL \rho$). All pairs from the off-diagonal lower triangle of the correlation matrix were included, and the $MaxL \rho$ for each module is reported. The $MaxL \rho$ results range from 0 to 1 with 0 representing no correlation and 1 signifying complete integration.

Method 2: relative eigenvalue dispersion (VE_{SD})

Eigenvalue dispersion was computed following procedures set out by Pavlicev *et al.* (2009), using the *llsde* function (Habar 2011). Obtained values encapsulate the combined effects of eigenvalue variance, which scales linearly with mean correlation, and the standard deviation which scales with the average level of correlation (for a full overview of the relative eigenvalue dispersion method see Pavlicev *et al.* 2009). Obtained VE_{SD} values range from 0 to 1, and are directly comparable across different datasets. Higher eigenvalue dispersals indicate higher magnitudes of integration as higher values reflect smaller numbers of eigenvectors needed to capture a larger proportion of total correlated shape variation.

To test the equivalence of these methods, we calculated integration magnitudes for both methods for the whole primate order on the *shape*, *PIC*, and *allo data* sets.

3.4.4 Module morphological disparity analyses

We used Procrustes variance (Pv) as a measure to quantify morphological disparity (MD). Pv is calculated as the sum of the diagonal elements of the covariance matrix divided by the number of observations of the data set (Zelditch *et al.* 2012), thus taking sample size into account. Significance of the absolute differences in Pv between the clades and between the locomotory groups was assessed in a pairwise manner through 1000

permutations, where the vectors of residuals were randomized among groups. Calculations were made using the *morphol.disparity* function of the *geomorph* package (Adams and Otárola-Castillo 2013).

3.4.5 Relationship between integration and morphological disparity

Results of the integration and morphological disparity analyses were paired to measure the strength and direction of the association between integration and disparity distributions using Spearman's rank correlation. Here, the correlation coefficient falls on a scale of -1 (perfect inverse relationship), to 0 (dissimilarity), to +1 (perfect direct relationship). The correlation coefficient enables us to compare obtained results to the model predictions of constraint (inverse relationship), facilitating model (direct relationship), or neither (dissimilarity). Integration and disparity distributions were plotted to visualize the relationship between these two factors.

3.5 Results

3.5.1 Morphological variation and influencing factors.

Results of the principal component analysis illustrate the variation present within primate pelvic girdle shape (figs 3.1-3.4). PC 1 – PC3, and PC1 – PC15 captured 68.44% and 95% respectively of primate pelvis shape variation in morphospace. PC1 captures 39.70% of shape variation. Variation along PC1 mainly reflects morphological variation of the ilium blade: mediolateral flaring amongst Hominoidea versus the narrower iliac planes present within the non-Hominoidea taxa. The negative values of the axis also represent a relative decrease in sacrum width, and a relative shortened and flattened pubis symphysis compared to the extreme positive end of the first PC. PC1 predominantly contrasts shape variation of large-bodied hominoids at the negative end, whilst smaller bodied monkeys and lemurs occupy a morphospace at the centre and positive end of PC1. The regression of size (pelvis log(centroid)) on PC1 confirms that the correlation between shape and size is high for PC1: 72.76% ($F = 116.92, p = .001$). Within Hominoidea, *Hylobates lar*'s position is the closest to other non-Hominoidea primate taxa in the morphospace (fig. 3.3 - 3.4).

PC2 and PC3, representing 17.32% and 11.42% of shape variation respectively, structure variation predominantly in the non-Hominoidea groups. Positive values of PC2 describe a pelvic shape characterised by relatively highly positioned sacra, thinner medially oriented ischia and long caudal pubic rami, while negative values of PC2 represent a relatively deeper sacral position, broader laterally projected ischia, and short pubic rami. The main factor structuring PC3 relates to the differentiation of Lemuroidea from the other primates. Lemuroidea's typical flaring iliac crest and curved blades are described by the negative values of PC3 whilst rounder iliac crests and straighter ilia blades represent the positive end of the scale(fig.3.3 - 3.4).

Visual inspection of the PCA plots suggests that variation in the primate pelvis is influenced by evolutionary history (fig 3.3 - 3.4). This phylogenetic structuring of the primate pelvis morphologies is also visually evident in the phylomorphospace plots provided in figure 3.1 and 3.2. The phylogenetic signal test confirms these observations: there is a detectable phylogenetic signal within the *shape data*: $K_{\text{mult}} 0.4057, p = .001$, effect size: 9.827 (table 3.3). Our findings are complementary with those of Lycett and Cramon-Traubel (2013), who recovered a significant phylogenetic signal when

reconstructing a neighbour cluster phenogram based on primate pelvis morphology. Furthermore, analyses by Martin-Serra *et al.* (2014) revealed that the carnivore pelvis carried higher levels of phylogenetic signal than other bones of the appendicular skeleton, which may equally be the case for primates.

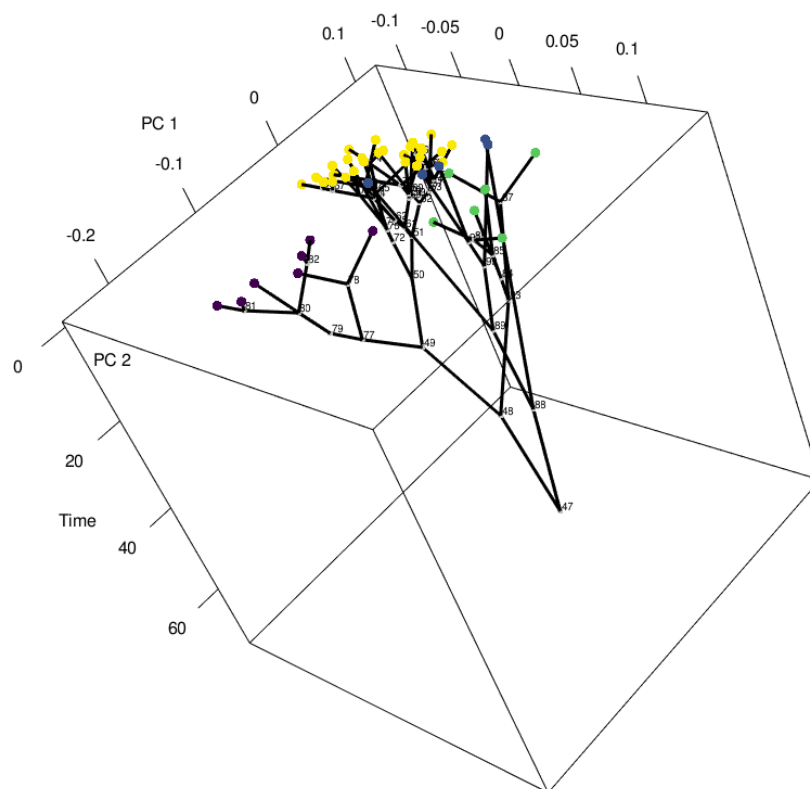


Fig 3.1. Phylomorphospace of *shape data* variation along the PC1- PC2- time axes.

Time axis represents millions of years. Colours represent the following primate groups: purple = Hominoidea, blue = Lemuroidea, green = New World monkeys (Ceboidea), yellow = Old World monkeys (Cercopithecoidea).

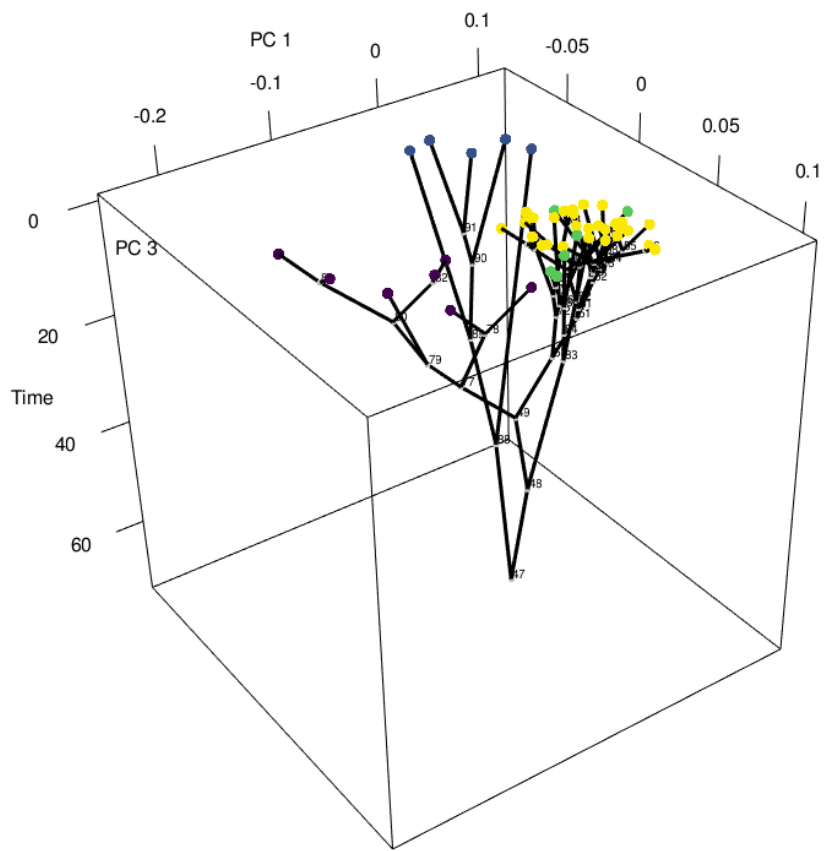


Fig 3.2. Phylomorphospace of *shape data* variation along the PC1- PC3- time axes.

Time axis represent millions of years. Colours represent the following primate groups: purple Hominoidea, blue = Lemuroidea, green = Ceboidea (New World monkeys), yellow = Old World monkeys (Cercopithecoidea).

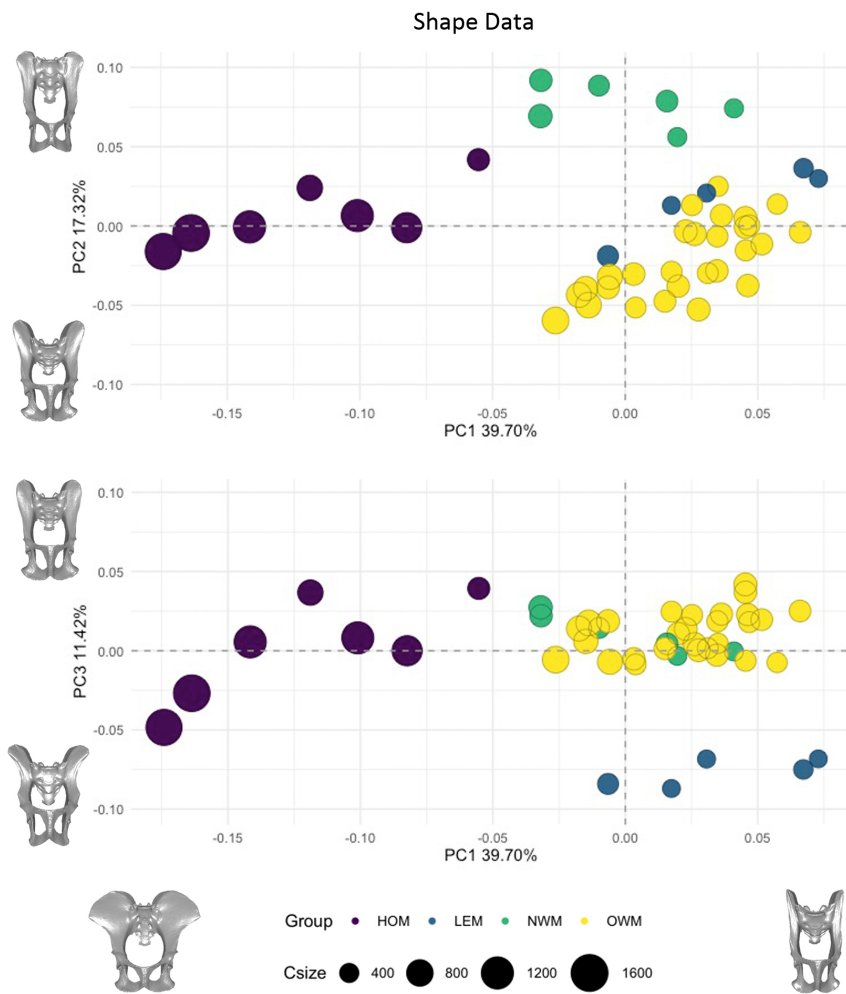


Fig 3.3. Morphospace of *shape data* variation along the PC1- PC3 axes by clade

HOM =Hominoidea, *LEM* = Lemuroidea, *NWM* = Ceboidea (New World monkeys), *OWM*= Cercopithecoidea (Old Word monkeys). Differences in plot point size correspond to differences in primate taxa centroid size

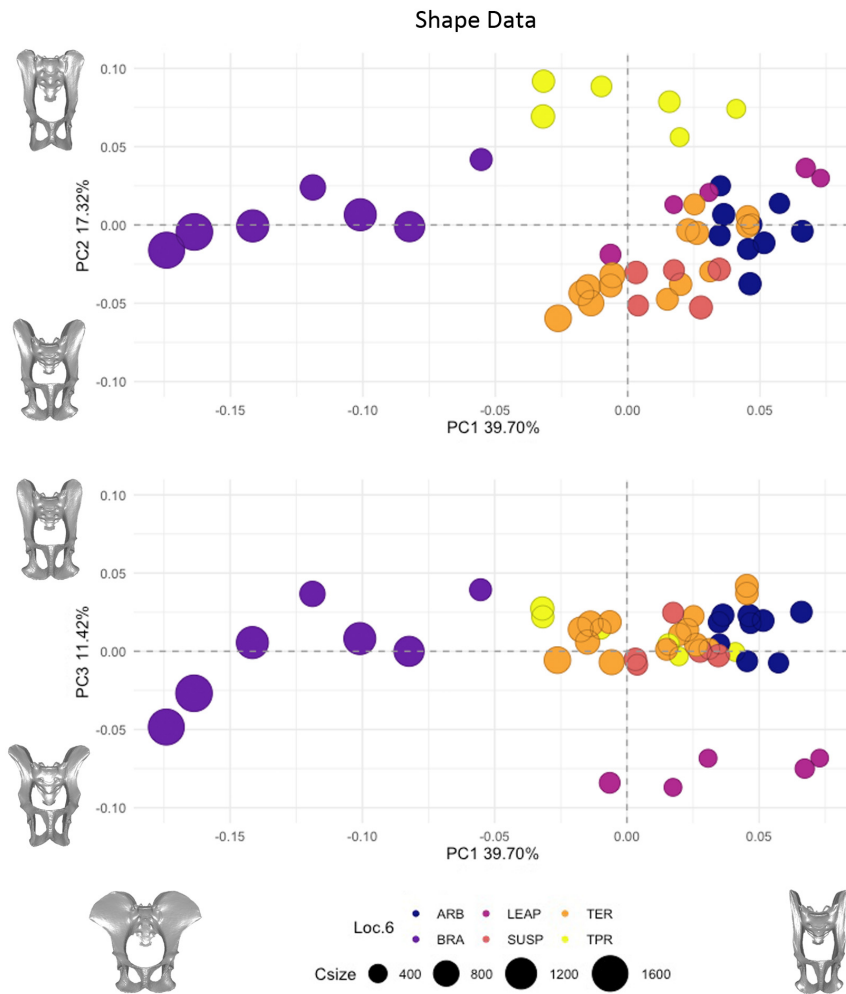


Fig 3.4. Morphospace of *shape data* variation along the PC1- PC3 axes by locomotion

ARB = arboreal, *BRA*= brachiation, *LEAP* = leaping, *SUSP* = Old World Monkey Suspensory, *TER*= terrestrial, *TPR*= Tail prehensility suspensory locomotion. Differences in plot point size correspond to differences in primate taxa centroid size.

The results of the linear and multiple linear regression (table 3.2) indicated that 30.85% ($p < .001$) of primate pelvis shape is predicted by size, 59.02% ($p < .001$) by locomotory group (but reduced to 6.12% after accounting for allometry), and 53.16% by phylogenetic group association, reduced to 30.70% after similarities due to allometry are taken into account. When phylogenetic context is taken into account within the regressions, both locomotion ($z = -0.329$) and clades ($z = -0.927$) lose their predictive power and become non-statistically significant ($p = .708$ and $p = .834$ respectively). Only allometry continues to play a part: $z = 4.673$ ($p < .001$).

Whilst the influence of allometry, clade and locomotion on the module morphologies are variable across the pelvic girdle modules (table 3.2), the results from the linear regression reveal the large extent to which all modules are predominantly defined by locomotion and clade association, and this remains the case even after allometry is taken into account, except for the ilium where allometry itself carries a greater predictive power than allometric-corrected clade and locomotory association. However, as we observed with the overall pelvic shape, when phylogeny is considered, the predictive power of clade and locomotion disappears and even allometric impact on ischium and pubis becomes statically non-significant. K_{mult} phylogenetic signal tests quantitatively confirm that variation in module morphology is impacted by their ancestral histories. The K_{mult} effect sizes (z) indicate that this is most prevalent in ischium and pubis morphologies.

	Allo	Clade	Loc	Allo*	Clade*	Loc*	Clade**	Loc**
Pelvis	0.3085	0.5316	0.5902	4.673	-0.927	-0.329	0.3070	0.0612
Il	0.4417	0.5500	0.6144	4.801	-0.026	1.048	0.2287	0.2696
Is	0.2043	0.4698	0.5432	1.848	-1.8310	-2.386	0.3112	0.3687
Pu	0.1030	0.5326	0.5640	0.689	-0.457	-0.554	0.4690	0.4872
Ac	0.2473	0.4790	0.5200	2.479	-1.204	-1.717	0.2784	0.3087
Sa	0.1282	0.5982	0.6388	1.538	0.476	-0.168	0.5107	0.5372

Table 3.2. Overview analyses influencing factors.

*Il=Ilium, Is= ischium, Pu=Pubis, Ac= Acetabulum, Sa= Sacrum; * denotes phylogenetic regression (procD.pgls function) and Z value is reported, in all other instances values are reported in R^2 ; ** denotes clade and locomotion variable after allometry has been taken into account. Italic values indicate non-statistical significance at p 0.001.*

	K_{mult}	$K_{mult} p$	$K_{mult} Z$
Pelvis	0.4057	.001	9.827
Il	0.3969	.001	6.749
Is	0.4175	.001	10.846
Pu	0.4139	.001	9.720
Ac	0.4098	.001	8.658
Sa	0.4101	.001	7.196

Table 3.3. Overview influence phylogenetic signal.

Il=Ilium, Is= ischium, Pu=Pubis, Ac= Acetabulum, Sa= Sacrum.

3.5.2 Module Integration

The results of *MaxL* ρ analyses for primate order pelvic modules (fig. 3.5, table 3.4) for *shape*, *PIC*, and *allo* data demonstrate that integration levels of the modules are highly variable, ranking in *shape* data from low (ilium: 0.390), to moderate (ischium: 0.490, pubis: 0.570, sacrum: 0.650) to high (acetabulum: 0.850). The influences of phylogeny and allometry are also variable, as indicated by the percentage difference of *shape* with *PIC* and *allo data* integration levels: ilium (-%5, -3%), ischium (+2%, -4%), pubis (-5%, +2%), acetabulum (-2%, -4%), and sacrum (-8%, +3%). The absence of equivalent tests in other integration studies, however, limits our assessment of the observed integration differences between the different data sets.

The primate VE_{SD} results confirm the *MaxL* ρ findings, although some differences exist between the two methods: VE_{SD} slightly increases the low values (ilium) and reduces the high values (acetabulum) comparatively to *MaxL* ρ integration distribution. Other modules obtained a mix of minor lower and higher values. Yet despite these differences, similar integration trends are revealed by the two methods as table 3.4 and figure 3.6 demonstrate, and for our study the VE_{SD} validates the *MaxL* ρ findings.

Results of the *shape data* integration levels across the clades (table 3.5, fig. 3.6) reveal that each clade has similar integration distribution, even though some variability can be observed. Lemuroidea (LEM) group associate with the highest registered level of integration for the ilium, the New World monkey (NWM) group for the ischium, pubis, and acetabulum, and Hominoidea (HOM) in the sacrum. Conversely, the acetabulum aside, the Old World monkey (OWM) group obtain the lowest levels of module integration. To ensure this is not an artefact of this group being more numerously sampled, we randomly re-sampled the OWM species and re-run the analyses with $n=10$. The same results were obtained for the resampled OWM data (table 3.5), demonstrating that this integration signal is present within the OWM group and confirms the stability of the used methods. We obtained a similar pattern when examining the *allo data* and can in most cases note a minor reduction in integration levels (table 3.5, fig. 3.6). The Hominoidea sacrum stands out, where a reduction of 15% is observed compared to the *shape data* integration value.

Continuing with the locomotory groups (table fig 3.7), the results indicate that the locomotory groups have variable integration distributions whilst adhering to the overall integration pattern seen in the primate order: from low in the ilium, to moderate in the ischium, pubis and sacrum, to high in the acetabulum. The brachiation (BRA) group equates to the Hominoidea where due to sample size true and modified brachiation are combined. This may affect the integration values for this locomotory group. Clingers and leapers (LEAP) phylogenetically cluster in the Lemuroidea, whereas New World monkeys display a specific type of suspensory locomotion, here represented by the TPR group. We do gain more information about the OWM clade group which is represented in this study by three different types of locomotion: arboreal (ARB), suspensory (SUSP), and terrestrial locomotion (TER). The results indicate that the arboreal, suspensory, and terrestrial locomotory groups display each higher levels of integration compared to the overall OWM clade group in which these monkeys reside. The only exception to this observation is the acetabulum of the terrestrial locomotory group, which obtains an integration value of 0.860 compared to 0.870 of the OWM group. The low OWM integration values thus may be due to the different locomotory behaviours represented within this clade.

The arboreal and terrestrial groups are generalised quadrupeds in which fore- and hindlimb are approximately equal in lengths, whereas the brachiation, vertical clingers and leapers, suspensory and tail prehensile locomotory species all exhibit greater variations in limbs proportions and are associated with specialized forms of locomotion (Fleagle 1999) (see table 3.1). Previous studies (Young 2010) demonstrate that limbs of specialist primate species are characterised by lower integration between limb modules (tested modules: humerus, radius, metacarpal – femur, tibia, and metatarsal) compared to those of generalists. The noted lower integration is posited to have decreased constraints and facilitated the more independent evolution of the fore- and hind limbs morphologies and functionality. For the pelvis modules, however, we observe that the arboreal and terrestrial groups obtain relative low integrations levels compared to the specialist groups. We also find a similar signal for the between module integration levels (tables S4.1- S4.4) whereby the arboreal and particularly the terrestrial locomotory group obtained low if not the lowest between integration values. This is likely an effect of the

more upright (orthograde) posture of specialists, resulting in increased biomechanical loading on the pelvis and its constituent modules (Fleagle 2013). If so, this offers an alternative explanation for the relatively lower integration values amongst the OWM clade since this group is predominantly associated with quadrupedalism, the generalist form of locomotion. The integration levels calculated from *allo data* demonstrate that allometry plays a variable contributing factor, with the ilium of the brachiation group displaying the greatest allometric influence.

Overall, the integration analyses reveal: 1) integration levels of the modules are highly variable, ranging from low (ilium), to moderate (ischium, pubis, sacrum) to high (acetabulum); 2) similar distribution of integration magnitudes exist across all data sets and groups, and 3) allometry seems to play a minor but variable role in the realised integration magnitudes. The largest integrating effects of allometry is associated with the hominoid/brachiation sacrum (9%).

<i>Primates</i>	<i>MaxL ρ</i>					<i>VE_{SD}</i>				
	Il	Is	Pu	Ac	Sa	Il	Is	Pu	Ac	Sa
Shape	0.390	0.490	0.570	0.860	0.650	0.420	0.500	0.590	0.840	0.590
PIC	0.340	0.510	0.520	0.840	0.570	0.390	0.520	0.550	0.820	0.550
Allo	0.360	0.450	0.590	0.820	0.680	0.400	0.470	0.600	0.790	0.610

Table 3.4. Primate integration magnitudes: *MaxL ρ* and *VE_{SD}*

<i>MaxL ρ</i>	<i>Shape Data Clades</i>					<i>Allo Data Clades</i>				
	Il	Is	Pu	Ac	Sa	Il	Is	Pu	Ac	Sa
HOM	0.430	0.550	0.630	0.820	0.790	0.410	0.550	0.600	0.840	0.660
LEM	0.480	0.610	0.590	0.740	0.650	0.480	0.600	0.590	0.780	0.600
NWM	0.450	0.620	0.770	0.900	0.720	0.400	0.580	0.740	0.910	0.740
OWM	0.390	0.440	0.500	0.870	0.530	0.370	0.450	0.510	0.850	0.530
OWM*	0.390	0.440	0.500	0.870	0.530	0.370	0.450	0.510	0.850	0.530

Table 3.5. Clade integration magnitudes

HOM = Hominoidea, LEM = Lemuroidea, NWM = New World monkeys (Ceboidea), OWM= Old World monkeys (Cercopithecoidea).

<i>MaxL ρ</i>	<i>Shape Data Locomotion</i>					<i>Allo Data Locomotion</i>				
	Il	Is	Pu	Ac	Sa	Il	Is	Pu	Ac	Sa
ARB	0.400	0.540	0.650	0.890	0.650	0.430	0.540	0.650	0.880	0.640
BRA	0.430	0.550	0.630	0.820	0.790	0.420	0.550	0.600	0.850	0.680
LEAP	0.480	0.610	0.590	0.740	0.650	0.480	0.590	0.590	0.780	0.610
SUSP	0.390	0.540	0.630	0.910	0.650	0.370	0.550	0.640	0.910	0.630
TER	0.400	0.510	0.520	0.860	0.670	0.390	0.510	0.530	0.850	0.670
TPR	0.450	0.620	0.770	0.900	0.720	0.400	0.580	0.740	0.910	0.740

Table 3.6. Locomotion integration magnitudes

ARB = arboreal, BRA= brachiation, LEAP = leaping, SUSP = Old World Monkey Suspensory, TER= terrestrial, TPR= Tail prehensility suspensory locomotion.

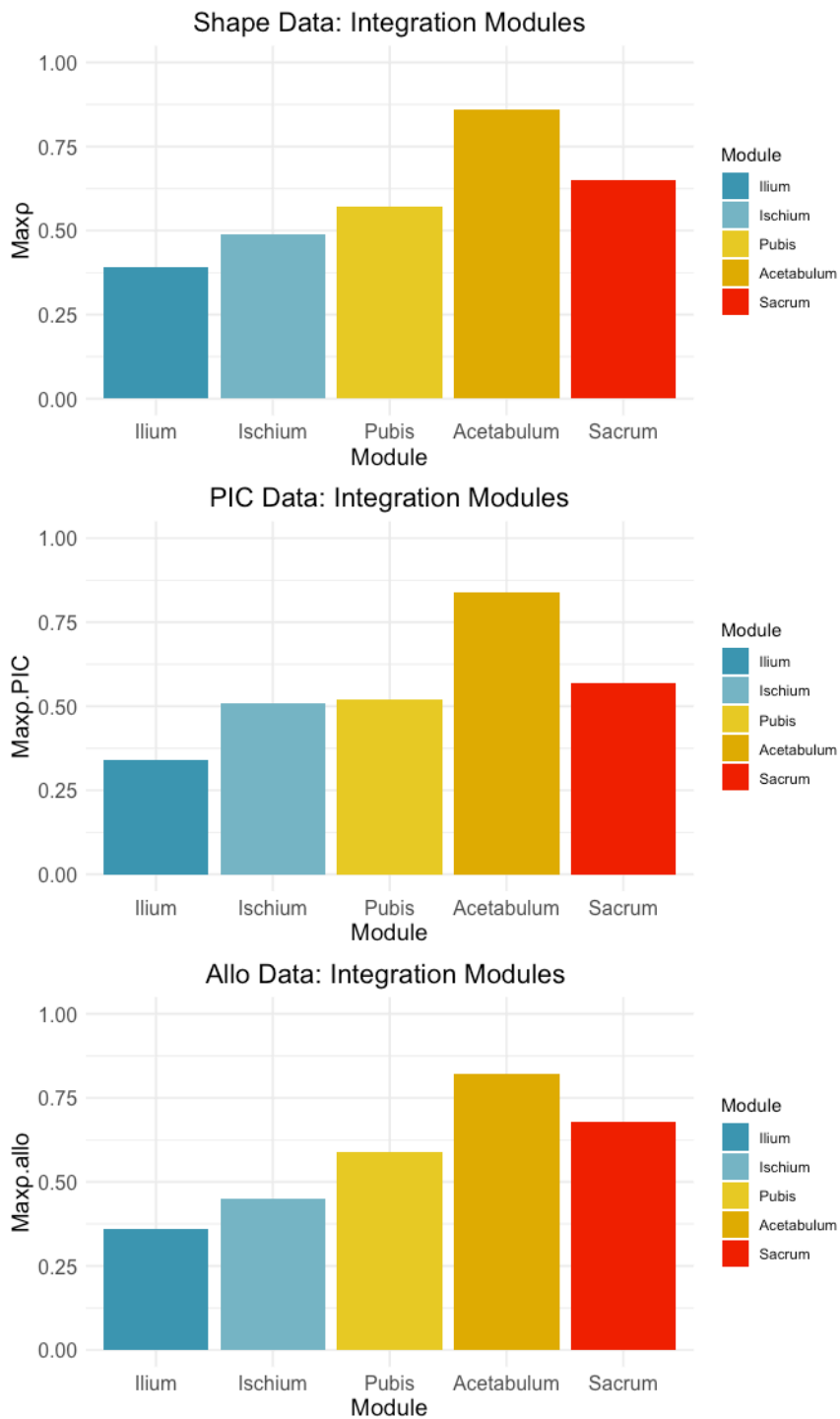


Fig 3.5. Primate module integration

Top: *shape data*; middle: *PIC data*; bottom: *allo data*

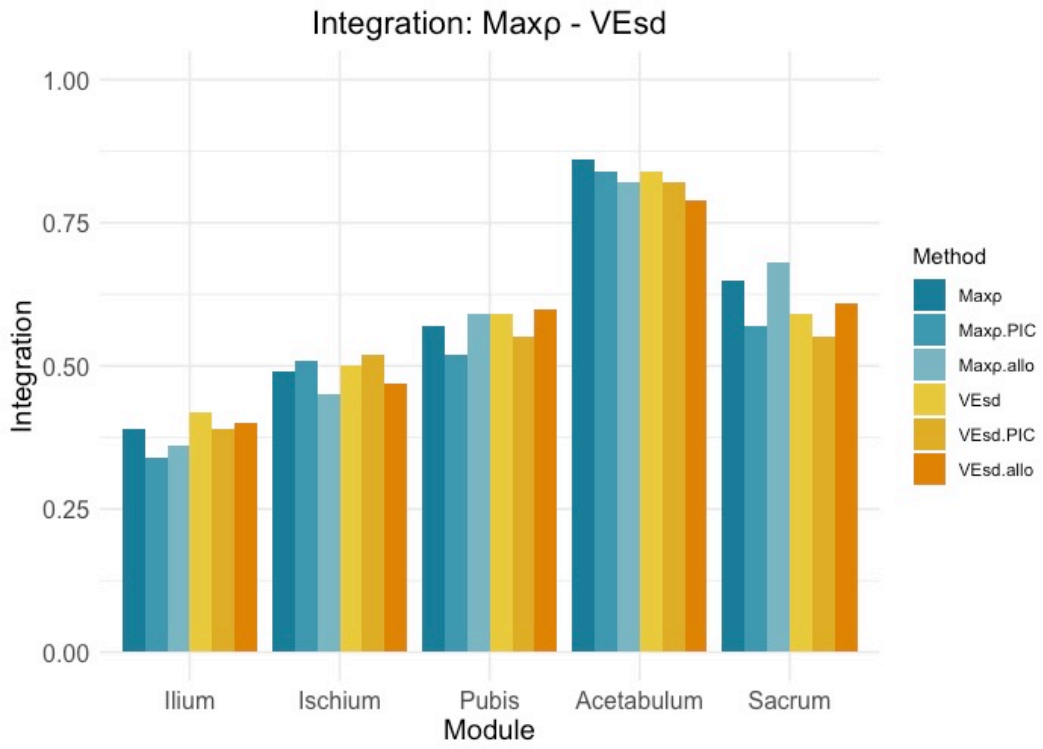


Fig 3.6. Primate module integration: $R_{MaxL} \rho - VE_{SD}$ method comparison

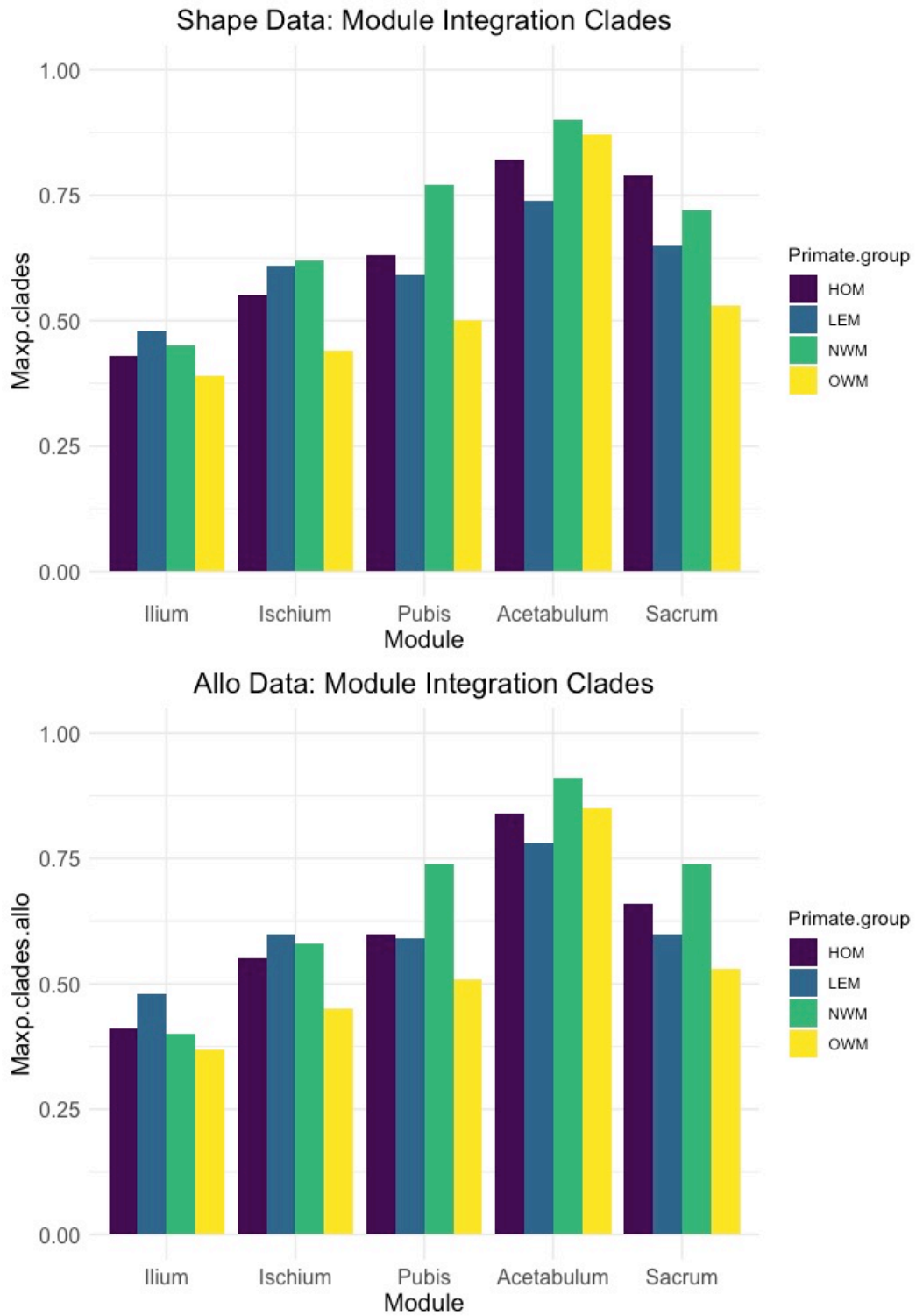


Fig 3.7. Clade module integration

Top: shape data; bottom: allo data. HOM =Hominoidea, LEM = Lemuroidea, NWM = New World monkeys (Ceboidea), OWM= Old World monkeys (Cercopithecoidea)

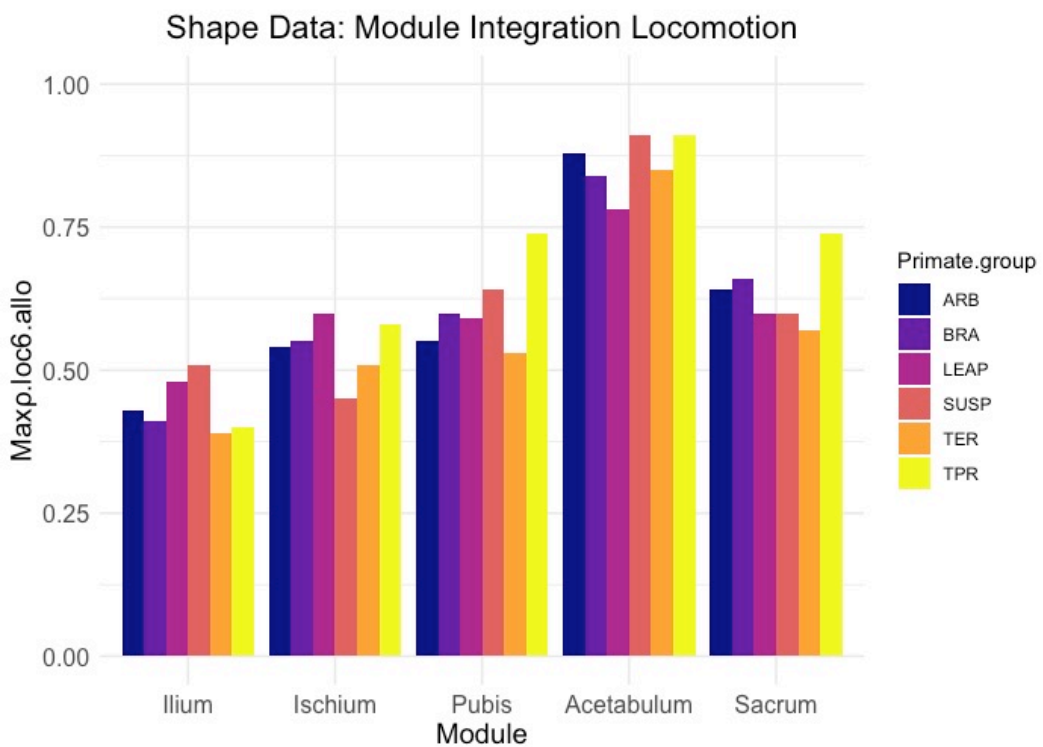
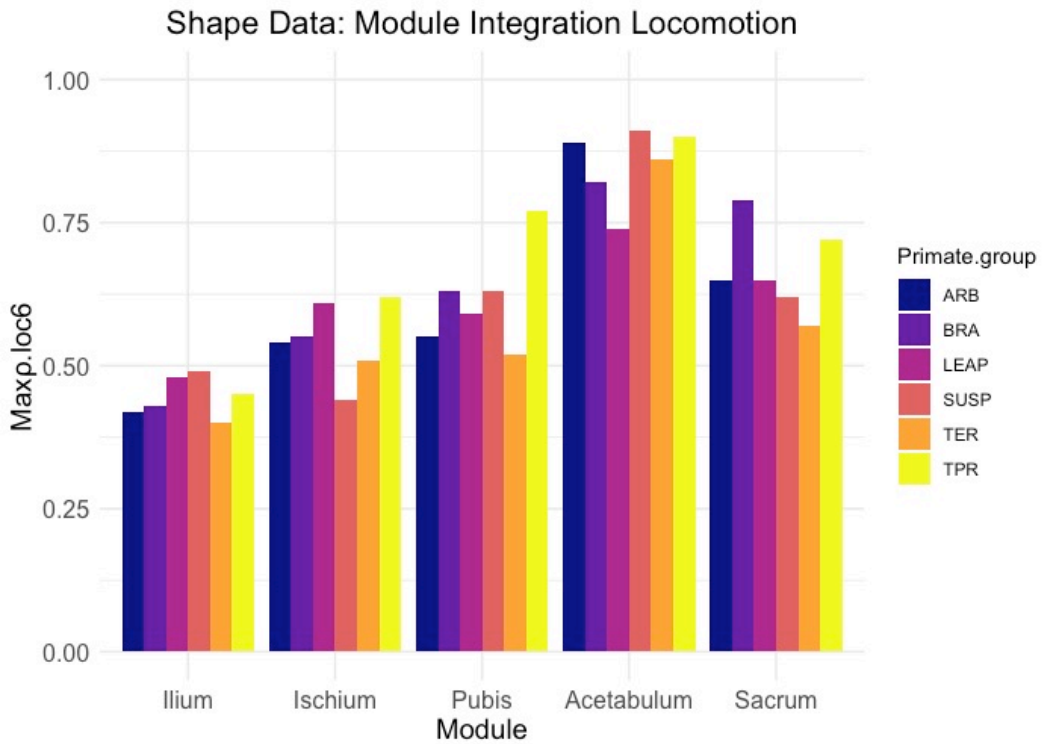


Fig 3.8. Locomotion module integration

Top: shape data; bottom: allo data. ARB = arboreal, BRA= brachiation, LEAP = leaping, SUSP = Old World Monkey Suspensory, TER= terrestrial, TPR= Tail prehensility suspensory locomotion.

3.5.3 Morphological disparity

Morphological disparity, reported here as the Procrustes Variance ($Pv \times 10^5$) for each module of the primate pelvis, reveals variance ranging in *shape data* from high (ilium: 21.513) to moderate (ischium: 9.351, and sacrum: 7.903) to low (pubis: 4.173, and acetabulum: 3.191) (table 3.7, fig 3.9). Similar patterns are detected when the effects of phylogeny and allometry are taken into account, albeit with a notable absolute and relative reduction of primate ilium disparity (PIC ilium: 17.082, -20.60%; *allo* ilium: 13.245 -37.83%) (table 3.7, fig. 3.9). Results of the clade and locomotion group disparity analyses demonstrate that ilium reduction is largely driven by the brachiating Hominoidea (table 3.8 – 3.9, fig. 3.10 – 3.11). The large difference in ilium disparity between *shape* and *allo data* demonstrate the extent to which allometry plays a role in ilium morphology diversification. Allometry also plays a role in increasing ischium and acetabulum morphology disparity albeit to a smaller extent (table 3.4). Conversely, pubis and sacrum disparity increase after the impact of allometry is considered, indicating that these two modules are under allometric morphological constraint. These results highlight the variable role allometry plays in pelvic morphological disparity. Similarly, we observe a variable yet different pattern in relation to phylogenetic influence on morphological disparity: if the role of allometry appears relatively limited for the primate pubis and sacrum modules, phylogenetic relatedness does play a larger extent in the morphological disparity for these two modules (table 3.7, fig 3.9).

Pairwise clade tests (table 3.10) reveal that the hominoid ilium morphology is significantly more variable than the New and Old World monkey groups ($p = 0.001$ and $p = 0.004$ respectively), although these differences become statistically not significant once allometry is taken into account (table 3.11). We note a similar observation for the locomotory groups (table 3.12), whereby the ilium of the brachiation group is significantly more variable compared to all other locomotory groups. When the allometric influence is considered, the pairwise absolute difference between the arboreal and the brachiating groups remains significant, in addition to the arboreal and leaping groups becoming significant (table 3.13).

Statistical clade differences in disparity also exist between the sacrum variability of the two monkey groups ($p = 0.002$) (table 3.10). The locomotory groups data in table 3.12

informs us that these differences are difference exist in the three locomotory groups which comprise the Old World monkey clade (arboreal, suspensory and terrestrial locomotory groups) compared to the tail prehensile suspensory mode of locomotion exhibited by the New World monkey clade. Once the data is corrected for allometry, sacrum disparity remains significant between the two monkey whilst the differences between Old World monkeys and Hominoidea also become statistically importance (tables 3.10-3.11). For the locomotory groups, sacrum disparity for the arboreal and tail prehensile modes of locomotion remains significantly different. Significant differences between the arboreal and brachiating group are now also noted. Interestingly, we also observe in our locomotory *allo data* a significant difference in morphological disparity between the ischium of the brachiating Hominoidea and the Old World monkey suspensory locomotory behaviour. In all other instances, differences in disparity amongst clades and locomotory groups were not statistically significant.

MD	<i>Primates (Pv x10⁵)</i>				
	Il	Is	Pu	Ac	Sa
<i>Shape</i>	21.513	9.351	4.173	3.191	7.903
<i>PIC</i>	17.082	9.755	3.383	3.344	6.031
<i>Allo</i>	13.370	8.108	4.358	2.401	7.713

Table 3.7. Primate module disparity: Pv values

MD	<i>Shape data (Pv x10⁵)</i>					<i>Allo Data (Pv x10⁵)</i>				
	Il	Is	Pu	Ac	Sa	Il	Is	Pu	Ac	Sa
Clades										
All	21.513	9.351	4.173	3.191	7.903	13.370	8.108	4.358	2.401	7.713
HOM	18.537	6.139	2.818	2.333	4.444	10.389	6.650	1.952	2.122	5.299
LEM	11.866	5.678	2.532	1.804	2.528	10.167	5.529	2.671	2.011	2.469
NWM	5.709	4.634	2.255	1.805	5.997	4.625	4.033	2.086	2.055	5.405
OWM	7.926	4.604	1.564	1.439	2.392	6.326	4.053	1.466	1.227	1.959

Table 3.8. Clade module disparity: Pv values

HOM = Hominoidea, LEM = Lemuroidea, NWM = New World monkeys (Ceboidea), OWM = Old World monkeys (Cercopithecoidea); Gen = Generalist, Spe = Specialist locomotion

MD	<i>Shape data (Pv x10⁵)</i>					<i>Allo Data (Pv x10⁵)</i>				
	Il	Is	Pu	Ac	Sa	Il	Is	Pu	Ac	Sa
Loc										
ARB	3.452	3.794	0.935	1.303	1.542	4.116	3.558	0.968	1.183	1.466
BRA	18.537	6.139	2.818	2.333	4.444	10.389	6.65	1.952	2.122	5.299
LEAP	11.866	5.678	2.532	1.804	2.528	10.167	5.529	2.671	2.011	2.469
SUSP	3.439	1.211	1.357	1.105	1.501	4.421	1.355	1.256	1.054	1.511
TER	7.859	4.081	1.614	1.215	2.157	5.86	3.674	1.583	1.059	1.774
TPR	5.709	4.634	2.255	1.805	5.997	4.625	4.033	2.086	2.055	5.405

Table 3.9. Locomotion module disparity: Pv values

ARB = arboreal, BRA= brachiation, LEAP = leaping, SUSP = Old World Monkey Suspensory, TER= terrestrial, TPR= Tail prehensility suspensory locomotion.

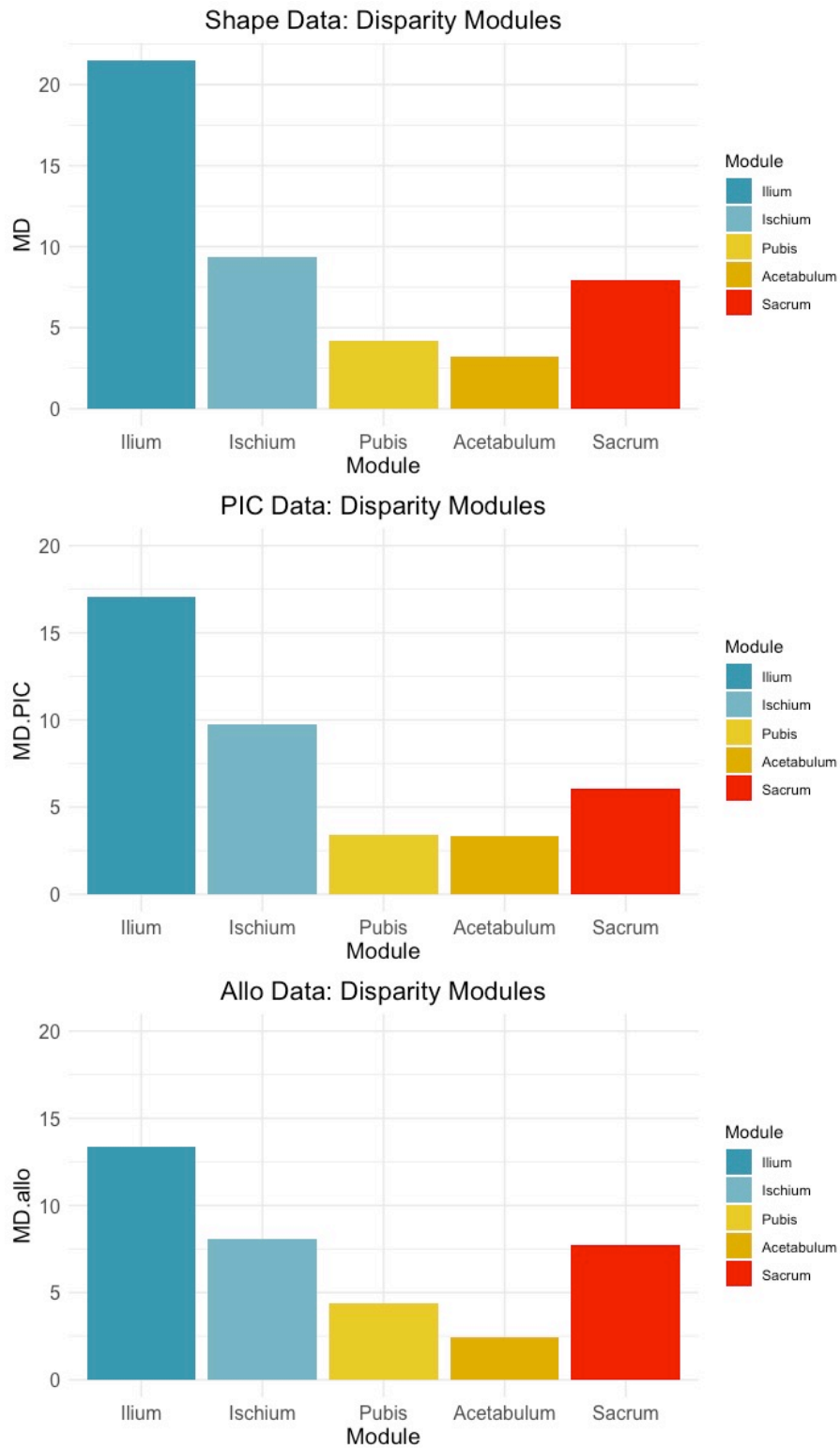


Fig 3.9. Primate module disparity

top: shape data; bottom: allo data

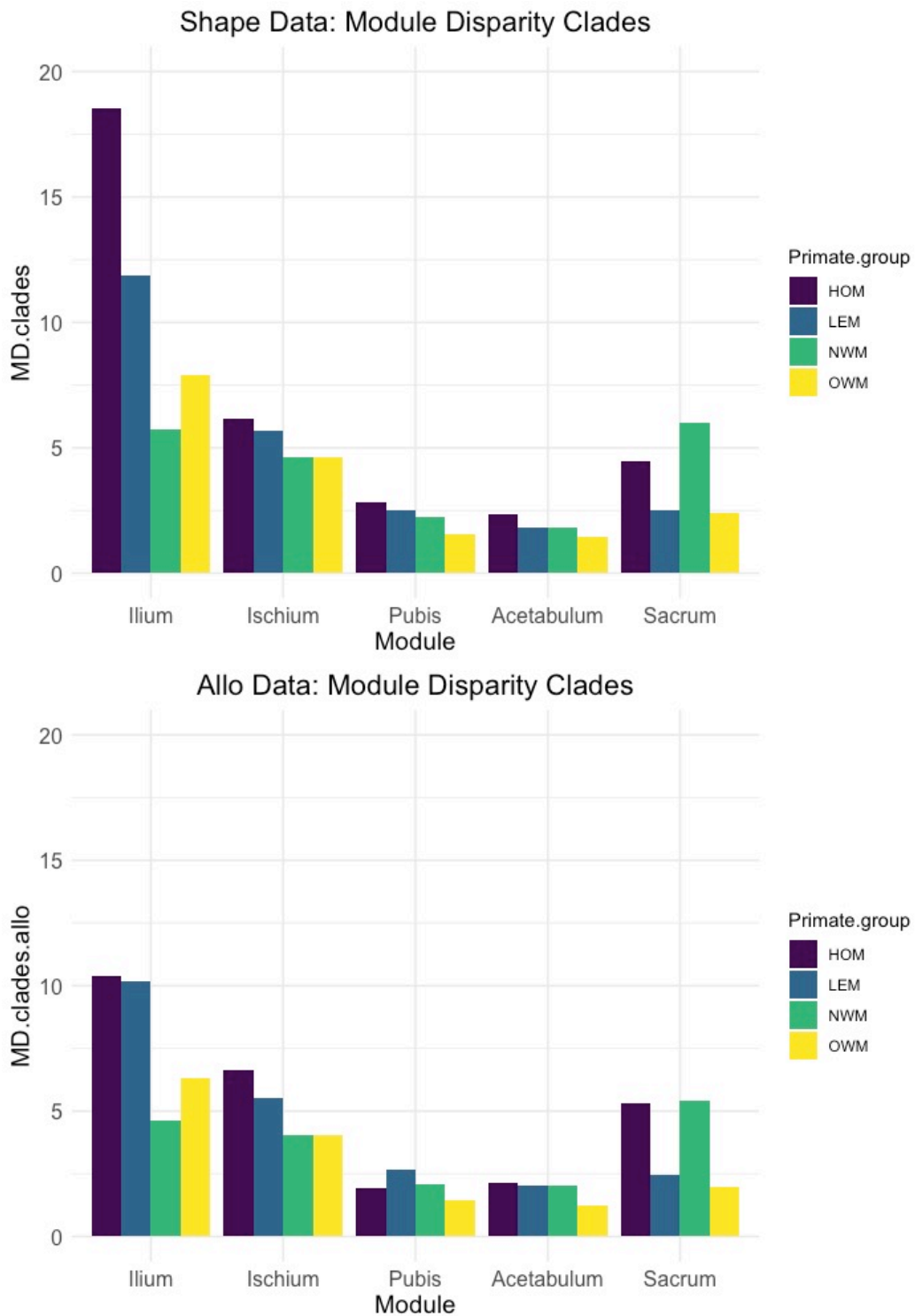


Fig 3.10. Clade module disparity

Top: shape data; bottom: allo data. HOM = Hominoidea, LEM = Lemuroidea, NWM = New World monkeys (Ceboidea), OWM = Old World monkeys (Cercopithecoidea).

<i>Shape data</i>		HOM	LEM	NWM	OWM
Il	HOM		0.147	0.001	0.004
	LEM	6.671		0.166	0.290
	NWM	12.827	6.157		0.530
	OWM	10.610	3.940	2.217	
Is	HOM		0.792	0.362	0.241
	LEM	0.461		0.589	0.474
	NWM	1.505	1.044		0.989
	OWM	1.534	1.073	0.029	
Pu	HOM		0.741	0.480	0.033
	LEM	0.285		0.766	0.151
	NWM	0.563	0.278		0.284
	OWM	1.253	0.968	0.690	
Ac	HOM		0.494	0.440	0.084
	LEM	0.529		0.998	0.573
	NWM	0.527	0.001		0.553
	OWM	0.894	0.365	0.366	
Sa	HOM		0.160	0.227	0.039
	LEM	1.917		0.015	0.907
	NWM	1.553	3.470		0.002
	OWM	2.052	0.136	3.606	

Table 3.10. *Shape data*: pairwise absolute differences of clade disparity and p-values

Il = ilium, *Is* = ischium, *Pu* = pubis, *Ac* = acetabulum, *Sa* = sacrum. *HOM* = Hominoidea, *LEM* = Lemuroidea, *NWM* = New World monkeys (*Ceboidea*), *OWM* = Old World monkeys (*Cercopithecoidea*). Bold values indicate $p \leq 0.005$

<i>Allo data</i>		HOM	LEM	NWM	OWM
Il	HOM		0.926	0.006	0.018
	LEM	0.222		0.021	0.033
	NWM	5.764	5.542		0.344
	OWM	4.062	3.841	1.701	
Is	HOM		0.514	0.123	0.038
	LEM	1.120		0.401	0.295
	NWM	2.617	1.497		0.983
	OWM	2.597	1.477	0.020	
Pu	HOM		0.304	0.836	0.343
	LEM	0.719		0.431	0.042
	NWM	0.134	0.585		0.274
	OWM	0.486	1.205	0.620	
Ac	HOM		0.863	0.915	0.044
	LEM	0.111		0.949	0.150
	NWM	0.067	0.044		0.094
	OWM	0.895	0.784	0.828	
Sa	HOM		0.042	0.932	0.004
	LEM	2.830		0.043	0.673
	NWM	0.106	2.936		0.005
	OWM	3.339	0.509	3.445	

Table 3.11. *Allo data*: pairwise absolute differences of phylogenetic group disparity and p-values.

Il = ilium, *Is* = ischium, *Pu* = pubis, *Ac* = acetabulum, *Sa* = sacrum. *HOM* = Hominoidea, *LEM* = Lemuroidea, *NWM* = New World monkeys (Ceboidea), *OWM* = Old World monkeys (Cercopithecoidea). Bold values indicate $p \leq 0.005$

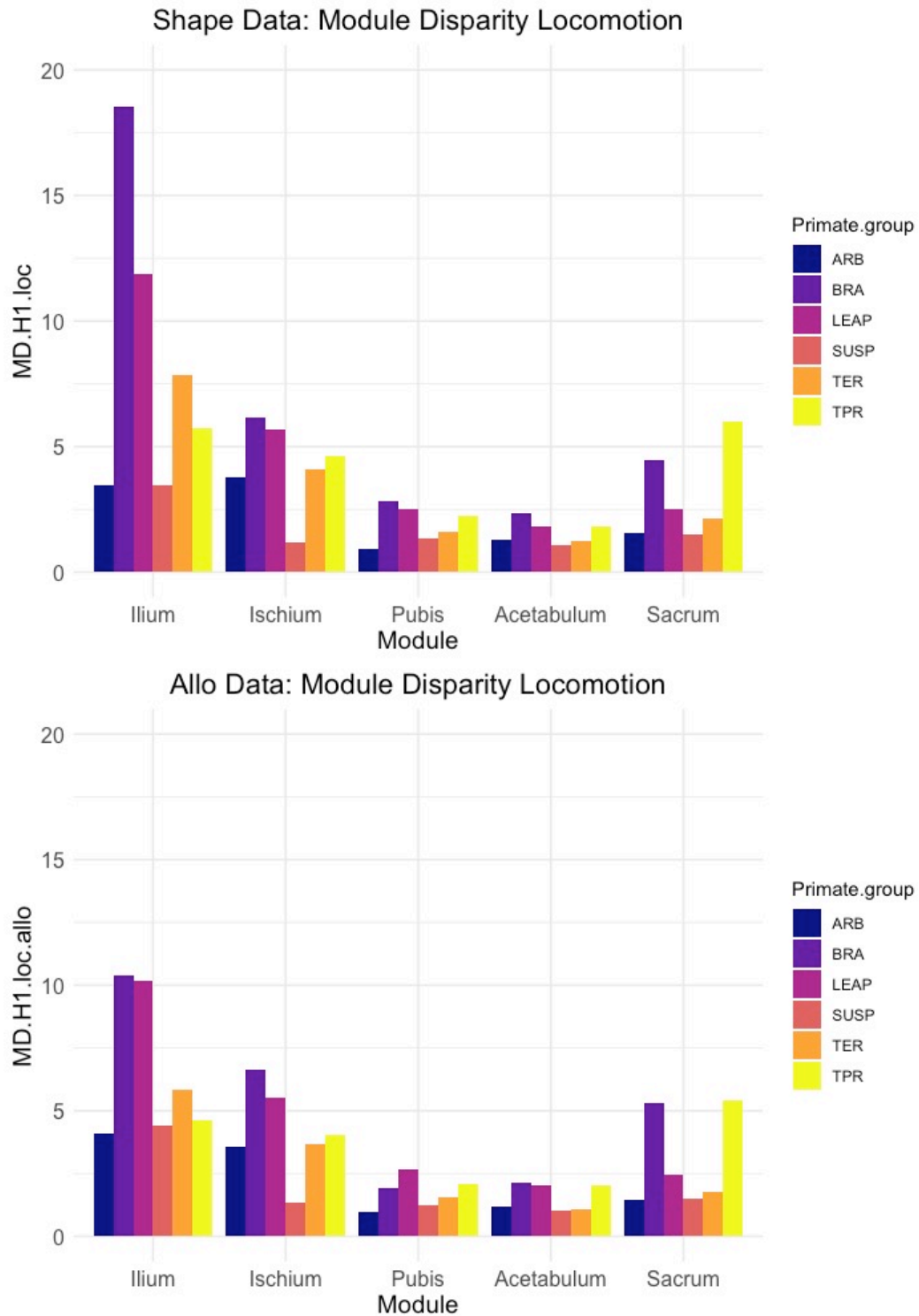


Fig 3.11. Locomotion module disparity

Top: shape data; bottom: allo data. ARB = arboreal, BRA= brachiation, LEAP = leaping, SUSP = Old World Monkey Suspensory, TER= terrestrial, TPR= Tail prehensility suspensory locomotion.

<i>Shape data</i>		ARB	BRA	LEAP	SUSP	TER	TPR
Il	ARB		0.001	0.044	0.997	0.183	0.592
	BRA	15.085		0.161	0.003	0.004	0.003
	LEAP	8.414	6.671		0.096	0.339	0.189
	SUSP	0.013	15.098	8.427	1.000	0.316	0.629
	TER	4.407	10.678	4.007	4.420		0.586
	TPR	2.258	12.827	6.157	2.270	2.150	
Is	ARB		0.107	0.223	0.118	0.808	0.565
	BRA	2.344		0.785	0.008	0.141	0.314
	LEAP	1.883	0.461		0.022	0.295	0.548
	SUSP	2.583	4.928	4.466		0.067	0.051
	TER	0.286	2.058	1.597	2.870		0.687
	TPR	0.839	1.505	1.044	3.423	0.553	
Pu	ARB		0.007	0.033	0.619	0.256	0.078
	BRA	1.883		0.724	0.092	0.074	0.523
	LEAP	1.598	0.285		0.223	0.237	0.758
	SUSP	0.422	1.460	1.175		0.764	0.327
	TER	0.679	1.204	0.919	0.256		0.394
	TPR	1.320	0.563	0.278	0.898	0.641	
Ac	ARB		0.057	0.428	0.745	0.848	0.418
	BRA	1.030		0.442	0.070	0.034	0.403
	LEAP	0.501	0.529		0.367	0.348	0.996
	SUSP	0.198	1.228	0.699		0.870	0.326
	TER	0.088	1.117	0.589	0.110		0.298
	TPR	0.502	0.527	0.001	0.700	0.590	
Sa	ARB		0.017	0.450	0.979	0.568	0.001
	BRA	2.902		0.165	0.035	0.051	0.240
	LEAP	0.985	1.917		0.500	0.769	0.020
	SUSP	0.041	2.943	1.027		0.606	0.004
	TER	0.614	2.288	0.371	0.656		0.002
	TPR	4.455	1.553	3.470	4.497	3.841	

Table 3.12. *Shape data*: pairwise absolute differences of locomotory group disparity and p-values

Il = ilium, *Is* = ischium, *Pu* = pubis, *Ac* = acetabulum, *Sa* = sacrum, *ARB* = arboreal, *BRA* = brachiation, *LEAP* = leaping, *SUSP* = Old World Monkey Suspensory, *TER* = terrestrial, *TPR* = Tail prehensility suspensory locomotion.

<i>Allo data</i>		ARB	BRA	LEAP	SUSP	TER	TPR
Il	ARB		0.001	0.005	0.883	0.309	0.797
	BRA	6.272		0.926	0.010	0.009	0.006
	LEAP	6.051	0.222		0.010	0.026	0.015
	SUSP	0.304	5.968	5.746		0.473	0.938
	TER	1.743	4.529	4.307	1.439		0.479
	TPR	0.509	5.764	5.542	0.204	1.235	
Is	ARB		0.031	0.213	0.200	0.922	0.755
	BRA	3.091		0.510	0.003	0.035	0.125
	LEAP	1.971	1.120		0.033	0.241	0.409
	SUSP	2.203	5.295	4.174		0.152	0.157
	TER	0.116	2.976	1.855	2.319		0.812
	TPR	0.474	2.617	1.497	2.678	0.359	
Pu	ARB		0.114	0.011	0.683	0.230	0.083
	BRA	0.984		0.328	0.362	0.512	0.846
	LEAP	1.703	0.719		0.096	0.114	0.462
	SUSP	0.288	0.697	1.415		0.648	0.306
	TER	0.615	0.369	1.088	0.328		0.440
	TPR	1.118	0.134	0.585	0.831	0.503	
Ac	ARB		0.073	0.157	0.799	0.799	0.126
	BRA	0.939		0.852	0.099	0.033	0.917
	LEAP	0.828	0.111		0.188	0.096	0.943
	SUSP	0.129	1.068	0.957		0.996	0.120
	TER	0.124	1.063	0.952	0.005		0.057
	TPR	0.872	0.067	0.044	1.000	0.996	
Sa	ARB		0.005	0.448	0.971	0.791	0.005
	BRA	3.833		0.050	0.007	0.006	0.946
	LEAP	1.003	2.830		0.536	0.601	0.050
	SUSP	0.046	3.788	0.958		0.844	0.009
	TER	0.309	3.524	0.694	0.263		0.006
	TPR	3.939	0.106	2.936	3.894	3.630	

Table 3.13. *Allo data*: pairwise absolute differences of locomotory group disparity and p-values

Il = ilium, *Is*= ischium, *Pu* = pubis, *Ac*= acetabulum, *Sa*=sacrum, *ARB* = arboreal, *BRA*= brachiation, *LEAP* = leaping, *SUSP* = Old World Monkey Suspensory, *TER*= terrestrial, *TPR*= Tail prehensility suspensory locomotion.

3.5.4 Relationship between integration and morphological disparity

Our results indicate that integration and disparity relate broadly in an inverse way (table 3.14). This trend is observable for the primate order as whole (fig. 3.12, table 3.14), the clades (fig. 3.13, table 3.14), and the locomotory groups (fig. 3.14, table 3.14), and this is equally true across all data sets. The presence of this inverse relationship is in accordance with predictions of the M_1 constraining model, indicative of integration acting as a constraining mechanism on adaptive responses.

A few other interesting points are of note. The morphological disparity of the pubis is low compared to that of the ischium and sacrum despite containing similar levels of integration. Conversely, variability in the breadth of the pubis is not too dissimilar to the variability of the acetabulum, which contains a higher level of integration. This remains the case when the effects of allometry are considered. The low pubis disparity could also be a sign of high occurrence of convergent evolution. If so, as suggested by the ‘fly in the tube’ model (Felice *et al.* 2018), we can expect the evolutionary tempo of the pubis to be higher relative to its morphological disparity since similar shapes occupy the same area of morphospace. In such scenarios, integration limits the area of morphospace in which species evolve but not the tempo at which they move around this preferred region of morphospace.

To test this idea, we post-hoc calculated the evolutionary tempo of the primate pelvic constituents using the *compare.evol.rates* function (Adams 2014c) in *geomorph* package (Adams and Otárola-Castillo 2013). The results indicate that the evolutionary tempo of the pubis is very low, even lower than the acetabulum with the latter containing a much higher level of integration (fig. 3.15). Convergent evolution is thus not a likely contributing factor to the low morphological disparity. The pubis, therefore, has another, here unidentified factor constraining morphological disparity. The functional demands related to obstetrics may play a part, necessitating coordination beyond the boundary of the pubis module and thus influencing pubis disparity. The obstetric explanation will, however, require further study. Conversely, ilium phenotypes have a broader than expected amount of disparity in relation to their level of integration. However, this is partly the effect of allometry acting as a facilitating factor for this module, and particularly notable in the large-bodied brachiating Hominoidea group.

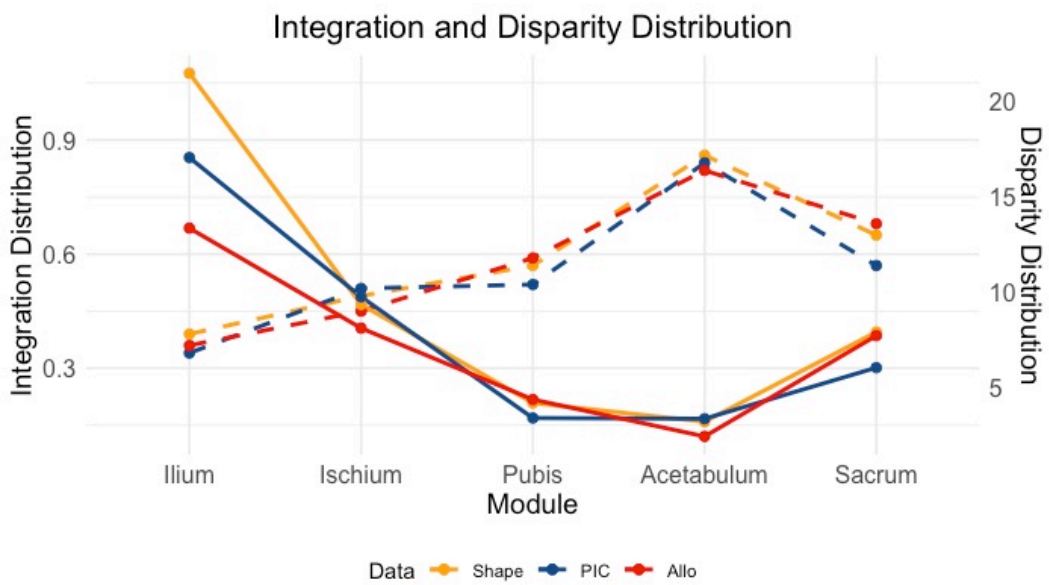


Fig 3.12. Primate integration and morphological disparity distribution patterns

Dashed lines illustrate the MaxL ρ integration values on the left y-axis (Integration Distribution) whilst full lines represent the Pv values plotted according the right y-axis (Disparity Distribution).

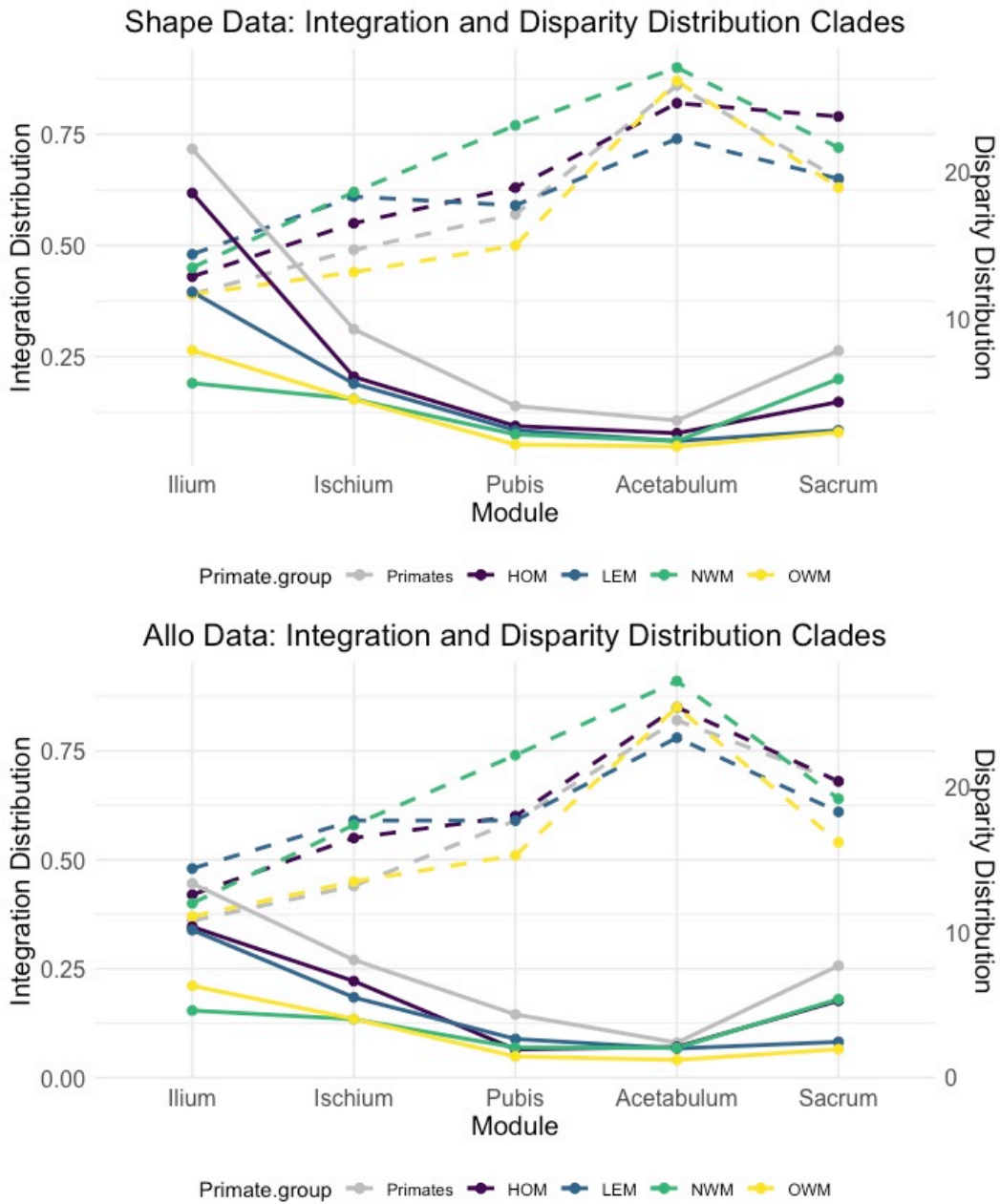


Fig 3.13. Clade integration and morphological disparity distribution patterns

Dashed lines illustrate the $MaxL \rho$ integration values on the left y-axis (Integration Distribution) whilst full lines represent the P_v values plotted according the right y-axis (Disparity Distribution). Primates = Primate order, HOM = Hominoidea, LEM = Lemuroidea, NWM = New World monkeys (Ceboidea), OWM = Old World monkeys (Cercopithecoidea).

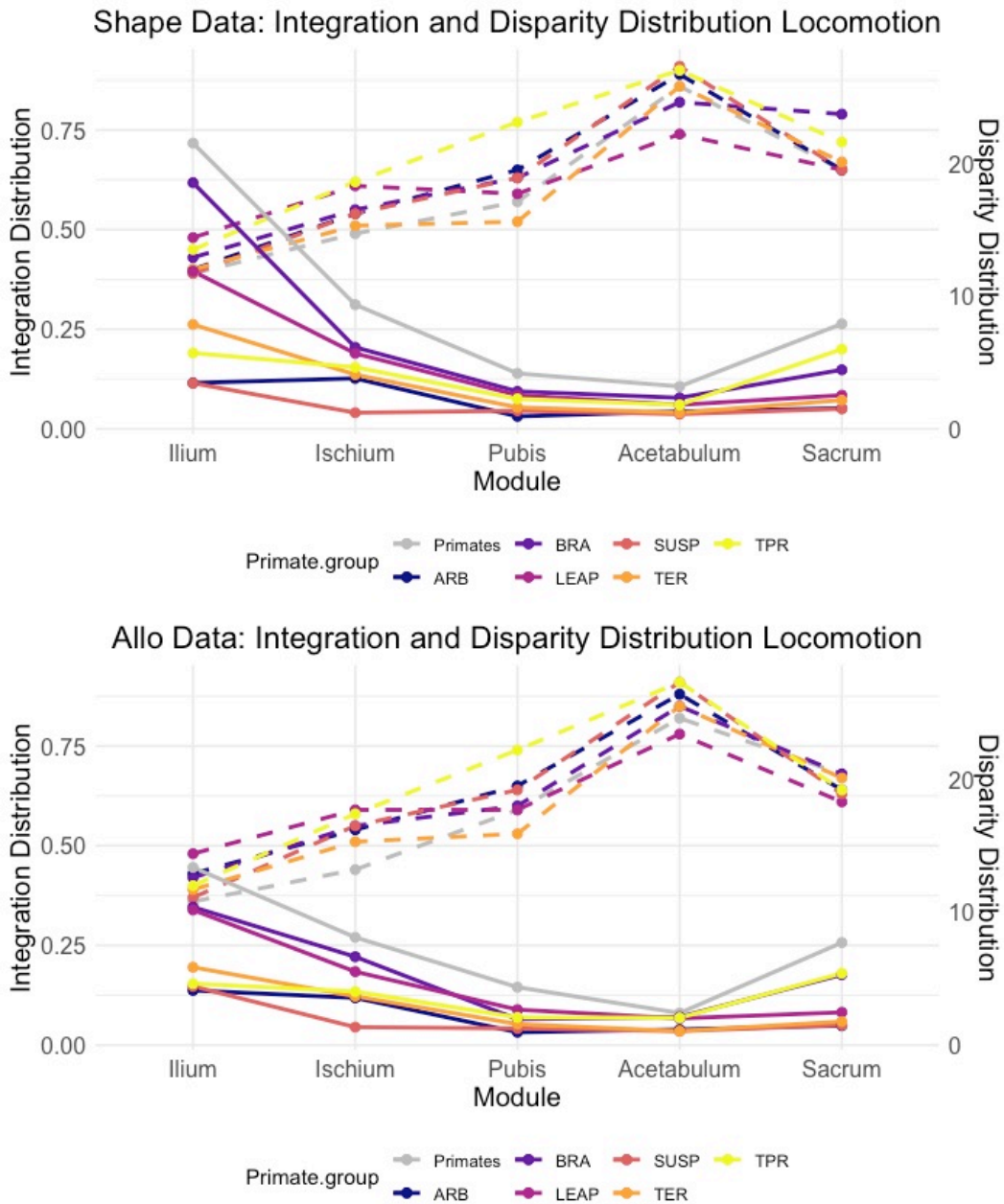


Fig 3.14. Integration and morphological disparity distribution patterns locomotion

Dashed lines illustrate the $MaxL p$ integration values on the left y-axis (Integration Distribution) whilst full lines represent the Pv values plotted according to the right y-axis (Disparity Distribution). Primates = primate order, ARB = arboreal, BRA= brachiation, LEAP = leaping, SUSP = Old World Monkey Suspensory, TER= terrestrial, TPR= Tail prehensility suspensory locomotion.

<i>r (MaxL ρ – Pv)</i>	<i>Shape Data</i>	<i>Allo Data</i>
Primates	-0.7813	-0.8517
HOM	-0.8035	-0.7952
LEM	-0.8573	-0.7744
NWM	-0.7584	-0.7364
OWM	-0.7069	-0.7345
ARB	-0.7416	-0.8099
BRA	-0.8035	-0.7952
LEAP	-0.8573	-0.7779
SUSP	-0.7363	-0.7744
TER	-0.7537	-0.8198
TPR	-0.7584	-0.7364

Table 3.14. Correlation coefficient between integration (*MaxL ρ*) and morphological disparity (*Pv*)

Primates = Primate order, HOM = Hominoidea, LEM = Lemuroidea, NWM = New World monkeys (Ceboidea), OWM = Old World monkeys (Cercopithecoidea), ARB = arboreal, BRA= brachiation, LEAP = leaping, SUSP = Old World Monkey Suspensory, TER= terrestrial, TPR= Tail prehensility suspensory locomotion.

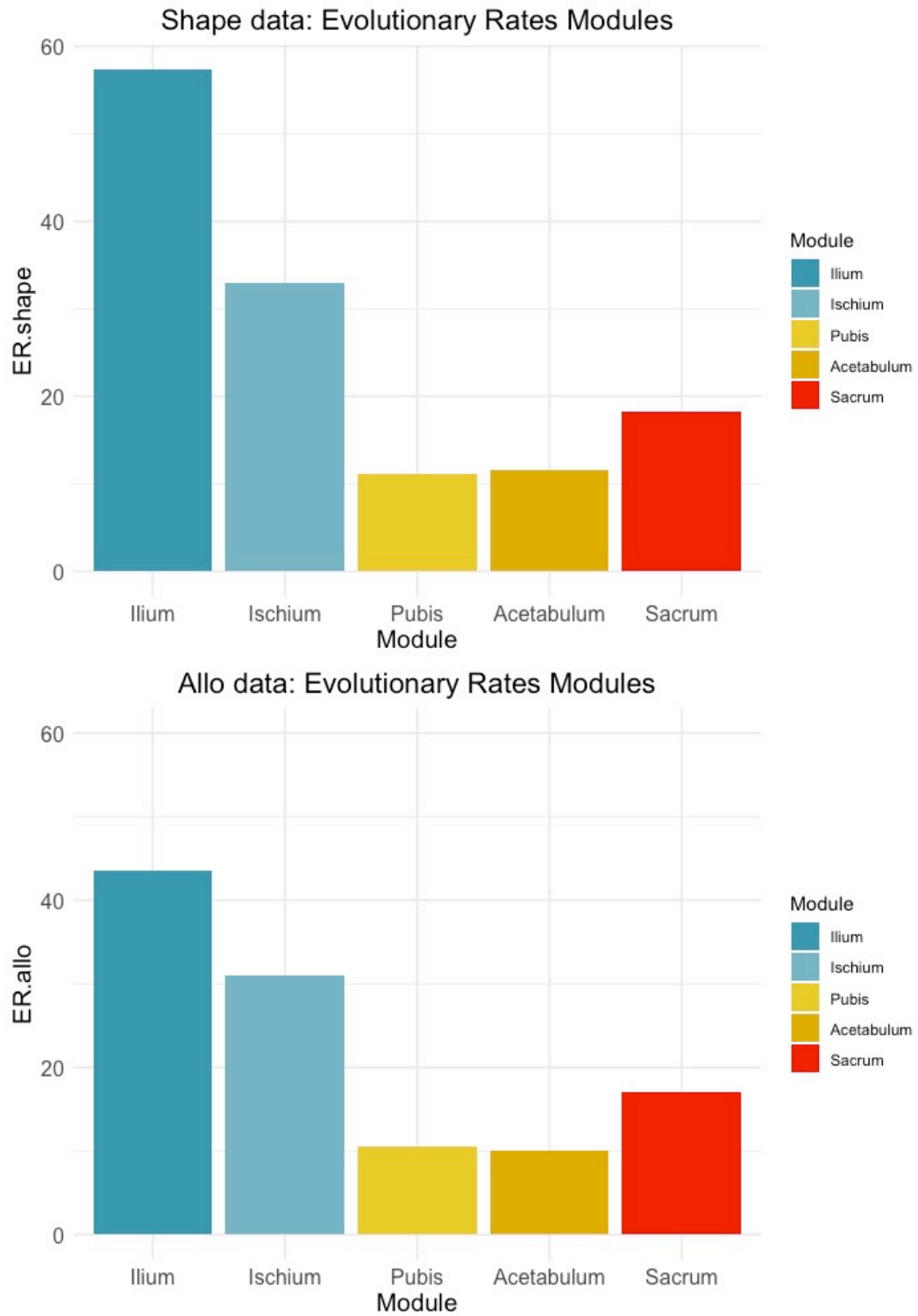


Fig 3.15. Primate evolutionary rates of modules

Top: shape data; bottom: allo data.

3.6 Discussion

Here, we have analysed the magnitudes of integration and disparity for the primate order, and for its phylogenetic and locomotion groups. Based upon the results of the previous modularity chapter, the pelvis was divided into its constituent modules: ilium, ischium, pubis, acetabulum and sacrum. The results demonstrate that there is significant variation in the magnitude of integration of the different modules, ranking from low (ilium), to moderate (ischium, pubis, sacrum), to high (acetabulum). This pattern of integration is present across all data sets, indicative that it is conserved across primates and its groups. The effects of allometry on integration are variable, but overall it did not impact on the observed integration distribution. We also found that the methods of relative eigenvalue variance and the estimated product-moment correlation coefficient produced the same ranking and similar levels of integration magnitudes, and thus conclude that both methods are stable indices of integration.

Differences in morphological disparity in the ilium and sacrum among the phylogenetic groups were statistically significant. Allometry plays a contributing role in ilium shape differentiation; this is particularly the case among the large-bodied hominoid ilia. Factors involved in differing sacrum disparities are less straightforward to explain. The sacrum is itself a modular composite structure with varying segmentation, as exemplified by the different numbers of sacral vertebrae across the primate order (Schultz 1945). The large range of sacral vertebra within Hominoidea (ranging from three to six sacral vertebrae as represented by the lesser and great apes) likely contributes to the high sacral disparity for this clade. Answers to the high sacral disparity amongst New World monkeys, however, must lie elsewhere as they have similar numbers of sacral vertebrae. The sampled New World monkey group ranged from the the fully-prehensile *Ateles* to the semi-prehensile *Cebus* and *Lagothrix*. Showalter (2018) has demonstrated that sacrum morphology differs amongst these genera, which likely contributes to the comparatively high level of morphological disparity within this group.

Differences in module variability across the phylogenetic and locomotory groups are variable. Overall though, the specialist locomotory groups exhibit the greatest amount of disparity compared to the generalist groups. A similar trend thus exists in specialist limb and pelvis disparity, although, unlike limbs, the increased disparity is not paired with a

significant reduction in integration levels (Young and Hallgrímsson 2005, Rolian 2009, Young 2010). Instead, we register a small increase in levels of integration. Specialists thus exhibit more variability in pelvic morphology without a reduction of integration magnitudes. Possible explanations must be sought beyond integration and effects of allometry as the higher disparity amongst specialists persist after the effects of body size are taken into account.

What then can be the cause for the observed increase in morphological disparity among specialists? Specialist taxa are characterised by greater joint mobility. This is seen in for e.g. specialist taxa displaying shallower acetabulum with less thick walls, and larger cranial aspects of the lunate surface (enabling greater mobility). They also share an upright body position which requires larger loadbearing cross-sectional areas such as auricular surfaces to cope with additional load transfers (Lewton 2015). One possible answer is that the observed disparity among the specialist locomotory groups reflects this enhanced joint mobility and the effects of the increased loading transmission regimes (Frost 1990 a,b, Lewton 2015).

On the other hand, the low disparity among generalists may relate to phylogeny. We note that overall the Old World monkey groups displays the least amount of disparity. Old World monkeys encompass three forms of locomotion: suspension, arboreal, and terrestrial. The latter two groups are generalized quadrupeds. Yet when we examine the Old World monkey specialist suspensory mode of locomotion group, we see that this group shares the low disparity signal with the arboreal and terrestrial quadrupedalism (generalists). This suggests that the differing locomotory groups within the Old World monkey clade share low disparity and that locomotion may play a less of a role in the observed disparity levels, or at least within this clade. The Old World monkey group may contain a constraining phylogenetic element when it comes to disparity, not present in the other clades. We do know though that the potential constraining element is not integration, since the Old World monkey clade and its locomotory groups do not exhibit greater integration levels. The effects of phylogeny and locomotion, however, are not mutually exclusive and likely interact within the observed levels of disparity. Despite the above described variability in clades and locomotory groups, the distribution of disparity

remains the same: low in acetabulum and pubis, moderate for ischium and sacrum, whilst high levels of disparity were uncovered for the ilium.

Combining the integration and disparity results reveals that these variables are characterized by an inverse relationship. The results thus follow the predicted pattern of the M_1 model, and support the view that primate pelvic modules are evolutionarily constrained. Specifically, this signifies that the developmental/functional correlation between the shape of different pelvis modules acts as a constraint on variation, and therefore, on the extent to which the primate pelvis may respond to selection, with the level of constraint mediated by the level of integration. Yet, complementary genetic and developmental analyses are needed to fully understand the observed magnitudes of integration, and the observed link between correlation and disparity.

Interesting observations were also made concerning the ilium and pubis. Ilium disparity is higher than expected under the constraining model. Its high variability can, to a large extent, be attributed to allometry. The assisting effect of increased body size on novel ilia forms is illustrated by the morphospace occupied by the large bodied hominoids along the main PC1 axis. The pubis is another interesting module. Pubis disparity is lower than expected in relation to its integration magnitude, indicative of another factor playing a constraining role on disparity. Allometry in this case does not provide an answer, nor does convergent evolution of the pubis shape. The pubis is, however, also an integral part of the pelvic inlet involved with the functional demands of parturition. This can necessitate correlation beyond this module boundary which may act as an additional constraint.

3.7 Conclusion

Attempts to understand the influence of integration on variation and the evolutionary consequences of their relationship have mainly taken place in a theoretical framework (Goswami *et al.* 2006b). The application of the theoretical framework on empirical data remains relatively rare. With our results, we add an empirical example of an inverse relationship between integration and disparity to the overall discussion of integration constraining or facilitating morphological divergence.

Our findings demonstrate a previously unquantified impact of integration on primate pelvic morphologies. This pattern is equally detectable within the various clades and within the differing locomotory groups, suggesting that this pattern is conserved and shared across all primates. If a similar relationship between integration and morphological expression of the pelvis modules exists in other mammalian orders remains to be determined. Furthermore, without detailed genetic and developmental information on the processes involved in morphogenesis, it is not possible to determine the precise drivers underpinning and governing the observed integration pattern. However, whilst a better understanding of the underlying causes requires further study, integration magnitudes and its impact on morphological expression are now identified.

Our findings have implications on how we interpret pelvic trait morphologies as adaptation, as the correlated response can act as a stabilising factor or even move the direction of morphological change away from the preferred direction of selection. Constraint is problematic when reconstructing the evolution of traits, and evolutionary models will need to consider integration magnitudes to accurately reconstruct evolutionary trait histories.

Another important aspect of our results is that even if the relationship between integration and morphological expression remains broadly similar across all primate groups, room for absolute differences in morphological disparity remain possible without major changes in integration magnitudes. How this is achieved remains currently unanswered, and raises interesting questions for future research.

3.8 Supplementary Information

S1: Supplementary Information Primate Specimen

Parvorder	Clade	Family	Species	N _F	N _M	N
Strepsirrhini	Lemuroidea	Daubentoniidae	<i>Daubentonia madagascariensis</i>	1	1	2
		Indridae	<i>Indris indris</i>	1	1	2
		Lemuridae	<i>Eulemur fulvus rufus</i>	1	2	3
			<i>Lemur catta</i>	1	1	2
			<i>Varecia variegata</i>	1	1	2
5	6	11				
Platyrrhini	Ceboidea (NWM)	Atelidae	<i>Alouatta semniculus</i>	0	1	1
			<i>Ateles geoffroy</i>	1	0	1
			<i>Ateles pansicus</i>	0	1	1
			<i>Lagothrix Lagothricha</i>	3	2	5
		Cebidae	<i>Cebus apella</i>	0	2	2
			<i>Cebus capucinus</i>	1	1	2
5	7	12				
Catarrhini	Cercopithecoidea (OWM)	Cercopithecidae	<i>Cercocebus galeritus</i>	1	1	2
			<i>Cercopithecus ascanius</i>	2	2	4
			<i>Cercopithecus cephus</i>	2	0	2
			<i>Cercopithecus hamlyni</i>	2	1	3
			<i>Cercopithecus lhoesti</i>	2	2	4
			<i>Cercopithecus mitis</i>	2	2	4
			<i>Cercopithecus mona</i>	2	2	4
			<i>Cercopithecus neglectus</i>	2	2	4
			<i>Cercopithecus nictitans</i>	2	2	4
			<i>Cercopithecus petaurista</i>	0	1	1
			<i>Cercopithecus pogonias</i>	0	1	1
			<i>Chlorocebus aetiops</i>	4	6	10
			<i>Colobus guereza</i>	2	2	4
			<i>Colobus polykomas</i>	3	3	6
			<i>Erythrocebus patas</i>	2	2	4
			<i>Lophocebus albigena</i>	4	4	8
			<i>Lophocebus aterrimus</i>	1	0	1
			<i>Macaca fascicularis</i>	2	3	5
			<i>Macaca maura</i>	2	2	4
			<i>Macaca mulatta</i>	1	1	2
			<i>Macaca nemestrina</i>	1	1	2
			<i>Mandrillus sphinx</i>	1	1	2
			<i>Papio anubis</i>	2	2	4
			<i>Papio cynocephalus</i>	2	2	4
			<i>Papio hamadryas</i>	5	5	10
			<i>Ptilocolobus badius</i>	2	2	4
			<i>Ptilocolobus kirkii</i>	2	0	2
			<i>Presbytis comata</i>	1	1	2
			<i>Pygathrix nemaus</i>	0	1	1
			<i>Semnopithecus entellus</i>	1	1	2
			<i>Theropithecus gelada</i>	1	1	2
			56	56	112	
	Hominoidea	Hominidae	<i>Gorilla beringei graueri</i>	4	5	9
			<i>Gorilla gorilla</i>	1	0	1
			<i>Pan paniscus</i>	3	5	8
			<i>Pan troglodytes</i>	2	2	4
			<i>Pongo pygmaeus</i>	1	2	3
			Hylobatidae	<i>Hylobates lar</i>	5	5
<i>Symphalangus syndactylus</i>	1	1		2		
17	20	37				
Overall total				172		

Table S1: Primate Specimen

S2: Primate Phylogenetic hypothesis

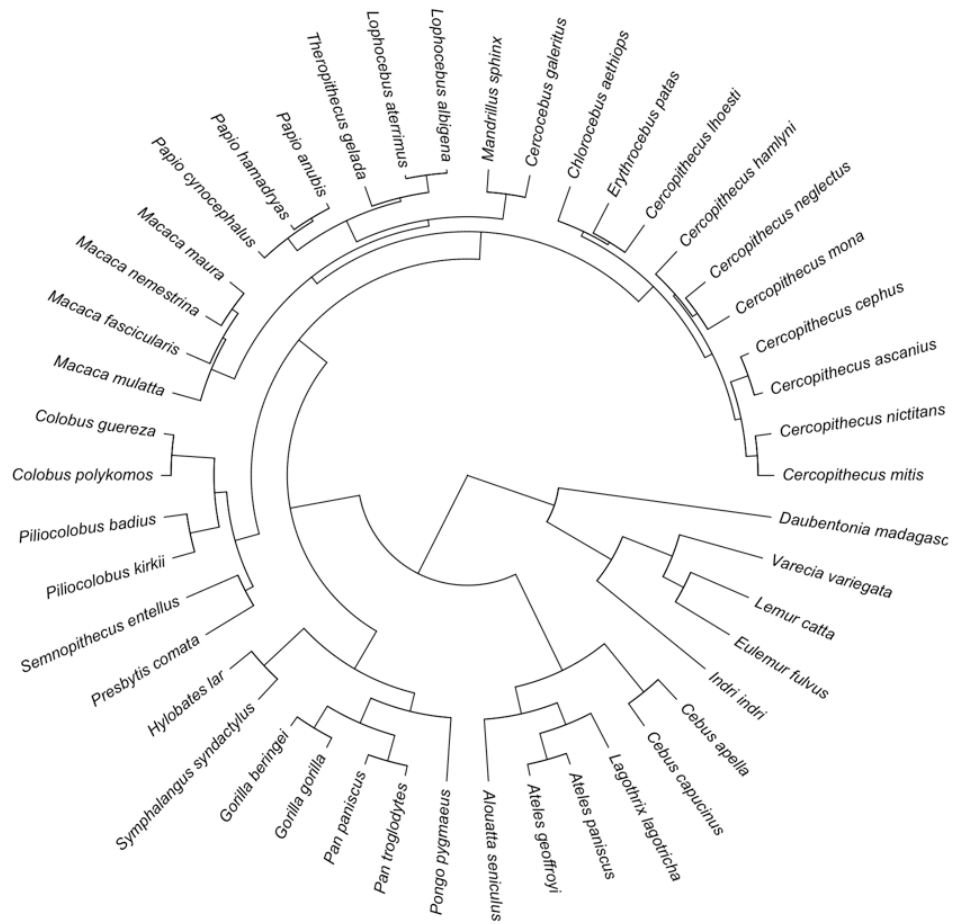


Fig. S2: Phylogenetic hypothesis of primates used within this study

S3: Size differences of phylogenetic and locomotory groups

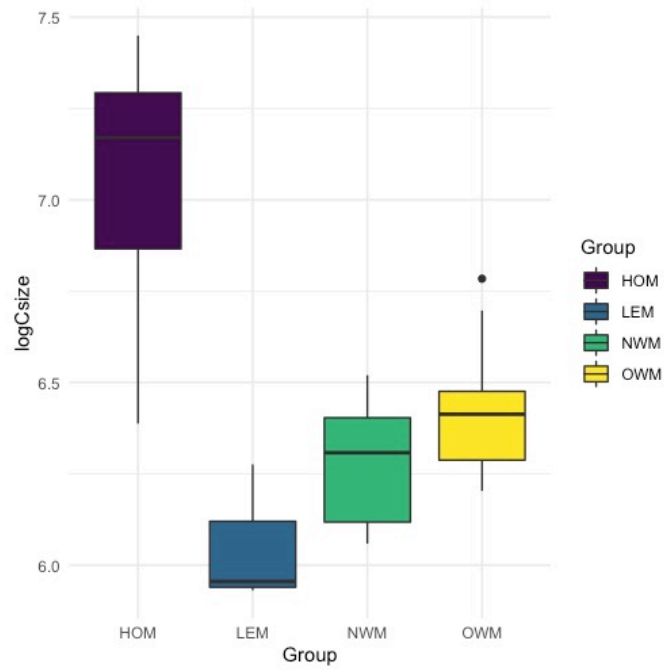


Fig. S3.1: Boxplot size differences of clades

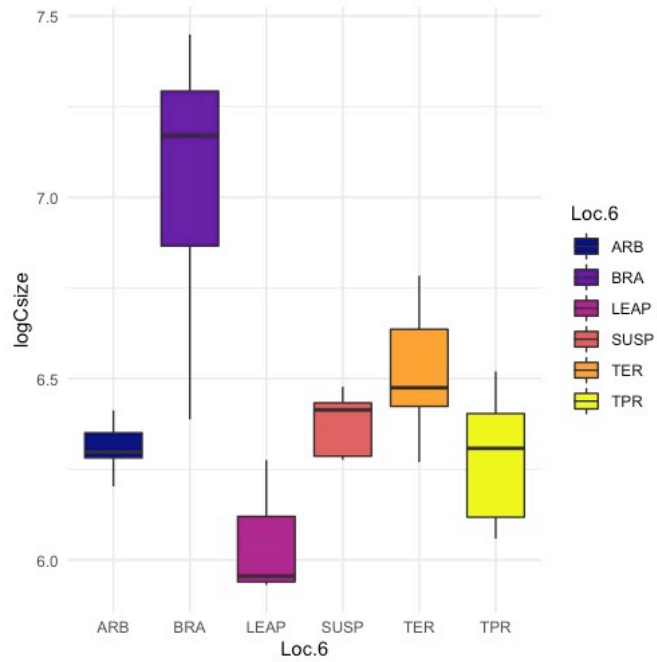


Fig. S3.2: Boxplot size differences of locomotory groups

Outlier for OWM represents Mandrillus sphinx

S4: Integration between modules

<i>MaxL ρ</i>	<i>Shape Data Clades</i>									
	Il-Is	Il-Pu	Il-Ac	Il-Sa	Is-Pu	Is-Ac	Is-Sa	Pu-Ac	Pu-Sa	Ac-Sa
HOM	0.300	0.340	0.330	0.320	0.340	0.450	0.290	0.430	0.240	0.440
LEM	0.320	0.330	0.370	0.400	0.270	0.390	0.320	0.290	0.410	0.360
NWM	0.230	0.240	0.410	0.380	0.280	0.210	0.250	0.330	0.290	0.490
OWM	0.220	0.170	0.330	0.210	0.150	0.310	0.200	0.320	0.170	0.180

Table S4.1 *Shape data* clades: integration between modules

<i>MaxL ρ</i>	<i>Allo Data Clades</i>									
	Il-Is	Il-Pu	Il-Ac	Il-Sa	Is-Pu	Is-Ac	Is-Sa	Pu-Ac	Pu-Sa	Ac-Sa
HOM	0.310	0.330	0.370	0.330	0.360	0.560	0.300	0.460	0.180	0.280
LEM	0.300	0.360	0.350	0.360	0.280	0.410	0.310	0.280	0.400	0.340
NWM	0.220	0.260	0.390	0.310	0.270	0.230	0.190	0.350	0.300	0.510
OWM	0.190	0.160	0.250	0.190	0.160	0.320	0.160	0.330	0.170	0.150

Table S4.2 *Allo data* clades: integration between modules

<i>MaxL ρ</i>	<i>Shape Data Locomotion</i>									
	Il-Is	Il-Pu	Il-Ac	Il-Sa	Is-Pu	Is-Ac	Is-Sa	Pu-Ac	Pu-Sa	Ac-Sa
ARB	0.420	0.540	0.550	0.890	0.650	0.420	0.540	0.550	0.890	0.650
BRA	0.430	0.550	0.630	0.820	0.790	0.430	0.550	0.630	0.820	0.790
LEAP	0.480	0.610	0.590	0.740	0.650	0.480	0.610	0.590	0.740	0.650
SUSP	0.490	0.440	0.630	0.910	0.620	0.490	0.440	0.630	0.910	0.620
TER	0.400	0.510	0.520	0.860	0.570	0.400	0.510	0.520	0.860	0.570
TPR	0.450	0.620	0.770	0.900	0.720	0.450	0.620	0.770	0.900	0.720

Table S4.3 *Shape data* locomotion: integration between modules

MaxL p Allo Data Locomotion

	Il-Is	Il-Pu	Il-Ac	Il-Sa	Is-Pu	Is-Ac	Is-Sa	Pu-Ac	Pu-Sa	Ac-Sa
ARB	0.330	0.250	0.380	0.220	0.320	0.540	0.240	0.330	0.260	0.170
BRA	0.310	0.330	0.370	0.330	0.360	0.560	0.300	0.460	0.180	0.280
LEAP	0.300	0.360	0.350	0.360	0.280	0.410	0.310	0.280	0.400	0.340
SUSP	0.240	0.330	0.320	0.250	0.320	0.390	0.220	0.410	0.330	0.380
TER	0.190	0.210	0.290	0.220	0.180	0.320	0.160	0.340	0.190	0.180
TPR	0.220	0.260	0.390	0.310	0.270	0.230	0.190	0.350	0.300	0.510

Table S4.4 *Allo data* locomotion: integration between modules

Chapter 4:

Divergence of the Human Pelvis Integration and Morphological Disparity.

Covid-19 Impact Statement:

The last years of the presented PhD research were conducted during the global COVID-19 pandemic, leading to closures of research institutions and musea worldwide. Travel was prohibited, and later severely restricted at the time of data collections. This has particularly impacted the study of chapter 4, resulting in a limited sample size. Further studies will benefit from enlarging the sample size and it will be of interest to review the presented findings in the future.

4.1 Abstract

The distinct human pelvis is widely considered to be shaped by selection for locomotor and obstetrical functionality. Yet the intrinsic pelvic mechanism which influences the response to selection remains poorly understood. Here, we examine humans in a comparative framework. We analyse pelvis module integration and morphological disparity magnitudes between humans, gorillas, bonobos, gibbons, and rhesus monkeys to gain insights into the intrinsic levels of constraint and evolutionary flexibility. The results demonstrate that the reduction of integration levels across the different anatomical pelvic elements is a defining human feature. The reduction of inherent constraint is paired with elevated levels of disparity. We found humans to be more variable in every examined element, apart from the pubis. The limited sample size of the present study must be considered in the interpretation of the results. However, our data suggests that the reduced constraint enabled human pelvic traits to evolve in a more autonomous way. This permits the human pelvic bauplan to be more responsive to multiple selective pressures, and be more flexible in shaping phenotypic and population specific solutions to configure optimal fitness. Another specific human characteristic is the marked disassociation between the pubis and ischium, along with integrational increases within these two elements. The high level of pubic integration acts as a constraint on its morphological variability, limiting its evolutionary possibilities. Yet the high ischial integration level pairs with a significant high level of disparity, providing us

with an empirical example of high integration not constraining but facilitating responsiveness. This 'liberated' ischium is a beneficial feature serving both efficient bipedalism and eases parturitions, allowing the relevant traits to respond with more ease and greater extent to the multiple directions of selection compared to those of the other analysed primates. This facilitated hominin pelvic evolution and its morphological divergence.

4.2 Introduction

Compared to other primates, humans are defined by two specific characteristics: we are the only extant primate to obligatorily walk upright, and the only large bodied-ape to birth large-headed neonates relative to our obstetric dimension (Rosenberg and Trevathan 2002). The human pelvis structure plays a pivotal role in both these characteristics. It is integral to the performance of bipedalism, and contains the birth canal crucial to successful parturition. The morphology of the human pelvis is strikingly different from other primates. In the false pelvis, the shape and orientation of the iliac blades differ between primates and humans. Human iliac blades are shorter, placed more laterally, and curve along the side of the body to produce the characteristic bowl shape. The reduced iliac height free the lumbar vertebrae to curve lordotically (inwards). These changes have been associated with more efficient balancing of the upper body during upright walking, and reduce the energetical cost of side-to-side shifting during walking (Aiello and Dean 1990, Lovejoy 2005, Lovejoy and McCollum 2010, Tuttle 2014). Alterations in the true pelvis – sacrum, ischium, and pubis include the sacrum being shorter, wider, and more ventrally concave, whereas the ischium is much shortened, more robust and differently angled. The differences have been proposed to relate to resisting the increased loading of upper body weight during bipedalism and improving hamstring leverage (Aiello and Dean 1990, Warrener 2011, Tuttle 2014). The observed alterations also impact the shape of the human birth canal. In other primates the birth canal is elongated whereby the larger dimension is anteriorly-posteriorly (sagittal) orientated and this orientation remains the same throughout the birth canal (inlet, mid-plane, and outlet). Humans, on the other hand, have a relative narrow sagittal pelvic inlet dimension due to the medio-lateral (transverse) orientation of the upper pelvis. The mid-plane and outlet are, however, wider in the in the sagittal than transverse dimension. This results in a twisted birth canal that requires neonates to rotate their head and shoulders

as they pass through the birth canal (i.e. rotational birth process) (Fig 4.1) (Rosenberg 1992, Rosenberg and Trevathan 2002, Rosenberg and Trevathan 2005).

The human pelvic morphology is widely considered to be the evolutionary outcome of selection for locomotory and obstetrical functions, both being essential to the survival and reproductive success of our species (Rosenberg 1992, Ruff 2010, Grabowski and Roseman 2015, Gruss and Schmitt 2015, Gruss *et al.* 2017, but do see Betti *et al.* 2013 and Betti and Manica 2018 for the role of neutral evolution and response by Mitteroecker *et al.* 2021). Previous studies have mainly focused on employing biomechanical modelling to link specific pelvic traits with adaptations to functional demands and the evaluation of the fossil record for the presence or absence of these trait. However, whilst these studies have provided many insights into the biomechanical demands placed upon the pelvis structure, it is unlikely that these morphological changes occurred in isolation. Instead, complex biological organisms are systems composed of traits (modules) with varying degrees of correlations within and between these traits (i.e. integration) (Olson and Millar 1958, Cheverud 1982).

Morphological integration acts in a similar way to the genetic concept of pleiotropy whereby one gene influences multiple phenotypic traits (i.e correlated traits). These correlations or genetic integration are quantitatively described in the additive genetic variance-covariance matrices (**G** matrices). Conversely, morphological integration relates to morphological correlated traits, be it due to genetic, developmental, and/or functional correlation, as described by the phenotypic variance-covariance matrices (**P** matrices). Much overlap exists between genetic and morphological integration as the phenotype and genotype operate in a feedback loop, and ultimately it is this interaction that drives the mechanisms of evolution. For example, if a specific change to development or functional integration provides an individual phenotype with a fitness advantage over time this can lead to genetic integration at population/species level since individuals with this type of developmental or functional integration become more numerous due to their fitness advantage. In this way, change at phenotype level becomes a change in genotype. Genetic integration in turn becomes evolutionary integration when the integrated traits co-evolve together in response to selection (Cheverud 1984, Cheverud 1996a, Cheverud *et al.* 1996, Rolian and Willmore 2009, Grabowski 2012, Rolian 2014, Mitteroecker *et al.*

2021). Past studies have demonstrated this link, as seen in the broadly similar levels of integration between the **P** and **G** matrices (e.g. see Cheverud 1988, Cheverud 1995, 1996b, Marroig *et al.* 2009, Porto *et al.* 2009, but do see Willis *et al.* 1991 for a different view).

Morphological integration may constrain or facilitate morphological evolution. Integration is predominantly thought of as an inherent constraining mechanism. This safeguards the cohesion of genetic, developmental and/or functional traits, yet limits evolutionary change since the correlated traits must co-evolve. The correlated traits potentially act as a stabilizing factor or even direct the response to selection away from its preferred direction (Marroig *et al.* 2009, Porto *et al.* 2009, Goswami *et al.* 2014). Importantly, high levels of integration between traits may mask the target of selection since non-targeted traits co-evolve. The observed changes thus may be as a side-effect and not a response to selection (Gould and Lewontin 1979, Wagner 1996, Lynch and Walsh 1998, Hansen 2003, Hansen and Houle 2004, Hansen and Houle 2008). Conversely, low levels of integration enable traits to evolve in a more autonomously manner, promoting a response to the direction of selection (Marroig *et al.* 2009, Porto *et al.* 2009). In these scenarios, the magnitudes of integration relate to the inherent level of constraint. In specific circumstances, however, high integration levels may facilitate responsiveness. This occurs when the correlated response aligns with the preferred direction of selection (Goswami *et al.* 2014, 2015). Importantly, the concept of integration is equally applicable to integration within and between organismal traits. Patterns and magnitudes of integration may evolve in response to natural selection. This occurs through altered levels of integration within or between traits, resulting in a higher/lower magnitude of inherent constraint which alters how species can respond to selection (Wagner 1995, 1996, Pavlicev *et al.* 2011). Reduced integration, for example, may enable the evolution of new morphological forms previously not possible due to prior inherent constraints. From an evolutionary perspective, identifying changes to integration magnitudes between closely related species thus may provide a window into past selective divergence.

To understand human pelvic adaption thus requires an understanding of the internal patterns of morphological integration that influences its evolutionary trajectories. Only a few studies have approached the human pelvis evolution from this angle. Grabowski *et*

al. (2011) found that the evolution of the human hip bone was facilitated by decreased levels of integration and increased evolutionary flexibility compared to other apes. Lewton (2012), tested Grabowski's hypothesis but did obtain different results. Instead she found *Pan* to be the least integrated species in her extended comparative analyses. She did observe, however, that low levels of hip bone integrations are a common feature amongst primates, likely a contributing factor to the great diversity of extant primate pelvic morphology and expanded locomotory repertoire. As such, no consensus has yet been reached about the role integration may have played in the extensive morphological divergence of the human pelvis structure. Both these studies employed linear distances and focused on the overall integration of the hip bone without considering the internal modular patterns present within the primate pelvis (Chapter 2). Grabowski considered this subject again in 2013, this time focusing on obstetrics. He once again found humans to be characterised by low levels of integration between obstetric and non-obstetric traits, and once again humans to be more evolutionary flexible.

Here we revisit this topic to explore how the human pelvis is able to differ to such great extent from other primates. We investigate and compare its integration pattern to other primates, its impact on evolutionary flexibility, and discuss the role these changes may have played in hominin evolution. To do so, we use geometric morphometric shape configurations of the human, gorilla, bonobo, hylobate, and rhesus monkey pelvic structure. We partition the pelvis along its developmental and functional partitions as identified in Chapter 2, and quantify the magnitude of integration and the morphological disparity – how morphologically different the examined species are from each other - as described in more detail in Chapter 3. Next, we pair the results of integration and morphological disparity to determine: 1) whether integration acts in a constraining or facilitating manner, and 2) the extent by which it does. We discuss our results in relation to hominin evolution to contextualise the significance of our findings.

4.3 Data

4.3.1 Osteological sample

Three-dimensional (3D) landmarks ($n = 153$) were collected of the fully articulated pelvis of four extant Hominoidea species: *Gorilla beringei* (gorillas), *Homo sapiens* (humans),

Hylobates lar (gibbons), and *Pan paniscus* (bonobos) to investigate similarities/differences in integration patterns of humans compared to their closest living ape species. The *Macaca mulatta* (rhesus monkeys) shares the long anterior-posterior inlet dimension within a cranial-caudal elongated pelvic morphology of the non-human ape species, though shares with extant humans a close fit between neonate head and the maternal pelvic inlet dimensions (Schultz 1949, Rosenberg and Trevathan 2005) (figure 4.1). Despite their more distant phylogenetic relationship, this similarity between rhesus monkeys and humans may make a comparison between these two species particularly informative for the obstetric - locomotion analyses. For this reason, the *Macaca mulatta* was added to our data set. Each sampled species is represented by eight specimens and each group includes an even distribution of males and females.

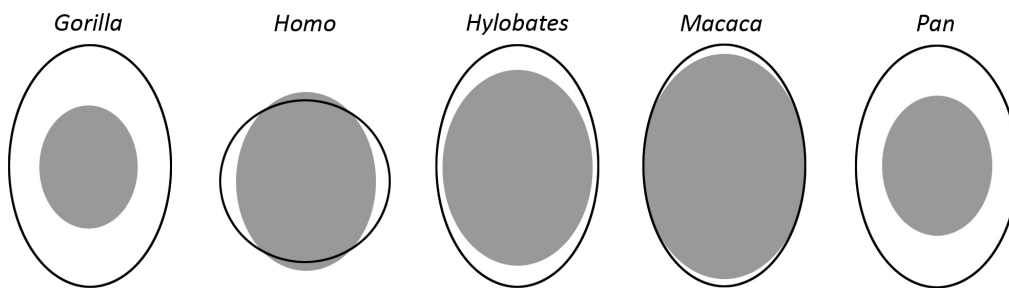


Fig 4.1. Pelvic inlet relative to neonate dimensions of the sampled species

Illustration of the sampled primate species relating the size of the maternal pelvic inlet (black outline) to the size of the neonatal heads (grey ovals). The diagrams are standardised according to the transverse diameter. In humans, the neonatal cranium dimensions are larger than the anterior-posterior (sagittal) inlet dimension, necessitating the neonate to enter the birth canal in a medio-lateral (transverse) orientation. The mid-plane and outlet are however wider in the sagittal than transverse dimension, requiring the neonate to twist and rotate its head and shoulders as it descend along long the birth canal (= rotational birth process). In all other primates, the orientation of the birth canal (i.e inlet, mid-plane and outlet) remain the same throughout, being more elongated than wide.

Source: adaptation after Schultz 1949 and Rosenberg and Trevathan 2005

4.3.2 Geometric morphometric data

The geometric data collection follows methodology as detailed in Chapter 2. We collected 53 landmarks and semi-landmarks on both the left and right sides of the pelvis. Shape data was extracted by performing a Generalised Procrustes Analysis (GPA). During the GPA, the landmark configurations are superimposed and variance due to position, rotation and isometric size are removed. We included the left and right side of the primate pelvis girdle in the Procrustes fit as symmetrical structures obtain more robust alignment (Cardini 2016, 2017). The resulting Procrustes shape variables were orthogonally projected into its linear tangent space to obtain variables amenable to statistical analysis (Dryden and Mardia 1998, Klingenberg 2009, Baab *et al.* 2012, Zelditch *et al.* 2012). The GPA procedure was performed using the *geomorph* package in R (Adams and Otarola-Castillo 2013).

4.4 Analyses

Our previous study (Chapter 2) revealed how the primate pelvis is dominantly characterised by a strong developmental modularity with the ilium, ischium, pubis, acetabulum, and sacrum all acting relatively independently from one another (Chapter 2: H_1 hypothesis). For the functional modules, following Huseynov *et al.* (2017), we partitioned the pelvis landmarks along bone morphologies hypothesized to be mainly involved with obstetric and locomotory function (Chapter 2: hypothesis H_5). To preserve biological information due to relative size, position, and orientation of the modules within the pelvic girdle, we used the within configuration approach (Klingenberg 2009, Baab *et al.* 2012, Baab 2013). For the analyses, we used data characterising the left and midline of the pelvis landmark configuration.

4.4.1 Integration analyses

The pelvis is sexually dimorphic, and species vary in their level of sexual dimorphism (Schultz 1949, Leutenegger 1974, Leutenegger and Larson 1985, Wood and Chamberlain 1986, Tague 1995). We opt to retain sexual dimorphism information in our study since this directly relates to the species reproductive success. Human pelvic sexual dimorphism is widely accepted to be the product of evolutionary adaptation (Tague 1992, Rosenberg

and Threvathan 2005, Weaver and Hublin 2009, Grabowski and Roseman 2015, Pavlicev *et al.* 2020). This view is further supported by the high levels of heritability of the male and female pelvic shape and size which demonstrates substantial involvement of inherent factors shaping and maintaining sexual dimorphism (Sharma 2002).

To calculate comparable magnitudes of integration of the modules, we first created a trait congruence coefficient correlation matrix for each module of each sampled species. The congruent vector is a proven stable measurement for small data sets, often employed within the field of palaeontology where large sample sizes are not a feasible option (Goswami and Polly 2010a). Next, we computed integration magnitudes with the method of estimated Pearson product-moment correlation method. The estimated Pearson product-moment correlation method produces similar results to relative eigenvalue dispersal method as previously demonstrated in the Chapter 3. The estimated Pearson product-moment correlation coefficient ($MaxL \rho$) ranges from 0 to 1 with 0 indicative of no correlation and 1 signifying complete integration. All pairs from the off-diagonal lower triangle of the vector correlation matrix were included and the $MaxL \rho$ from across the matrix is reported. Values were obtained using the *EMMLi* function of the *EMMLi* package (Goswami and Finarelli 2016). Integration within and between the modules of the developmental and functional partitions were calculated.

4.4.2 Morphological disparity analyses

To examine the variational properties of the sampled species, disparity was quantified by Procrustes variance (Pv) and calculated using the 'morphol.disparity' function in *geomorph*, for each module of the developmental and functional partition. Pv is calculated as the sum of the diagonal elements of the group's variance-covariance matrix divided by the number of observations of the data set (Zelditch *et al.* 2012). Significance of the disparity between the species was assessed in a pairwise manner through 1000 permutations. Calculations were made using the *morphol.disparity* function of the *geomorph* package (Adams and Otarola-Castillo 2013).

Primate sexual dimorphism is the product of trait changes in both males and females (Plavclan 2001). The magnitudes of divergence between males and females is a product of evolutionary adaptation, with higher levels of disparity associated with higher past

adaptive pressure to diverge (Plavclan 2001). For example, higher levels of pelvic sexual dimorphism have been noted in mammal and primate species that birth relatively large-headed and large-bodied neonates compared to species with smaller offspring (Ridley 1995, Tague 2016, Moffett 2017, Gunstra *et al.* 2019). To examine the level of sexual dimorphism - a measure of past selective pressure - of each sampled species and their impact on morphological disparity, we ran the morphological disparity analysis on the shape variables (*shape* data) and *sex-corrected* data. The latter data set was obtained by regressing biological sex on shape, and using the obtained residuals as the *sex-corrected* data.

4.4.3 Relationship of integration and disparity

For the developmental modules, the results of the integration and morphological disparity analyses were paired to evaluate the relationship between integration and disparity. This enables us to evaluate whether integration acts as a constraint or a facilitator, and the extent by which it does so. We also employ Spearman's rank correlations to measure the strength and direction of the association between integration and disparity distributions. Here, the correlation coefficient falls on a scale of -1 (perfect inverse relationship), to 0 (dissimilarity), to +1 (perfect direct relationship). The correlation coefficient enables us to compare obtained results, as well as whether integration predominately acts as a constraint (inverse relationship), mixed or no detectable relationship (dissimilarity), or facilitator (direct relationship). As in Chapter 3, Integration and disparity distributions are plotted to visualize the relationship between these two factors. Given that the functional partition only consists of two modules, no such analyses were needed.

4.5 Results

Developmental partition

4.5.1 Integration

The developmental intra- and inter-integration module analysis reveals that much variation exists among the examined species. Module intra-integration levels between species vary and may rank differently per species, indicative of each species containing its own set of alterations to suits its needs. *Homo* and *Gorilla* species share rank of integration magnitudes (ilium, sacrum, acetabulum, pubis, ischium), as do *Hylobates* and *Pan* (ilium, sacrum, ischium, acetabulum, pubis), whilst *Macaca* ranks ilium, sacrum, ischium, pubis, acetabulum in an ascending integration order. Focusing on humans: the high integration levels of the pubis and particularly the ischium stand out whilst the sacrum and acetabulum register lower levels. The human ilium integration falls in mid-range (table 4.1, fig 4.2).

Continuing with the between-module integration magnitudes (table 4.2), a marked reduction is notable between the covariation of the human ischium and pubis. The extensive disassociation of ischium-pubis signifies that these two elements can vary in a comparative increased independent manner, with each element able to respond more directly to natural selection.

Specifically looking at modules involved in shaping the pelvic inlet, the integration magnitude between the ilium and pubis is the lowest in humans, as are the integration levels between the ilium and sacrum. In the latter case, this observation is shared with *Macaca mulatta*, another species under relative obstetric constraint. The third between-module integration magnitude of interest is between the pubis and sacrum. In this case, humans do fall at the lower end of obtained *MaxL* ρ values; however, it is notable that great apes share this signal of low shared cohesion between these elements. Overall, aside from between-integration magnitudes of the acetabulum and ischium, and acetabulum and the pubis, *Homo sapiens* is marked by low if not the lowest level of between-module integration values of the examined species, enabling its developmental modules to vary more independently from one another.

<i>MaxL ρ</i>					
	Il	Is	Pu	Ac	Sa
Gor	0.370	0.670	0.630	0.640	0.480
Hom	0.420	0.800	0.800	0.520	0.500
Hyl	0.460	0.630	0.750	0.730	0.710
Mac	0.390	0.690	0.570	0.860	0.520
Pan	0.460	0.640	0.720	0.650	0.620

Table 4.1. Integration of developmental modules

Species: Gor = Gorilla beringei, Hom = Homo sapiens, Hyl = Hylobates lar, Mac = Macaca mulatta, and Pan = Pan paniscus. Modules: Il = Ilium, Is = ischium, Pu = pubis, Ac= acetabulum, and Sa = sacrum

<i>MaxL ρ between modules</i>										
	Il-Is	Il-Pu	Il-Ac	Il-Sa	Is-Pu	Is-Ac	Is-Sa	Pu-Ac	Pu-Sa	Ac-Sa
Gor	0.270	0.210	0.320	0.280	0.270	0.440	0.200	0.290	0.150	0.150
Hom	0.230	0.160	0.260	0.240	0.170	0.380	0.150	0.260	0.170	0.130
Hyl	0.240	0.200	0.280	0.310	0.270	0.370	0.190	0.230	0.260	0.310
Mac	0.250	0.200	0.230	0.240	0.240	0.450	0.220	0.240	0.230	0.210
Pan	0.240	0.230	0.280	0.260	0.280	0.290	0.150	0.200	0.150	0.120

Table 4.2. Integration between developmental modules

Species: Gor = Gorilla beringei, Hom = Homo sapiens, Hyl = Hylobates lar, Mac = Macaca mulatta, and Pan = Pan paniscus. Modules: Il = Ilium, Is = ischium, Pu = pubis, Ac= acetabulum, and Sa = sacrum

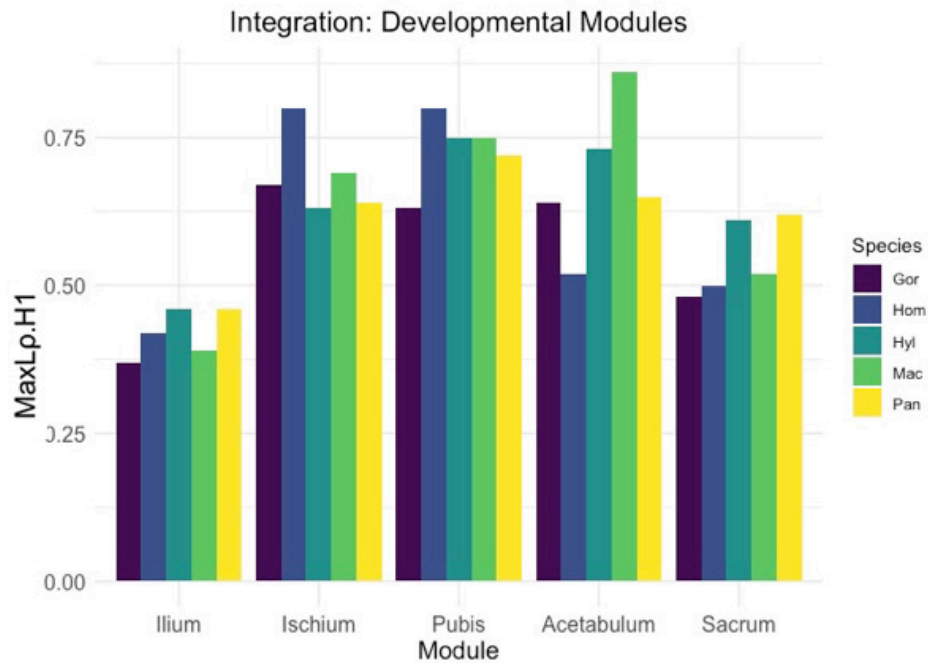


Fig 4.2. Developmental module integration

Species: Gor = Gorilla beringei, Hom = Homo sapiens, Hyl = Hylobates lar, Mac = Macaca mulatta, and Pan = Pan paniscus. Modules: Il = Ilium, Is = ischium, Pu = pubis, Ac= acetabulum, and Sa = sacrum

4.5.2 Morphological Disparity

Within the *shape data* analyses, human phenotypes are more variable in every aspect, apart from the pubis (table 4.3, fig 4.3). The disparity analysis reveals remarkable high variability of the human ischium. It is worth re-iterating that we employ the within configuration approach, meaning that the captured variation is due to morphological and relative position differences of the module within the pelvic girdle. In this context, the high ischial disparity is less surprising since a well-known human characteristic is the sexual dimorphic differential position of the ischial tuberosity in males and females. Compared to males, the ischial tuberosity of females are less robust, and points outwardly away from the pelvic cavity to increase the female pelvic outlet size (Buikstra and Ubelaker 1994, White *et al.* 2012). The pairwise disparity comparison underlines the extent of ischium variation, where *Homo sapiens'* disparity statistically differs from all

other sampled primates ($p < 0.005$). Additionally, the human sacrum is also significantly more variable in shape and relative position within the pelvis, apart from the pairwise comparison with *Macaca mulatta*. Differences in the human male and female sacrum size and morphology have been well documented (Buikstra and Ubelaker 1994, White *et al.* 2012), with the male sacrum tending to be longer, narrower and flatter whilst the female sacrum is shorter, wider, curved, and more posteriorly positioned (as to create wider birth canal). Another human element of interest is the ilium. In males, ilium morphology is narrower, taller, and has a more pronounced S-shaped iliac blade compared to females. The different male and female sacrum width also influence the position of the ilium in the pelvis (White *et al.* 2012). Morphological disparity of the human ilium differs statically to *Pan*. Pairwise data and associated p-values are provided in S3.

When we remove shape variation associated with sexual dimorphism (*sex-corrected data*), a different pattern emerges. Noteworthy are the similarities between *Homo sapiens* and *Macaca mulatta*, and, in line with expectations, the reduction of ischium disparity within *Homo sapiens*. The pairwise data (S3) confirm that humans no longer diverge at a significant level. The sex-corrected data reveal: 1) the comparatively high level of sexual dimorphism present within humans, indicative of past selective pressure for the sexes to diverge; and 2) that species associated with obstetric limitations not only express - as expected - higher divergence levels between the sexes, but already contain higher variability within the underlying shared male-female pelvic template.

	<i>MD (Pv x10⁵)</i>					<i>MD (Pv x10⁵)</i>				
	<i>Shape Data</i>					<i>Sex-Corrected Data</i>				
	Il	Is	Pu	Ac	Sa	Il	Is	Pu	Ac	Sa
Gor	9.770	6.276	1.373	2.327	3.189	6.8766	3.2452	0.9837	1.5393	2.9094
Hom	14.204	16.990	2.500	3.116	6.941	8.2022	4.7465	1.8369	1.8170	3.3236
Hyl	8.472	3.500	2.512	1.125	3.458	6.6671	2.9439	2.3056	0.9909	2.5513
Mac	9.201	7.190	3.221	2.592	4.432	8.0397	5.2579	2.4317	2.0883	3.4268
Pan	7.021	5.168	2.324	1.624	2.793	5.0788	3.8589	1.6734	1.2753	1.9188

Table 4.3. Developmental module disparity

Species: Gor = Gorilla beringei, Hom = Homo sapiens, Hyl = Hylobates lar, Mac = Macaca mulatta, and Pan = Pan paniscus. Modules: Il = Ilium, Is = ischium, Pu = pubis, Ac= acetabulum, and Sa = sacrum

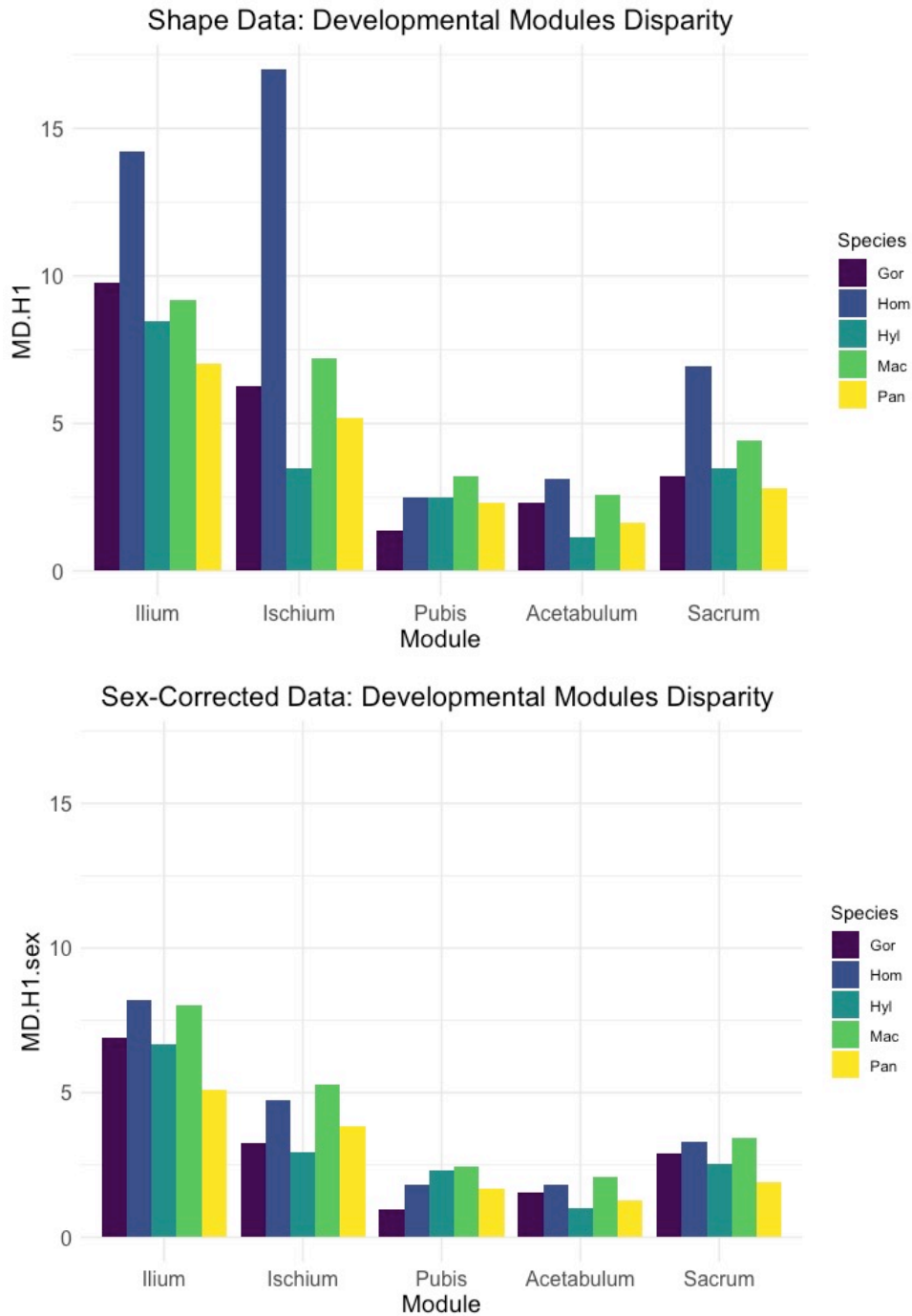


Fig 4.3. Developmental module disparity

Shape data top, sex-corrected data bottom. Species: Gor = Gorilla beringei, Hom = Homo sapiens, Hyl = Hylobates lar, Mac = Macaca mulatta, and Pan = Pan paniscus. Modules: Il = Ilium, Is = ischium, Pu = pubis, Ac = acetabulum, and Sa = sacrum

4.5.3 Relationship developmental integration and disparity

Paring the integration and disparity (*shape data*) results (fig 4.4 and table 4.4) reveals that, except for *Homo sapiens*, the relationship between integration and disparity distribution of the examined species are of an inverse nature, whereby high levels of integration are paired with low levels of morphological disparity and vice-versa. This inverse relationship is indicative of the constraining model, whereby high levels of integration act as a constraint on morphological variability and low levels of integration reduce this constraint (Wagner 1996, Lynch and Walsh 1998, Hansen 2003, Hansen and Houle 2004, Hansen and Houle 2008, Marroig *et al.* 2009, Porto *et al.* 2009, Goswami *et al.* 2014, Felice *et al.* 2018). Humans, however, do deviate from the general primate pattern (figure 4.4). The high morphological ischium disparity paired with high level of integration suggest that integration is not acting as a constraining but facilitating factor not seen in any of the other species sampled. Sacrum and ilium variation are higher than expected under the constraining model, whereas the high acetabulum variation is paired with decreased internal integration, and the pubis low variation is paired with high internal integration. The Spearman's correlation test results are indicative of how very differently humans are in this respect (table 4.4).

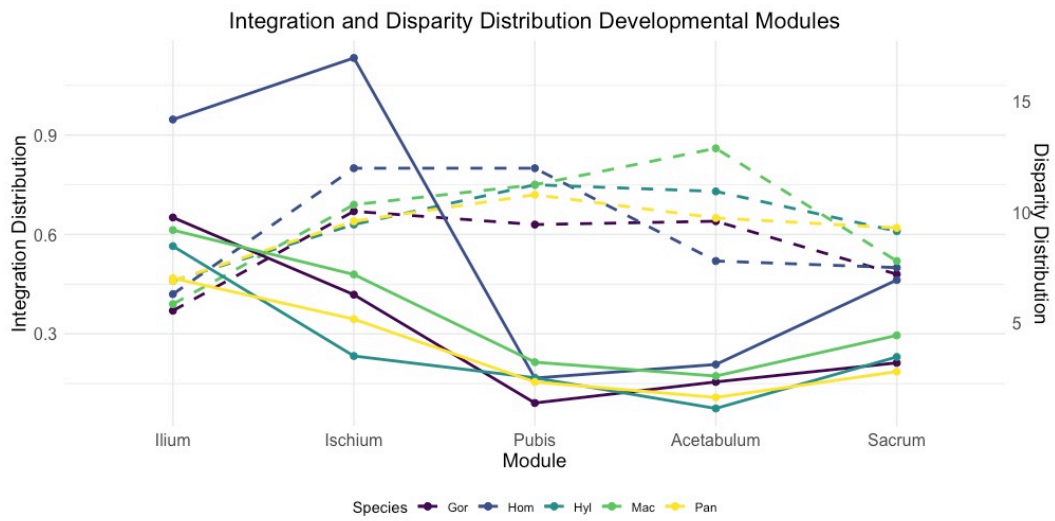


Fig 4.4. Integration and disparity distribution of the developmental partition

Dashed lines illustrate the Rho integration values on the left y-axis (Integration Distribution) whilst full lines represent the Pv values plotted according the right y-axis (Disparity Distribution). Species: Gor = Gorilla beringei, Hom = Homo sapiens, Hyl = Hylobates lar, Mac = Macaca mulatta, and Pan = Pan paniscus.

	$r (MaxL \rho - Pv)$
Gor	-0.7403
Hom	+0.0102
Hyl	-0.9415
Mac	-0.7665
Pan	-0.8126

Table 4.4. Correlation coefficient between integration (Rho) and morphological disparity (Pv).

Species: Gor = Gorilla beringei, Hom = Homo sapiens, Hyl = Hylobates lar, Mac = Macaca mulatta, and Pan = Pan paniscus.

Functional partition

4.5.4 Integration of the functional partition

Whilst the developmental partition is the dominant modular configuration within the primate pelvis structure, a significant - albeit lower in strength - partitioning also exist between its functional modules (Chapter 2). The integration analyses indicate similar levels of integration are present within the locomotory and obstetric modules of the sampled species (table 4.5, figure 4.5). Differences are, however, observed in integration magnitudes between these two modules (table 4.5). Here, *Homo sapiens* shows low inter-module integration. *Macaca mulatta* also registers comparatively less integration between its functional modules, but not to the same extent as humans. Thus, whilst the two species associated with obstetric limitations register similar levels of integration within the obstetric module, they do have comparatively lower levels of integration between the obstetric and locomotory modules. This low level of integration between obstetric and locomotory modules would have facilitated a more autonomous response to selection of relevant structures supporting each function without compromising the other, and thus assisting divergence between the functional demands placed upon the pelvis structure.

	<i>MaxL ρ</i>		
	Loc	Obs	Loc-Obs
Gor	0.360	0.410	0.280
Hom	0.360	0.430	0.200
Hyl	0.370	0.440	0.280
Mac	0.360	0.440	0.250
Pan	0.340	0.450	0.280

Table 4.5. Integration within and between the functional modules

Species: Gor = Gorilla beringei, Hom = Homo sapiens, Hyl = Hylobates lar, Mac = Macaca mulatta, and Pan = Pan paniscus. Modules: Il = Ilium, Is = ischium, Pu = pubis, Ac= acetabulum, and Sa = sacrum

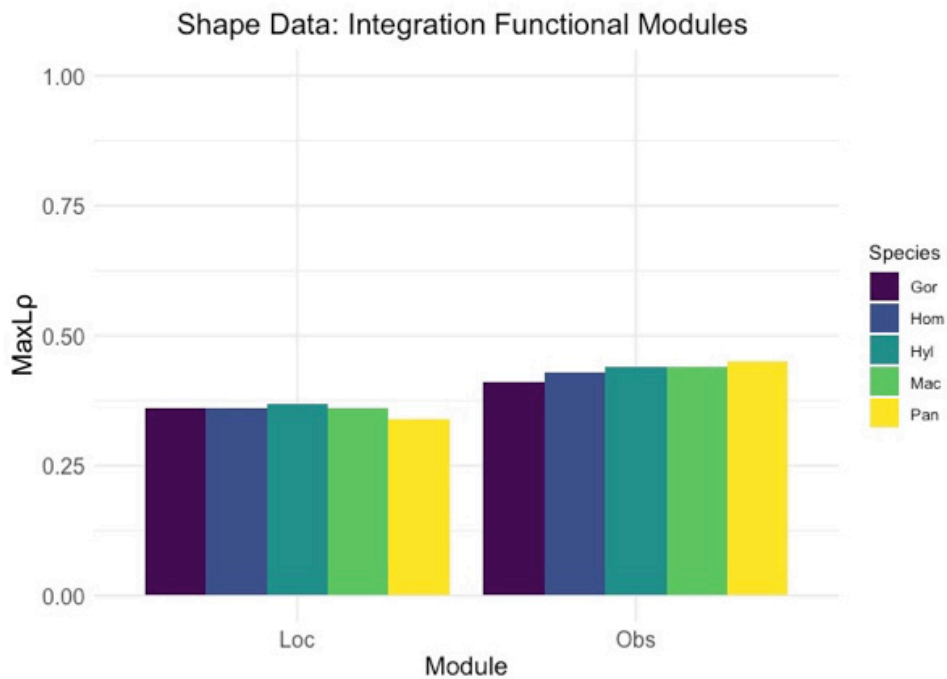


Fig 4.5. Functional module integration

Species: Gor = Gorilla beringei, Hom = Homo sapiens, Hyl = Hylobates lar, Mac = Macaca mulatta, and Pan = Pan paniscus. Modules: Il = Ilium, Is = ischium, Pu = pubis, Ac= acetabulum, and Sa = sacrum

4.5.6 Disparity of the functional partition

The results of the morphological disparity analyses (P_v) (table 4.6, figure 4.6) reveal high human variability of both obstetrical and locomotory morphologies. The pairwise comparison (S4) indicated that humans were significantly more variable than all other sampled species for the locomotory module, although only more than *Gorilla gorilla* for the obstetric module. Human variability is not solely a product of sexual dimorphism, although this contributes markedly to the observation as demonstrated by difference between *shape* and *sex-corrected* disparity. The *sex-corrected* data show, similar to the observation made in relation to developmental disparity, that *Homo sapiens* and *Macaca mulatta* express similar levels of disparity and are already more variable in the underlying shared male-female pattern than the other primate species studied,.

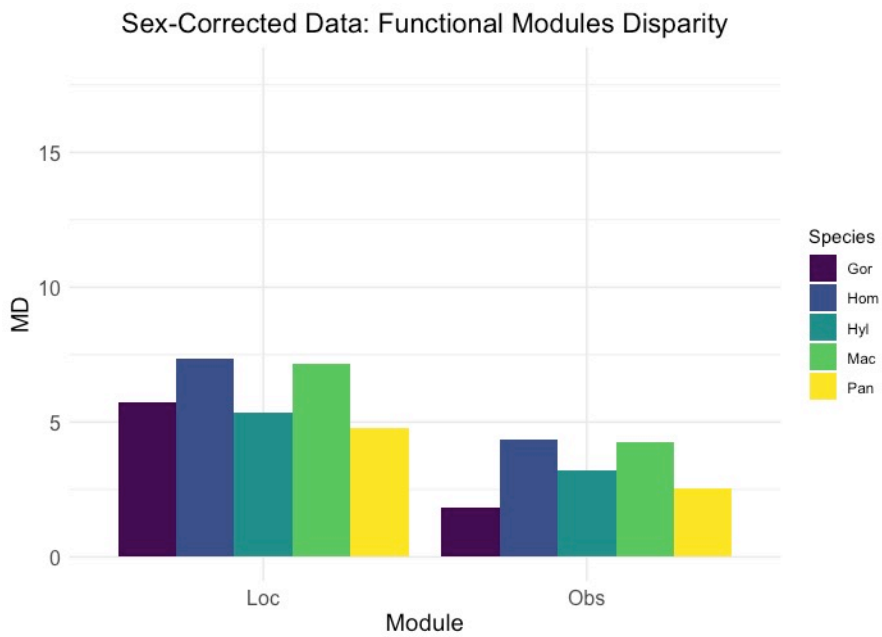
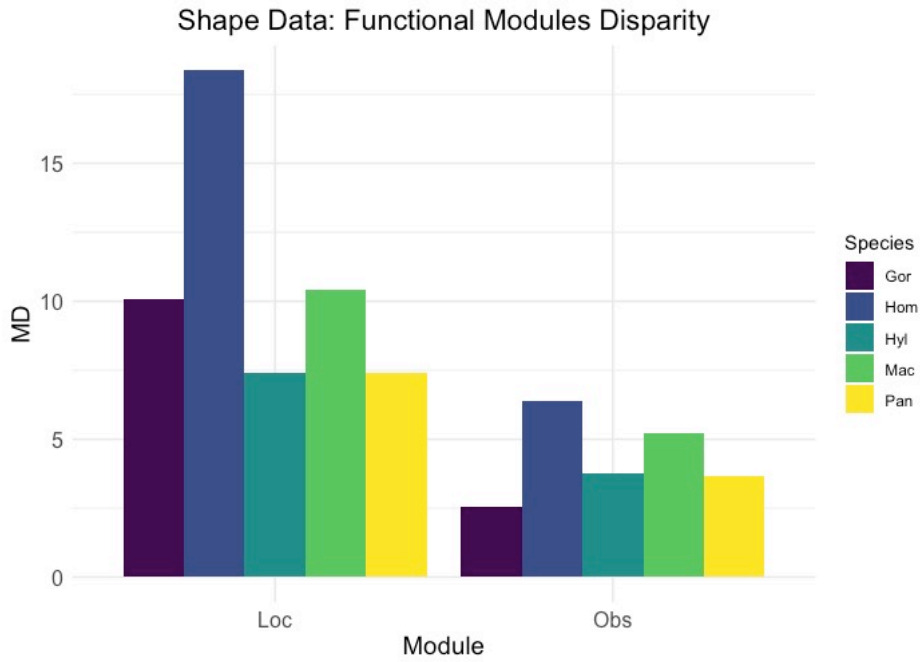


Fig 4.6. Functional module disparity

Shape data top, sex-corrected data bottom. Species: Gor = Gorilla beringei, Hom = Homo sapiens, Hyl = Hylobates lar, Mac = Macaca mulatta, and Pan = Pan paniscus.

Species: Gor = Gorilla beringei, Hom = Homo sapiens, Hyl = Hylobates lar, Mac = Macaca mulatta, and Pan = Pan paniscus. Modules: Il = Ilium, Is = ischium, Pu = pubis, Ac= acetabulum, and Sa = sacrum

	<i>MD (Pv x10⁵)</i>		<i>MD (Pv x10⁵)</i>	
	<i>Shape Data</i>		<i>Sex-Corrected Data</i>	
	Loc	Obs	Loc	Obs
Gor	10.062	2.567	5.725	1.829
Hom	18.369	6.392	7.362	4.370
Hyl	7.412	3.784	5.343	3.231
Mac	10.399	5.204	7.153	4.233
Pan	7.406	3.655	4.797	2.559

Table 4.6. Disparity within and between the functional modules

Species: Gor = Gorilla beringei, Hom = Homo sapiens, Hyl = Hylobates lar, Mac = Macaca mulatta, and Pan = Pan paniscus. Modules: Il = Ilium, Is = ischium, Pu = pubis, Ac= acetabulum, and Sa = sacrum

4.6 Discussion

In this study, we compared human pelvic integration and disparity to those of other primates. We will first discuss the development results. The results of the developmental integration analyses reveal that integration magnitudes within the developmental modules of humans are somewhat differently structured. The ischium and pubis register comparatively higher integration magnitude than observed in other primates, while the magnitudes are similar for the ilium and lower for the acetabulum and sacrum, although admittedly species variability exists throughout the sampled primates. The in-between module integration provides us with a more interesting observation: humans are characterised by reduced levels of between-module integration. This increases the relative independence of its developmental modules and enables each element to respond more directly along the direction of selection, facilitating evolutionary divergence. The reduction aids the divergence of male/female morphologies, as seen by the high morphological and sexual dimorphic disparity levels observed within our species.

In Chapter 2, we highlighted that, unlike the carnivore pelvis, the primate pelvis bauplan consists of a separate ischium and pubis modules. In this chapter, we find that modern humans have taken the disassociation of ischium and pubis one step further. The marked disassociation of the human pubis and ischium features along high internal integration levels of these elements. Pairing integration with morphological disparity demonstrates that high levels of integration within the pubis acts as a constraint; however, the increased ischium integration acts in a facilitating manner promoting responsiveness as observed in the high morphological disparity values (fig 4.4). This association of high integration and high disparity occurs when the high covariation coordinates the response to selection along the direction of selection (Goswami *et al.* 2014, Klingenberg 2014). This theoretical expectation, however, has not often been observed empirically. Randau and Goswami 2017 did find a similar signal present in the Felidae vertebral column, as did we in Chapter 3 pertaining to the allometric effect on the Hominoidea ilium. Here we can add another empirical example to the theoretical discussion: the *Homo sapiens* ischium.

The human ischium is characterised by relatively high autonomy and high variability. This phenomenon is not observed in any of the other primates included within our study, and

warrants further thought as to what may have instigated such a change. Compared to apes, the human ischium is shorter, and the ischial tuberosity more robust and differently angled. The ischium is the attachment site of the hamstring, and changes to the ischium are associated with improved leverage of the hamstring making upright walking more economical (Gruss and Schmitt 2015, Kozma *et al.* 2018). In this light, changes to ischium position may have required increased independence due to bipedal locomotory demands, but not necessarily higher variability. Conversely, high ischium variability facilitates easing the human birthing process as, compared to males, the female ischial tuberosity points outwards and is much further apart to increase the female pelvic outlet size of the birth canal. The increased independence of the human ischium and its associated high variability thus also helps meet obstetrics demands in humans, and plays an important role in the high level of sexual dimorphism expressed within the human pelvis as, for example, seen in the sub-pubic angle. The observed novel human ischium alteration thus serves multiple needs.

What can the fossil record tell us about the potential origin and timing of an increased independent ischium within hominin evolution? The fossil evidence suggests bipedalism traces its origins not long after divergence from our closest ancestor the chimpanzee (8mya) as attested by cranial fragments of *Sahelanthropus tchadenis* (7 mya) (Brunet *et al.* 2002, Zollikofer *et al.* 2005, but see Wolpoff *et al.* 2006 and Macchiarelli *et al.* 2020 for a different interpretation) and proximal femora fragments of *Orrorin tugenensis* (6 mya) (Senut *et al.* 2001, Pickford *et al.* 2002, Almecija *et al.* 2013). The first fossil evidence of pelvic bipedal adaptation is from *Ardipithecus ramidus* (4.4 mya) (Lovejoy 2009, Lovejoy *et al.* 2009). Noted pelvic skeletal alterations of the *Ardipithecus ramidus* (4.4 mya) and *Australopithecus afarensis* (+/- 3.5 mya) (Berge 1994, Lovejoy 1988, Marchal 2003, Rak 1991, Stern and Susman 1983) include medio-lateral expanded iliac blades associated with increased pelvic balance needed during upright walking. The laterally flaring ilia give the overall pelvis a platypelloid shape. Other bipedal features include the craniocaudal shortening of the ilia, liberating the lumbar vertebrae to curve inwardly, providing stability when in an upright position, and the more posteriorly positioning of the sacroiliac joint to ensure effective load transfer between spine and legs (Lovejoy *et al.* 2009, Vleeming *et al.* 2012, Wagner *et al.* 2012). General agreement exists that these early hominins walked upright. However, whether this bipedalism was similar in style and frequency to modern

humans remains debated (Susman *et al.* 1984, Susman and Stern 1991, Ruff 1995, Stern 2000, Lovejoy 2005, Warrener 2013, Gruss and Schmitt 2015). Important to our discussion, the *Australopithecus afarensis* also retained ape-like pelvic features, such as the long ischium and the downwards direction of the ischial tuberosities. This suggests that the more extensive disassociation between the ischium and pubis had not yet taken place, and may not relate to bipedalism or at least not to bipedalism as performed at this time.

The arrival of full human-like gait walking alongside human-like body proportions appears with *Homo* (1.7 mya). Compared to the *Australopithecus afarensis*, the pelvis of *Homo erectus sensu lato* is narrower relative to its stature. The ilia now curve along in a sagittal direction and, along with a repositioned ischium, create the modern human-like bowl shape pelvis (Gruss and Schmitt 2015). Disassociation between the ischium and pubis thus likely occurred before or around this time. The derived *Homo* ischium relates to increased bipedal efficiency by reducing the distance between the acetabulae and the ischial tuberosities (Lovejoy *et al.* 1973, Lovejoy 2005). Furthermore, the ischium is now more robust, associated with increased leverage from the sacrotuberous ligament (Gruss and Schmitt 2015). Greater internal ischium cohesion (i.e. integration) may have been needed to withstand the increased functional demand. On the other hand, *Homo* is also associated with a shift in encephalization (increase in relative brain size) (Wells *et al.* 2012). Therefore, if the repositioned ischium noted at this stage is predominantly a response to changed locomotory, or obstetrics, or combined demands cannot be discerned.

Australopithecus sediba (1.9 mya), a contemporary with early *Homo*, may provide us with the answer. *Au. sediba* presents more *Homo*-like pelvic features, including changes to the ischium (Berger 2010, Churchill *et al.* 2017, Kibii *et al.* 2011). These fossils indicate that some form of ischium disassociation had occurred by this time. Yet the *Au. sediba*, in line with the earlier australopithecines, was a small-statured and small-brained species. Reconstructive modelling suggests *Au. sediba*'s birth canal was spacious in relation to its neonates dimensions (Laudicina and DeSilva 2019), suggesting that obstetrics limitations did not play a significant role in shaping the pelvis of this species. The low levels of sexual dimorphism within the *Au. sediba*'s pelvic form (Kibii *et al.* 2011) further supports this

suggestion. On this basis, we reason that the trend towards disassociation of the human ischium is more likely to be an initial response to improved bipedal efficiency. However, the encephalization events associated with *Homo*, and certainly with *Homo sapiens* (Wells *et al.* 2012), likely further amplified the disassociation to aide divergence of the sexes to help meet the changed obstetric needs. This proposed scenario however, remains to be empirically tested.

We now turn our attention to the functional integration and disparity within the pelvis. The human pelvis has traditionally been viewed as a 'compromise' or 'trade-off' solution to the antagonistic selective pressures of biomechanical efficiency favouring narrow pelvis versus an obstetrically efficient structure for birthing large-brained and large-bodied neonates requiring wide female pelvic inlets (i.e. the obstetric dilemma (OD) Wasburn 1960). Our results indicate that humans are characterized by a reduction of integration between these two aspects – narrow overall pelvis with wide inlets. This would be an effective response to the OD as a means to minimize covariation between traits under different directional selection. As a result, the functional partitions can evolve relatively more autonomously although constraints due to absolute physical limitations remain in place. The inclusion of Rhesus monkey (*Macaca mulatta*) within our analyses enables us to compare humans to another species experiencing obstetric limitations. We found a similar, albeit less pronounced, signal to be present. *Homo* and *Macaca* employ very different locomotory strategies but share the birthing of relative large-bodied neonates compared to their obstetric dimensions. Thus, this reduction in integration is more likely to be a response to obstetric demands than a locomotory need, although other shared variables beyond the present analyses cannot be excluded. The impact of the reduced inherent constraint due to lower integration is noticeable in the obstetric morphological disparity where both modern humans and rhesus monkeys are more disparate compared to the other species included in our analyses. Here, our results are in line with those of the obstetric investigation by Grabowski 2012, who found that 1) higher levels of integration between obstetric and non-obstetric pelvic traits limits the evolutionary potential of the birth canal, and 2) modern humans contain less integration between obstetric and other pelvic traits compared to other apes.

The integration levels of the obstetric partition itself, however, remain remarkably constant across all sampled species despite the development analyses highlighting how the pelvic birth canal - which crosses multiple developmental module boundaries - is likely to be internally structured differently across primate species. We speculate that the birth mechanism needs a certain level of cohesion to properly function. If obstetric integration is reduced, so would its internal cohesion, which may hinder its proper function. If so, for species under obstetric pressure, the only available option is to reduce integration with other non-obstetric pelvic traits. This increases the autonomy of the obstetric partition, enabling it to vary with more ease whilst safeguarding its internal cohesion. This thinking is consistent with the integration observations for humans and the rhesus monkeys. The employed mechanism may also provide greater species evolutionary flexibility as detected in the corresponding disparity values in these species. The tight fit between birth canal and neonate dimensions requires an optimal response to reduce the risk of cephalo-pelvic disproportion. Yet the optimal response may not be uniform across the species, instead it may be dependent on specific aspects of the phenotype and their environmental interaction. Greater plasticity and adaptability are achieved through the in-between reduction, which provides more room for phenotype and population-specific solutions to be formulated. This, in turn, results in a larger pool of species variation for natural selection to act upon.

The pelvis structure, however, is only one half of the equation when it comes to navigating obstetric limitations. Both the birth canal shape/dimension and those of the neonate passing through it are of importance. Past studies have demonstrated that the human pelvic shape co-varies with stature and head size (Bernard 1952, Fischer and Mitteroecker 2015, Holland *et al.* 1982, Tague 2000,). Tall females tend to have larger heads and give birth to large-headed neonates, have on average a more anthropoid (oval) shaped pelvic inlet compared to the more gynecoid (rounder) pelvis shape of shorter and smaller headed females who tend to give birth to smaller neonates. This integration between stature, head size, and pelvis shape is noted in females as well as males. Additionally, Fischer and Mitteroecker 2015 demonstrated that as females increase in head circumference an increase in outward tilt of the sacrum occurs in the female pelvis, thus enlarging the birth canal to enable their large-headed offspring to more easily descend through the birth canal. The integration of pelvis shape, stature, head-size, and neonate

reduces the risk of cephalo-pelvis disproportion, and enables correlated selection. Moreover, a recent study by Kawada *et al.* (2020) demonstrated that cephalo-pelvic covariation to reduce obstetric difficulties is not an exclusive human phenomenon, but is also present in rhesus monkeys. Whether cephalo-pelvic covariation evolved in parallel in *Macaca* and *Homo* due to comparable obstetric limitations, or is a more widely shared phenomenon amongst primates requires further study.

4.7 Conclusion

Here, we have quantified integration and disparity levels of the pelvic structure. The presented study is limited in its sample size, and this must be acknowledged. Nonetheless, based on this limited data we are able to draw similar interpretations as past studies: we find that the modern human integration pattern predominantly diverges from other primates by the reduction of integration across its components. The reduction aids responsiveness to selective pressures and provides a mechanism to generate phenotypic and population specific optimal fits. We found humans to be more disparate in every examined skeletal pelvic element, except for the pubis. A novel human trait is the marked integration disassociation between the ischium and pubis alongside increased integration magnitudes within these elements. For the pubis, the elevated integration translates into reduced levels of disparity indicative of constraints. The increased ischium integration, however, promotes variability in an empirical example of high integration acting not in a constraining but a facilitating manner. The 'liberated' ischium may be an initial response to selection towards increased bipedal efficiency; however, the increased ischium variability also plays a key role in easing parturition in modern humans.

Interestingly, past research by Mitteroecker and Bookstein (2008), Marroig *et al.* (2009), and Porto *et al.* (2009) also found reduced levels of integration and increased evolutionary flexibility in the human cranium compared to other primates. As bipedalism and encephalization are key hominin adaptations, the reduction of integration magnitudes in both the pelvis and cranium suggests that altered integration levels played a key role in facilitating human evolution. How these two elements are interlinked from an integration point of view, however, remains to be elucidated in future studies.

Our study also carries implications for the study of human obstetrics. Within our study, the inherent constraint levelled within human obstetrics and its corresponding variability could not have easily be understood by examining the birth canal in isolation. Only by placing obstetrics into the wider pelvis context did the observed increased in variability makes sense. Combined with past studies highlighting that the birth canal correlates beyond the pelvis structure (e.g see Fischer and Mitteroecker 2015), investigations in broader skeletal context have much potential to further our insights into the complex and interacting intrinsic mechanisms that govern obstetrics and indeed all other pelvic components.

4.8 Supplementary Information

S1: Morphospace of species

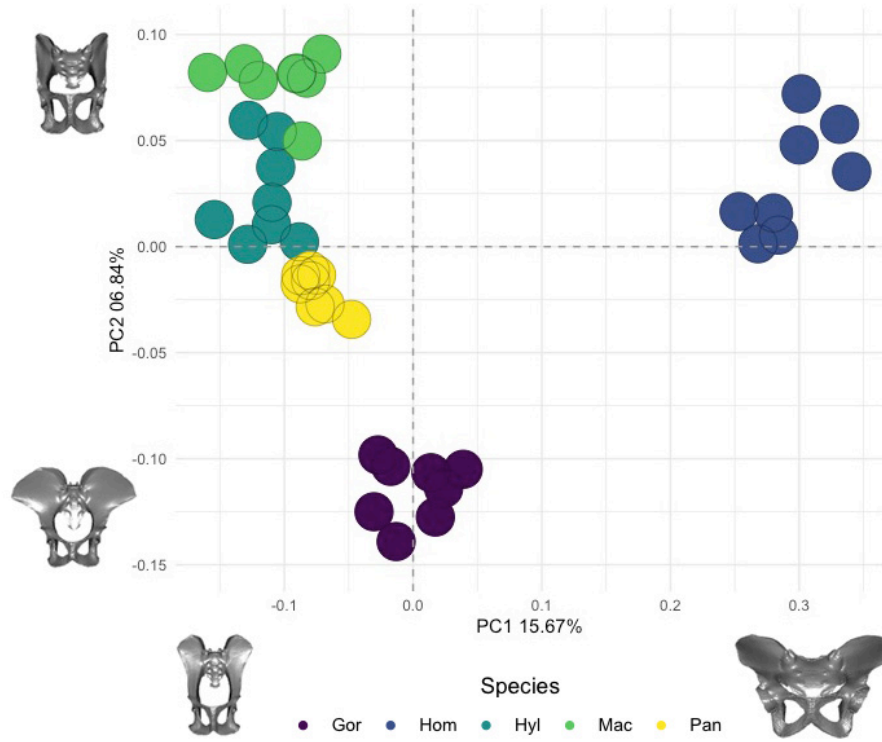


Fig S1. *Shape data*: morphospace of species variation along PC1-PC2 axes

S2: Size differences of species

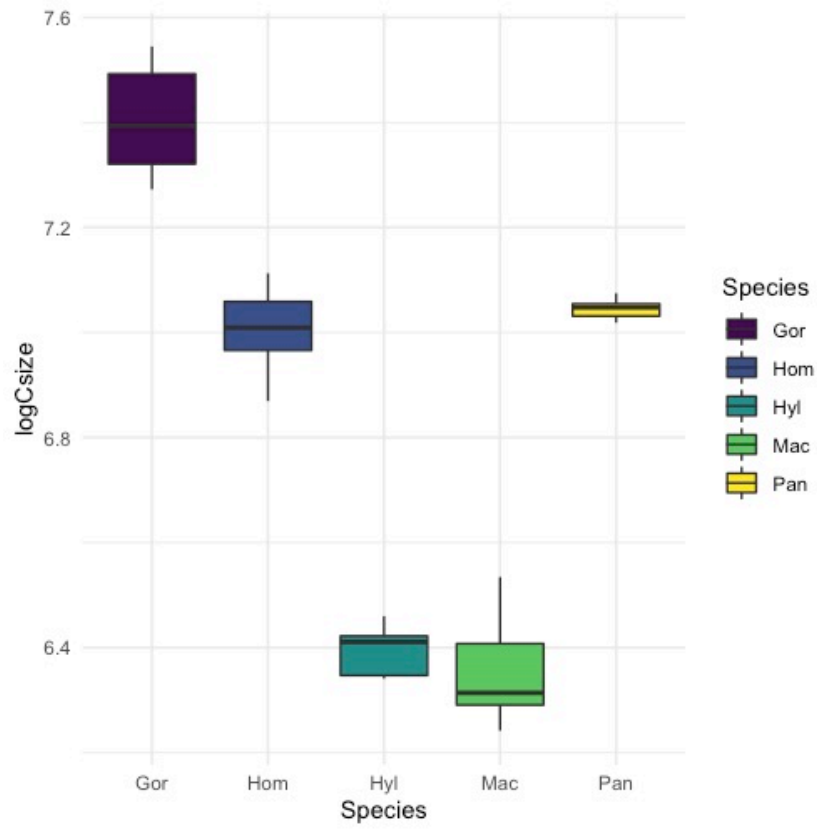


Fig S2. Boxplot size differences of species

S3: Developmental modules: pairwise differences of species disparity

<i>Shape Data</i>		Gor	Hom	Hyl	Mac	Pan
Il	Gor		0.043	0.586	0.789	0.210
	Hom	4.4342		0.006	0.023	0.002
	Hyl	1.2982	5.7324		0.752	0.501
	Mac	0.5697	5.0039	0.7285		0.306
	Pan	2.7494	7.1835	1.4511	2.1796	
Is	Gor		0.003	0.423	0.799	0.725
	Hom	10.714		0.001	0.004	0.001
	Hyl	2.7768	13.4907		0.271	0.651
	Mac	0.9137	9.8002	3.6905		0.567
	Pan	1.1078	11.8218	1.6689	2.0216	
Pu	Gor		0.229	0.242	0.053	0.318
	Hom	1.1272		0.990	0.450	0.850
	Hyl	1.1391	0.0119		0.464	0.857
	Mac	1.8481	0.7208	0.709		0.365
	Pan	0.9514	0.1758	0.1877	0.8966	
Ac	Gor		0.403	0.176	0.760	0.445
	Hom	0.7888		0.020	0.560	0.103
	Hyl	1.2020	1.9908		0.086	0.668
	Mac	0.2646	0.5242	1.4666		0.214
	Pan	0.7028	1.4916	0.4992	0.9674	
Sa	Gor		0.002	0.852	0.350	0.771
	Hom	3.752		0.005	0.057	0.003
	Hyl	0.2693	3.4827		0.461	0.625
	Mac	1.2436	2.5083	0.9744		0.235
	Pan	0.396	4.148	0.6653	1.6397	

Table S3.1 *Shape data*: developmental module pairwise differences of species disparity and p-values

<i>Sex-Corrected Data</i>		Gor	Hom	Hyl	Mac	Pan
Il	Gor		0.346	0.885	0.412	0.218
	Hom	1.3255		0.295	0.907	0.025
	Hyl	0.2095	1.5350		0.357	0.258
	Mac	1.1630	0.1625	1.3726		0.046
	Pan	1.7979	3.1234	1.5883	2.9609	
Is	Gor		0.258	0.818	0.127	0.645
	Hom	1.5014		0.178	0.693	0.523
	Hyl	0.3012	1.8026		0.079	0.476
	Mac	2.0127	0.5114	2.3139		0.277
	Pan	0.6137	0.8877	0.9149	1.399	
Pu	Gor		0.271	0.103	0.069	0.384
	Hom	0.8532		0.556	0.463	0.833
	Hyl	1.3219	0.4687		0.894	0.465
	Mac	1.4480	0.5948	0.1261		0.375
	Pan	0.6897	0.1635	0.6322	0.7583	
Ac	Gor		0.676	0.391	0.404	0.683
	Hom	0.2777		0.215	0.679	0.407
	Hyl	0.5484	0.8261		0.086	0.668
	Mac	0.5489	0.2713	1.0974		0.214
	Pan	0.264	0.5417	0.2844	0.813	
Sa	Gor		0.493	0.602	0.399	0.120
	Hom	0.4142		0.218	0.875	0.033
	Hyl	0.3581	0.7723		0.173	0.309
	Mac	0.5174	0.1032	0.8754		0.018
	Pan	0.9906	1.4048	0.6326	1.508	

Table S3.2. Sex-corrected data: developmental modules pairwise differences of species disparity and p-values

Disparity values (Pv) below the diagonal, associated p-values above. Bold values indicate $p \leq 0.005$. Species: Gor = Gorilla beringei, Hom = Homo sapiens, Hyl = Hylobates lar, Mac = Macaca mulatta, and Pan = Pan paniscus. Modules: Il = Ilium, Is = ischium, Pu = pubis, Ac= acetabulum, and Sa = sacrum.

S4: Functional modules: pairwise differences of species disparity

<i>Shape Data</i>		Gor	Hom	Hyl	Mac	Pan
Obs	Gor		0.001	0.270	0.013	0.285
	Hom	3.8259		0.006	0.279	0.006
	Hyl	1.2172	2.6087		0.167	0.905
	Mac	2.6376	1.1884	1.4204		0.146
	Pan	1.0886	2.7373	0.1286	1.549	
Loc	Gor		0.001	0.289	0.890	0.264
	Hom	8.3067	0	0.001	0.001	0.001
	Hyl	2.6502	10.9569		0.245	0.910
	Mac	0.337	7.9698	2.9871	0	0.244
	Pan	2.6563	10.963	0.0061	2.9932	

Table S4.1. *Shape data*: functional modules pairwise differences of species disparity and p-values

Disparity values (Pv) below the diagonal, associated p-values above. Bold values indicate $p \leq 0.005$. Species: Gor = Gorilla beringei, Hom = Homo sapiens, Hyl = Hylobates lar, Mac = Macaca mulatta, and Pan = Pan paniscus. Modules: Il = Ilium, Is = ischium, Pu = pubis, Ac= acetabulum, and Sa = sacrum.

<i>Sex-Corrected Data</i>		Gor	Hom	Hyl	Mac	Pan
Obs	Gor		0.003	0.083	0.003	0.371
	Hom	2.5414		0.152	0.853	0.016
	Hyl	1.4025	1.1389		0.192	0.372
	Mac	2.4045	0.1368	1.0020		0.028
	Pan	0.7300	1.8114	0.6725	1.6745	
Loc	Gor		0.162	0.750	0.223	0.441
	Hom	1.6366		0.089	0.873	0.030
	Hyl	0.3819	2.0185		0.123	0.643
	Mac	1.4283	0.2083	1.8102		0.060
	Pan	0.9276	2.5642	0.5457	2.3559	

Table S4.2. Sex-corrected data: functional modules pairwise differences of species disparity and p-values

Disparity values (Pv) below the diagonal, associated p-values above. Bold values indicate $p \leq 0.005$. Species: Gor = Gorilla beringei, Hom = Homo sapiens, Hyl = Hylobates lar, Mac = Macaca mulatta, and Pan = Pan paniscus. Modules: Il = Ilium, Is = ischium, Pu = pubis, Ac= acetabulum, and Sa = sacrum.

Chapter 5:

Conclusion and Future Directions

Evolutionary trajectories are most commonly reconstructed by comparing the shape and size of fossils to other fossils and extant life, using similarities and differences to draw inferences about behaviour, locomotion, and phylogenetic relatedness. This comparative approach has provided valuable information on past and current life forms, as have the many proposed hypotheses pertaining to the causes of the observed changes. Yet, such comparisons provide little information about the inherent evolutionary processes involved, and how these intrinsic mechanisms bias the evolutionary trajectories. Approaching evolutionary questions by employing modularity and integration enables us to focus on these processes and mechanisms, and to assess their role in influencing evolutionary trajectories and diversity. This allows for evolutionary questions to be approached from different points of view, and analyses built upon these theoretical foundations hold great potential to broaden and even change our understanding of particular evolutionary histories.

In the present thesis, I have focused on the morphology of the primate pelvis and applied such an approach. Specifically, the overarching aim of the thesis was to investigate the role of modularity and integration in shaping the primate pelvic girdle evolution. To do so, three research questions were posed, which I here revisit.

- 1) what is the inner modular structure of the pelvic girdle, and which processes underlie its structuring?
- 2) how may integration constrain or facilitate the ability of the pelvic girdle to respond to natural selection?
- 3) what is the role of integration in the morphological divergence of the human pelvis?

5.1 What is the inner modular structure of the pelvic girdle, and which processes underlie its structuring?

Chapter 2 addressed this question. To gain insights into the pelvis organisational structure, and the processes involved in modulating the primate pelvic girdle, I assessed four different developmental and one functional modular hypotheses. These hypotheses were tested upon the whole primate order, and four phylogenetic groups: Lemuroidea, Ceboidea (New World monkeys), Cercopithecoidea (Old World monkeys), and Hominoidea (excluding humans). The results indicated that, at macroevolutionary level, the primate pelvis is a modular structure, and that the developmental processes more strongly modulate the pelvis than shared functionality. I found that the modular organisational structure best matches the developmental partition along the ilium, ischium, pubis, acetabulum, and sacrum. Moreover, the uncovered pattern is ancestrally shared across primates apart from potentially lemuroids among whom the acetabulum appears less modular compared to the other primate groups.

The observed dominant primate modular pattern differs from carnivores (Martin-Serra *et al.* 2018) whereby in the latter group the ischium and pubis co-vary more closely compared to primates. Primates thus seem to be marked by an increased modular pubis and ischium. If this a primate-specific characteristic, or if such an increased parcellation of ischium and pubis is also present in other mammalian groups remains to be investigated. The presence of a relatively autonomous ischium and pubis is observed in all examined phylogenetic groups, suggesting this characteristic was present in basal primates although this remains to be confirmed until sufficient primate pelvis fossil data and outgroups can be added to the examined data set.

I did, however, also find a significant functional modular signal (locomotion-obstetrics) to be present within the primate pelvis, although it is less strong compared to the developmental partition. The existence of such a functional modulation indicates that the bony morphologies involved with locomotion and obstetrics can alter and evolve relatively autonomously from each other within the pelvis structure. This, in turn, may alleviate the difficulty of navigating potential different locomotion and obstetric selective directions, and may have played an assisting role in primate locomotory diversification

and sexual dimorphisms (Fleagle 2013, Gebo 2014). If such a modular structure is also present in other mammalian groups is currently untested and unknown.

Overall, the presence of both developmental and functional modularity demonstrates that the modularity pattern of the primate pelvic girdle is multi-layered with developmental processes meeting functional needs in a synergistically manner. Understanding how this is achieved will, however, require a hierarchical investigative approach. Unfortunately, the required statistical toolkit to combine geometric morphometric data with such a hierarchical methodology is lacking at the present time (Goswami *et al.* 2019). Hopefully, it will not be long before pursuing such an avenue will become possible in future studies.

5.2 How may integration constrain or facilitate the ability of the pelvic girdle to respond to natural selection?

Modular pattern and integration magnitudes do not only describe the manner and strength of the relationships of biological parts but also raise question as to how they may influence shape variability and bias evolutionary trajectories. In Chapter 3, I explicitly clarified the role of morphological integration in diversity and its impact on evolutionary possibility. Building upon the results of Chapter 2, I used the dominant modular structure - ilium, ischium, pubis, acetabulum, and sacrum – in order to examine whether the integration magnitudes of the developmental modules may constrain or facilitate evolution. I also explored whether the influence of integration is similar or different across phylogenetic and locomotory groups.

The results demonstrated that, overall, an inverse relationship exists between integration and morphological disparity, indicative of integration acting as a constraining factor on morphological diversity and evolutionary flexibility (Wagner 1996, Lynch and Walsh 1998, Hansen 2003, Hansen and Houle 2004, Hansen and Houle 2008, Goswami *et al.* 2014, Felice *et al.* 2018). This pattern of constraint is equally detectable in the primate order, in the clades, and in the locomotory groups, suggesting that this pattern is shared and conserved across the examined primates. Whether integration influences other mammalian pelvis structures in a similar way remains to be investigated. Furthermore,

access to detailed genetic and developmental information on the processes involved in morphogenesis are required to determine the precise drivers underpinning and governing the observed integration magnitudes. Nevertheless, whilst a better understanding of the underlying causes requires further study, integration magnitudes and their impact on evolutionary trajectories and diversity have now, for the first time, been identified.

Interesting observations were also made pertaining the ilium and pubis. Ilium disparity can, in part, be attributed to allometry. The assisting effect of increased body size on novel ilia shape is unsurprisingly particularly noticeable among the large-bodied hominoids. The pubis is another interesting module. Pubis disparity is lower than expected in relation to its integration magnitude, indicative of another factor playing a constraining role on disparity. Identifying the additional source of pubis constraint will require further investigations.

The study of the impact of integration within the locomotory groups raised interesting questions. Whereas overall the locomotory groups follow a pattern of constraint, differences in body position during locomotion does seem to play a part in obtained integration values. Terrestrial and arboreal quadrupeds (generalists) which hold their body in a pronograde position tend to display low module and particularly between module integration values compared to the specialist locomotion groups (vertical clinging and leaping, brachiation, suspension, and tail prehensility) which are performed with an orthograde trunk position. These differing locomotory forms and body positions translate into differing pelvic biomechanical loading and transmission regimes which may explain the observed integration magnitudes.

The findings have implications on how we may interpret morphological pelvic traits as adaptation. Since the results demonstrate that integration acts as a constraint, the correlated response can act as a stabilising factor or even move the direction of morphological change away from the direction of selection (Marroig *et al.* 2009, Porto *et al.* 2009, Goswami *et al.* 2014). The observed changes may be a side-effect and not a response to selection (Gould and Lewontin 1979). Constraint is problematic when reconstructing the evolution of traits, and evolutionary models will need to consider integration magnitudes to accurately reconstruct evolutionary trait histories. How our

field may effectively incorporate the effects of constraint within evolutionary models is an interesting but as of yet unanswered question.

5.3 What is the role of integration in the morphological divergence of the human pelvis?

In Chapter 4, I examined the human pelvis in a comparative framework. The human pelvis shape diverges significantly from other primates, making it an interesting research topic to investigate the role that integration may have played in facilitating this divergence. The study demonstrated that the reduction of integration levels across the different anatomical pelvic elements is a particular human characteristic. Moreover, elevated levels of evolutionary flexibility were observed alongside the reduced integration magnitudes, indicative of reduced constraints. The reduced constraint facilitates human pelvic traits to evolve in a more independent manner compared to the other sampled primate species. This permits the human pelvic bauplan to be more responsive to multiple selective pressures, and more flexible in shaping phenotypic and population specific solutions.

Another specific human characteristic I found was the increased disassociation between the pubis and ischium. This extended parcellation occurs alongside increased integration magnitudes within these two elements. The high level of human pubic integration acts as a constraint on its morphological variability, limiting its evolutionary possibilities. On the other hand, the high ischial integration level is linked to a high level of disparity, providing us with another empirical example of high integration facilitating evolutionary responsiveness. As mentioned above, and based on the current available information, the parcellation of pubis and ischium seems to be a defining primate characteristic (see Chapter 2). Humans built upon this primate pelvic architecture and further increased the ischium-pubis parcellation. From a human evolutionary perspective, the 'liberated' ischium is a beneficial feature serving both efficient bipedalism and parturitions of large-brained infants. The enhanced parcellation of ischium and pubis, combined with a general reduction of integration between the pelvic modules facilitated the relevant traits to respond with more ease and greater extent to the multiple directions of selection compared to those of the other analysed primates. Changes to the integration

magnitudes thus facilitated the evolution of the hominin pelvis and its morphological divergence.

Ischium variability is prominent among primates: quadrupeds have longer ischia than non-quadrupeds. Vertical clingers and Leapers (VLC) and bipeds (i.e. humans) are particular in this respect: they have shortened and dorsally bent ischia. Moreover, both VLC and bipeds share prominent ischial spines while these are small or absent in other primates (Waterman 1929, Abitol 1988, Lewton 2010). In this respect, humans may have perhaps more in common with VLC than our closest phylogenetic relatives. Further studies should consider the inclusion of VLC primates to examine if VLC primate species may carry a similar 'liberated' ischium signal as seen in humans.

The study of Chapter 4 is also important in two other aspects. Firstly, the investigation of the functional partitions enabled me to confirm the findings by Grabowski (2012), who found that the reduced integration between obstetrics and locomotion is key to increased human evolutionary flexibility of the obstetric partition. Grabowski employed linear measurement and Lande's (1979) breeder equation as a measure of evolutionary flexibility on a large data set. I found a similar signal in my study, yet I employed very different methods: geometric morphometrics combined with congruent vector correlation matrix and morphological disparity as a measure of evolutionary flexibility. I also used a small data set ($n=8$). This demonstrates that studies employing very different methods do obtain comparable results.

The second importance relates to how we approach the question of obstetric variability. The results indicated that the level of integration within the obstetrics module remains very similar across the sampled species; yet, humans displayed greater variation. Only by placing the obstetric partition in the wider pelvis context did the noted high human disparity make sense. Focusing on just obstetrics may not be conducive to understanding differences between species variability. Of course, such critique can equally, and rightly so, be levelled at the present studies. Indeed, the pelvis is not an isolated element within the overall integrated biological phenotype. How and the manner in which the pelvis co-varies with other elements remains to be investigated until such time that an appropriate data set can be constructed. It will be of particular interest to investigate the relationship

of the pelvis within the hind-limb structure, of which the pelvis forms a part, and the wider appendicular skeleton. Moreover, past studies (e.g. see Bernard 1952, Holland *et al.* 1982, Fischer and Mitteroecker 2015) have demonstrated a link between the pelvis and head morphologies. How and the manner in which these two elements co-vary from a modularity and integration perspective will be another interesting avenue to pursue in future studies.

5.4 The role of modularity and integration in shaping the primate pelvic girdle evolution

Overall, what can be said about the role of modularity and integration in shaping primate pelvis evolution and disparity? The primate pelvis is dominantly modulated by the developmental processes, with ilium, ischium, pubis, acetabulum, and sacrum all varying and evolving in a relative independent manner from one another. Primates, as an order, represents a diverse mammalian group (Lewton 2010, Fleagle 2013). Compared to the modular pattern of carnivores (Martin-Serra *et al.* 2018), primate diversity may be facilitated by the increased parcellation of the ischium and pubis. The pubis-ischium parcellation is present in all examined primate phylogenetic groups, suggestive that this was present among the basal primates. The integration of these modules acts as a constraint, limiting evolutionary possibilities and diversity. Yet allometry plays a role in facilitating novel ilia form, whereas the pubis contains another constraining factor not captured within this thesis.

It is within this primate context that humans evolved. The human integration levels are marked by reduction across pelvic constituents and further increased parcellation of pubis and ischium. The integration levels within the human pubis and ischium are remarkably high. In the case of the pubis, it translates to reduced variability and evolutionary flexibility. Conversely, the high ischium integration acts as a facilitator to increase disparity and evolutionary flexibility. The latter played a pivotal role in both bipedal efficiency and increased levels of sexual dimorphism, whereby the different positioning of the human female ischium is an important aspect to ease parturition. The overall reduction of integration between the human pelvis constituents provides the human pelvic bauplan with increased flexibility to respond to multiple selective pressures.

Nonetheless, in a biological context no element or trait is truly independent nor is the pelvis and its constituent modules. Future research should prioritise placing the pelvis into its broader context, and investigate pelvic integration and covariation within the wider skeletal structure. Equally, future research focussing on mammalian comparatives and deep time frameworks are needed to further our understanding of the role and impact of modularity and integration on primate and mammalian evolution and diversity of life.

References

- Abitbol, M.M. 1988. Evolution of the ischial spine and of the pelvic floor in the Hominoidea. *American Journal of Physical Anthropology* 75: 53-67
- Ackermann, R. R. 2005. Ontogenetic integration in the hominoid face. *Journal of Human Evolution* 48:175-197
- Ackermann, R.R., and Cheverud, J.M. 2004. Morphological integration in primate evolution. In (eds.) Pigliucci, M., and Preston, K.: *Phenotypic Integration: Studying the Ecology and Evolution of Complex Phenotypes*. Oxford: Oxford University Press. Pp. 302-319
- Adams, D.C. 2014a. A generalized K statistic for estimating phylogenetic signal from shape and other high-dimensional multivariate data. *Systematic Biology* 63: 685-697
- Adams, D.C. 2014b. A method for assessing phylogenetic least squares models for shape and other high-dimensional multivariate data. *Evolution* 68: 2675-2688
- Adams, D.C. 2014c. Quantifying and comparing phylogenetic evolutionary rates for shape and other high-dimensional phenotypic data. *Systems Biology* 63: 166-177
- Adams, D.C. 2016. Evaluating modularity in morphometric data: challenges with the RV coefficient and a new test measure. *Methods in Ecology and Evolution* 7: 565-572
- Adams, D.C., and Collyer, M.L. 2015. Permutation tests for phylogenetic comparative analyses of high-dimensional shape data: what you shuffle matters. *Evolution* 69: 823-829
- Adams, D. C., and Collyer, M. L. 2017. Multivariate phylogenetic comparative methods: evaluations, comparisons, and recommendations. *Systems Biology* 67: 14-31
- Adams, D.C., and Collyer, M.L. 2019. Comparing the strength of modular signal, and evaluating alternative modular hypotheses, using covariance ratio effect sizes with morphometric data. *Evolution* 73: 2352-2367
- Adams, D.C., and Otárola Castillo E. 2013. Geomorph: An R package for the collection and analysis of geometric morphometric shape data. *Methods in Ecology and Evolution* 4: 393-399
- Adams, D.C., Rohlf, F.J., and Slice, D.E. 2013. A field comes of age: Geometric morphometrics in the 21st century. *Hystrix* 27:7-14
- Adams, D.C., Rohlf, F.J., and Slice, D.E. 2004. Geometric morphometrics: ten years of progress following the 'revolution'. *Italian Journal of Zoology* 71(1): 5-16
- Aiello, L., and Dean, C. 1990. *An introduction to human evolutionary anatomy*. London, UK: Academic Press

- Almecija, S., Tallman, M., Alba, D.M., Pina, M., Muya-Sola, S., and Jungers, L.J. 2013. The femur of *Orrorin tugenensis* exhibits morphometric affinities with both Miocene apes and later hominins. *Nature Communications* 4:2888
- Altenberg, L. 1994. The evolution of evolvability in genetic programming. In K. E. Kinnear (ed.) *Advances in genetic programming*. Cambridge, MA: MIT Press. Pp. 47-74
- Altenberg, L. 2005. Modularity in evolution: some low-level questions. In W. Callebaut and D. Rasskin-Gutman (eds.) *Modularity: understanding the development and evolution of complex natural systems*. Cambridge, MA: MIT Press. Pp 99-128
- Anemone, R.L. 1993. The functional anatomy of the hip and thigh in primates. In D.L. Gebo (ed.): *Postcranial adaptation in nonhuman primates*. DeKalb, IL: Northern Illinois University Press. Pp 150-174
- Ankel-Simons F. 2000. *Primate Anatomy*. New York: Academic Press
- Arnold, S. J. 1992. Constraints on phenotypic evolution. *American Naturalist* 140(1): S85-S107
- Arnold, C., Matthews, L.J., and Nunn, C.L. 2010. The 10kTrees website: a new online resource for primate phylogeny. *Evolutionary Anthropology* 19:114-119
- Arnqvist, G., and Martensson, T. 1998. Measurement error in geometric morphometrics: Empirical strategies to assess and reduce its impact on measures of shape. *Acta zoologica Academiae Scientiarum Hungaricae* 44(1): 73-96
- Baab, K. L. 2013. The impact of superimposition choice in geometric morphometric approaches to morphological integration. *Journal of Human Evolution* 65: 689-692
- Baab, K.L., McNulty, K.P., and Rohlf, F.J. 2012. The shape of human evolution: a geometric morphometric perspective. *Evolutionary Anthropology* 21: 151-165
- Baab, K.L., Perry, J.M.G., Rohlf, F.J., and Jungers, W.L. 2014. Phylogenetic, ecological, and allometric correlates of cranial shape in malagasy lemuriforms. *Evolution*. 68: 1450-146
- Bardua, C., Fabre, A.-C., Bon, M., Das, K., Stanley, E.L., Blackburn, D.C., and Goswami, A. 2020. Evolutionary integration of the frog cranium. *Evolution* 76(3): 1200-1215
- Bardua, C., Felice, R.N., Watanabe, A., Fabre, A.C., and Goswami, A. 2019a. A practical guide to surface sliding semi-landmarks in morphometric analyses. *Integrative Organismal Biology* 1(1): obz016
- Bardua C., Wilkinson M., Gower D.J., Sherratt E., and Goswami A. 2019b. Morphological evolution and modularity of the caecilian skull. *BMC Evolutionary Biology* 19(30): s12862-018-1342-7

- Bezanson, M. 2017. Primate Positional Behavior Development and Evolution. *Annual Review of Anthropology* 46:279-298
- Bastir, M., and Rosas, A. 2005. Hierarchical nature of morphological integration and modularity in the human posterior face. *American Journal of Physical Anthropology* 128: 26e34
- Berg, R.L. 1960. The ecological significance of correlation pleiades. *Evolution* 14: 171-180
- Berge, C. 1994. How did the australopithecines walk? A biomechanical study of the hip and thigh of *Australopithecus afarensis*. *Journal of Human Evolution* 26: 259-273
- Berger, L.R., de Ruiter, D.J., Churchill, S.E., Schmid, P., Carlson, K.J., Dirks, P.H.G.M., and Kibii, J.M. 2010. Australopithecus sediba: A New Species of Homo-Like Australopith from South Africa. *Science* 328: 195-204
- Bernard, R.M. 1952. The shape and size of the female pelvis. *Edinburgh Medical Journal* 59(2): 1-15
- Betti, L., von Cramon-Traubadel, N., Manica, A., and Lycett, S.J. 2013. Global Geometric Morphometric Analyses of the Human Pelvis Reveal Substantial Neutral Population History Effects, Even across Sexes. *PLoS ONE* 8(2): e55909
- Betti, L., and Manica, A. 2018. Human variation in the shape of the birth canal is significant and geographically structured. *Proceedings of the Royal Society of London B* 285: 2018807
- Blomberg, S.P., Garland, T., and Ives, A.R. 2003. Testing for phylogenetic signal in comparative data: behavioral traits are more labile. *Evolution* 57:717-745
- Bon, M., Bardua, C., Goswami, A., and Fabre, A. C. 2020. Cranial integration in the fire salamander, *Salamandra salamandra* (Caudata: Salamandridae). *Biological Journal of the Linnean Society*, 130(1): 178-194
- Bookstein, F.L. 1991. Morphometric tools for landmark data: geometry and biology. Cambridge: Cambridge University Press
- Bookstein, F.L. 1997. Landmark methods for forms without landmarks: morphometrics of group differences in outline shape. *Medical Image Analysis* 1(3): 225-243
- Breuker, C.J., Debat, V., Klingenberg, C.P. 2006. Functional evo-devo. *Trends in Ecology & Evolution* 21: 488-492
- Brunet, M., Guy, F., Pilbeam, D., et al. 2002. A new hominid from the Upper Miocene of Chad, Central Africa. *Nature* 418: 145-151
- Buikstra, J.E., and Ubelaker, D. 1994. *Standards for data collections from human skeletal remains* (Research Series 44). Fayetteville: Arkansas, archaeological survey research

- Capellini, T.D., Handschuh, K., Quintana, L., Ferretti, E., Di Giacomo, G., and Fantini, S. 2011. Control of pelvic girdle development by genes of the Pbx family and Emx2. *Developmental Dynamics: An Official Publication of the American Association of the Anatomists* 240(5): 1173-1189
- Cardini, A. 2016. Lost in the other half: improving accuracy in geometric morphometric analyses of one side of bilaterally symmetric structures. *Systems Biology* 65: 1096-1106
- Cardini, A. 2017. Left, right or both? Estimating and improving accuracy of one-side-only geometric morphometric analyses of cranial variation. *Journal of Zoological Systematics and Evolutionary Research* 55: 1-10
- Cardini, A. 2019. Integration and modularity in Procrustes shape data: is there a risk of spurious results? *Evolutionary Biology* 46: 90-105
- Cheverud, J.M. 1982. Phenotypic, genetic, and environmental morphological integration in the cranium. *Evolution* 36: 499-516
- Cheverud, J.M. 1984. Quantitative genetics and developmental constraints on evolution by selection. *J. Theor. Biol.* 110: 155-171
- Cheverud, J.M. 1988. A comparison of genetic and phenotypic correlations. *Evolution* 42: 954-968
- Cheverud, J.M. 1995a. Morphological integration in the saddle-back tamarin (*Saguinus fuscicollis*) cranium. *American Naturalist* 145: 63-89
- Cheverud, J.M. 1996a. Developmental integration and the evolution of pleiotropy. *American Zoologist* 36: 44-50
- Cheverud, J.M. 1996b. Quantitative genetic analysis of cranial morphology in the cotton-top (*Saguinus oedipus*) and saddle-back (*S. fuscicollis*) tamarins. *Journal of Evolutionary Biology* 9: 5-42
- Cheverud, J.M., Routman, E.J., and Irschick, D.J. 1997. Pleiotropic effects of individual gene loci on mandibular morphology. *Evolution* 51: 2006-2016
- Churchill, S.E., Kibii, J.M, Schmid, P., Reed, N.D., and Berger, L.R. 2017. The Pelvis of *Australopithecus sediba*. *PaleoAnthropology* 2018: 334–356
- Clausen, J., and Hiesey, W.M. 1960. The balance between coherence and variation in evolution. *Proc. Natl.Acad. Sci. USA* 46: 494-506
- Clune, J., Mouret, J-B., and Lipson, H. 2013. The evolutionary origins of modularity. *Proceedings of the Royal Society B* 280: 20122863–20122863

- Collyer, M.L, Sekora, D.J., Adams, D.C. 2015. A method for analysis of phenotypic change for phenotypes described by high-dimensional data. *Heredity* 115: 357-365
- Darwin, C.R. 1859. *On the origin of species by means of natural selection*. London, John Murray
- Drake, A., and Klingenberg, C. 2010. Large-Scale Diversification of Skull Shape in Domestic Dogs: Disparity and Modularity. *The American Naturalist* 175: 289-301
- Dryden, I.L., and Mardia, K.V. 1998. *Statistical shape analysis*. Chichester: Wiley
- Dytham, C. 2011. *Choosing and using statistics: a biologist's guide*. Chichester: Wiley-Blackwell. Third edition.
- Eble, G.J 2004. The macroevolution of phenotypic integration. In M. Pigliucci and K. Preston (eds.): *Phenotypic integration: studying the ecology and evolution of complex phenotypes*. Oxford: Oxford University Press. Pp. 253-273
- Esteve-Altava, B. 2017. In search of morphological modules: a systematic review. *Biological Reviews* 92: 1332-1347
- Fabre, A.C., Bardua, C., Bon, M., Clavel, J., Felice, R.N., Streicher, J.W., Bonnel, J., Stanley, E.L., Blackburn, D.C., and Goswami, A. 2020. Metamorphosis shapes cranial diversity and rate of evolution in salamanders. *Nature Ecology and Evolution* 4: 1129-1140
- Felice R.N. and Goswami A. 2018. Developmental origins of mosaic evolution in the avian cranium. *Proceedings of the National Academy of Sciences of the United States of America* 115: 555-560.
- Felice, R.N., Randau, M., and Goswami, A. 2018. A fly in a tube: Macroevolutionary expectations for integrated phenotypes. *Evolution* 72: 2580-2594
- Fisher, R.A. 1958. *Statistical methods for research workers*. New York: Oliver and Boyd
- Fleagle, J. G. 2013. *Primate Adaptation and Evolution*. San Diego: Elsevier. Third Edition
- Fleagle, J.G., Anapol, F.C. 1992. The indriid ischium and the hominid hip. *Journal of Human Evolution* 22: 285-305
- Frost, H.M. 1990a. Skeletal structural adaptations to mechanical usage (SATMU): 1. Redefining Wolff's Law: The bone modelling problem. *The Anatomical Record* 226: 403-413
- Frost HM. 1990b. Skeletal structural adaptations to mechanical usage (SATMU): 2. Redefining Wolff's Law: The remodelling problem. *The Anatomical Record* 226: 414-422
- Gebo, D.L. 2014. *Primate comparative anatomy*. Maryland: John Hopkins University Press

- Goodall, C. R. 1991. Procrustes methods and the statistical analysis of shape (with discussion). *Journal of Royal Statistical Society B* 53: 285-340
- Gomez-Robles, A., Hopkins, W.D., and Sherwood, C.C. 2014. Modular structure facilitates mosaic evolution of the brain in chimpanzees and humans. *Nature Communications* doi 10.1038/ncomms5469
- Goswami, A. 2006. Cranial modularity shifts during mammalian evolution. *The American Naturalist* 168: 270-280
- Goswami, A. and Finarelli, J.A. 2016. EMMLi: a maximum likelihood approach to the analysis of modularity. *Evolution* 70(7): 1622-1637
- Goswami A., and Polly, P.D. 2010a. Methods for studying morphological integration and modularity. In J. Alroy and G. Hunt (eds.) *Quantitative methods in paleobiology*. Ithaca NY: Paleontological Society. Pp 213-243
- Goswami, A., and Polly, P.D. 2010b. The influence of modularity on cranial morphological disparity in Carnivora and Primates (Mammalia). *PLoS One* 5(3): e9517
- Goswami A., Binder W.J., Meachen, J. and O'Keefe F.R. 2015. The fossil record of phenotypic integration and modularity: a deep-time perspective on developmental and evolutionary dynamics. *Proceedings of the National Academy of Sciences of the United States of America (PNAS)* 112: 4891-4896
- Goswami, A., Randau, M., Polly, P.D., Weisbecker, V., Bennett, V. Hautier, L., and Sanchez-Villagra, M.R. 2016. Do developmental constraints and high integration limit the evolution of the marsupial oral apparatus? *Integrative and Comparative Biology* 56: 404-415
- Goswami, A., Smaers, J.B., Soligo, C., and Polly, P.D. 2014. The macroevolutionary consequences of phenotypic integration: from development to deep time. *Philosophical Transactions of the Royal Society B* 369: 20130254-20130254
- Goswami, A., Watanabe, A., Felice, R.N., Bardua, C., Fabre, A.-C. and Polly, P.D. 2019. High-density morphometric analysis of shape and integration: the good, the bad, and the not-really-a-problem. *Integrative & Comparative Biology* 59(3): 669-683
- Gould, S.J. 1966. Allometry and size on ontogeny and phylogeny. *Biological Reviews* 41(4): 587-638
- Gould, S.J. 1989. A developmental constraint in *Cerion*, with comments on the definition and interpretation of constraint in evolution. *Evolution* 43: 516-539
- Gould, S.J. 2002. *The Structure of Evolutionary Theory*. Cambridge, MA: Harvard

- Gould, S.J., and Lewontin, R.C. 1979. The spandrels of San Marco and the Panglossian paradigm: a 776 critique of the adaptationist programme. *Proceedings of the Royal Society of London B* 205(1161): 581-598
- Gower, J.C. 1975. Generalised Procrustes analysis. *Psychometrika* 40: 33-50
- Grabowski, M.W. 2012. Hominin obstetrics and the evolution of constraints. *Evolutionary Biology* 40: 57-75
- Grabowski, M.W., Polk, J.D., and Roseman, C.C. 2011. Divergent patterns of integration and reduced constraint in the human hip and the origins of bipedalism. *Evolution* 65: 1336-1356
- Grabowski, M.W., and Porto, A. 2016. How many more? Sample size determination in studies of morphological integration and evolvability. *Methods in Ecology and Evolution* 8(5): 592-603
- Grabowski, M.W., and Roseman, C.C. 2015. Complex and changing patterns of natural selection explain the evolution of the human hip. *Journal of human evolution* 85: 94-110
- Grunstra, N.D.S., Zachos, F.E., Herdina, A.N., Fisher, B, Paclicev, M., and Mitteroecker, P. 2019. Humans as inverted bats: A comparative 789 approach to the obstetric conundrum. *American journal of human biology: the official 790 journal of the Human Biology Council* e23227
- Gunz, P., and Mitteroecker, P. 2013. Semilandmarks: a method for quantifying curves and surfaces. *Hystrix* 24(1): 103-109
- Gunz, P., Mitteroecker, P., and Bookstein, F.L. 2005. Semilandmarks in three dimensions. In D.E. Slice (ed.): *Modern morphometrics in physical anthropology. Developments in primatology: Progress and prospects*. New York: Kluwer Academic Publishers-Plenum Publishers. Pp 73–98
- Gruss, L.T, Gruss, R. and Schmitt, D. 2017. Pelvic Breadth and Locomotor Kinematics in Human Evolution. *Anatomical record* 300(4): 739-751
- Gruss, L.T., and Schmitt, D. 2015. The evolution of the human pelvis: changing adaptations to bipedalism, obstetrics and thermoregulation. *Philosophical Transactions of the Royal Society B* 370(1663): 20140063
- Habar, A. 2011. A comparative analysis of integration indices. *Evolutionary Biology* 38: 476-488
- Hallgrímsson, B., Jamniczky, H., Young, N.M., Rolian C., Parsons, T.E., Boughner, J.C, and Marcucio R.S. 2009. Deciphering the palimpsest: studying the relationship between morphological integration and phenotypic covariation. *Journal of Evolutionary Biology* 36: 355-376

- Hammond, A.S., Plavcan, J.M., and Ward, C.V. 2016. A validated method for modelling anthropoid hip abduction in silico. *American Journal of Physical Anthropology* 160: 529–548
- Hansen, T.F. 2003. Is modularity necessary for evolvability? remarks on the relationship between pleiotropy and evolvability. *Biosystems* 69: 83-94
- Hansen, T.F., Armbruster, W.S., Carlson, M.L., and Pelabon, C. 2003. Evolvability and genetic constraint in dalechampia blossoms: genetic correlations and conditional evolvability. *Journal of Experimental Zoology Part B: Molecular and Developmental Evolution* 296: 23-39
- Hansen, T.F, and Houle, D. 2004. Evolvability, stabilizing selection, and the problem of stasis. In M. Pigliucci and K. Preston (eds.): *Phenotypic integration: studying the ecology and evolution of complex phenotypes*. Oxford: Oxford University Press. Pp. 130-150
- Hansen, T.F, and Houle, D. 2008. Measuring and comparing evolvability and constraint in multivariate characters. *Evolutionary Biology* 21: 1201-1219
- Hendrikse, J.L., Parsons, T.E., and Hallgrimsson, B. 2007. Evolvability as the proper focus of evolutionary developmental biology. *Evolution & Development* 9: 393-401
- Hirata, S., Fuwa, K., Sugama, K., Kusunoki, K., and Takeshita, H. 2011. Mechanism of birth in chimpanzees: Humans are not unique among primates. *Biology Letters* 7: 686-688
- Holland, E.L., Cran, G.W., Elwood, J.H., Pinkerton, J.H., and Thompson, W. 1982. Associations between pelvic anatomy, height and year of birth of men and women in Belfast. *Annals of Human Biology* 9(2): 113-120
- Huseynov, A., Ponce de Leon, M.S., and Zollikofer, C.P.E. 2017. Development of modular organisation in the chimpanzee pelvis. *The Anatomical Record* 300: 675-686
- Itou, J., Kawakami, H., Quach, T., Osterwalder, M., Evans, S.M., and Zeller, R. 2012. Islet1 regulates establishment of the posterior hindlimb field upstream of the Hand2-Shh morphoregulatory gene network in mouse embryos. *Development* 139(9): 1620-1629
- Jenkins, F.A., and Camazine, S.M. 1977. Hip structure and locomotion in ambulatory and cursorial carnivores. *Journal of Zoology* 181(3):351-370
- Jouffroy, F.K. 1975. Osteology and myology of the lemuriform postcranial skeleton. In: Tattersall, I., and Sussman, R.W. (eds.): *Lemur biology*. New York: Plenum Press. Pp 149-192
- Katz, D., and Friess, M. 2014. Technical note: 3D from standard digital photography of human crania: a preliminary assessment. *American Journal of Physical Anthropology* 154: 152-158

- Kawada, M., Nakatsukasa, M., Nishimura, T., Kaneko, A., and Morimoto, N. 2020. Covariation of fetal skull and maternal pelvis during the perinatal period in rhesus macaques and evolution of childbirth in primates. *Proceedings of the National Academy of Sciences of the United States of America (PNAS)* 117(35): 21251-21257
- Kendall, D.G. 1984. Shape manifolds, Procrustean metrics, and complex projective spaces. *Bulletin of the London Mathematical Society* 16: 81-121
- Kendall, D.G., Barden, D., Carne, T.K., and Le, H. 1999. *Shape and shape theory*. Chichester: Wiley
- Kenney-Hunt, J.P., Wang, B., Norgard, E.A., Fawcett, G., Falk D., Pletscher, L.S., Jarvis, J.P., Roseman, C., Wolf, J., and Cheverud, J.M. 2008. Pleiotropic patterns of quantitative trait loci for 70 murine skeletal traits. *Genetics* 178: 2275–228
- Kibii, J.M., Churchill, S.E., Schmid, P., Carlson, K.J., Reed, N.D., de Ruiter, D.J., and Berger, L.R. 2011 partial pelvis of *Australopithecus sediba*. *Science* 333: 1407-1411
- Klingenberg, C.P. 2005. Developmental constraints, modules and evolvability. In B. Hallgrímsson and B. K. Hall (eds.): *Variation*. San Diego: Academic Press. Pp. 219-247
- Klingenberg, C.P. 2008. Morphological integration and developmental modularity. *Annual Review of Ecology and Systematics* 39: 115-132
- Klingenberg, C.P. 2009. Morphometric integration and modularity in configurations of landmarks: Tools for evaluating a-priori hypotheses. *Evolution & Development* 11: 405-421
- Klingenberg, C.P. 2010. Evolution and development of shape: integrating quantitative approaches. *Nature Reviews Genetics* 11: 623-635
- Klingenberg, C.P. 2013. Cranial integration and modularity: Insights into evolution and development from morphometric data. *Hystrix* 24: 43-58
- Klingenberg, C.P. 2014. Studying morphological integration and modularity at multiple levels: Concepts and analysis. *Philosophical Transactions of the Royal Society B* doi:10.1098/rstb.2013.0249
- Klingenberg, C.P. 2020. Walking on Kendall's shape space: understanding shape spaces and their coordinate systems. *Evolutionary Biology* 47: 334-352
- Klingenberg, C.P., and Leamy, L.J. 2001. Quantitative genetics of geometric shape in the mouse mandible. *Evolution* 55: 2342-2352
- Klingenberg, C.P., Leamy, L.J., and Cheverud, J. M. 2004. Integration and modularity of quantitative trait locus effects on geometric shape in the mouse mandible. *Genetics* 166: 1909-1921

- Klingenberg, C.P., and Marugan-Lobon, J. 2013. Evolutionary Covariation in Geometric Morphometric Data: Analyzing Integration, Modularity, and Allometry in a Phylogenetic Context. *Systematic Biology* 62 (4): 591-610
- Kohn, L.A.P., and Atchley, W.R. 1988. How similar are genetic correlation structures? Data from mice and rats. *Evolution* 42(3): 467-481
- Kozma, E.E., Webb, N.M., Harcourt-Smith, W.E.H., Raichlen, D.A., D'Août, K., Brown, M.H., Finestone, E.M., Ross, S.R., Aerts, P., and Pontzer, H. 2018. Hip extensor mechanics and the evolution of walking and climbing capabilities in humans, apes, and fossil hominins. *Proceedings of the National Academy of Sciences of the United States of America (PNAS)* 115(16): 4134-4139
- Lande, R. 1979. Quantitative genetic analysis of multivariate evolution, applied to brain: body size allometry. *Evolution* 33: 402-416
- Laudicina, N.M., Rodriguez, F., and DeSilva J.M. 2019. Reconstructing birth in *Australopithecus sediba*. PLOS One. DOI: 10.1371/journal.pone.0221871
- Lawing, A.M., and Polly, P.D. 2010. Geometric morphometrics: recent applications to the study of evolution and development. *Journal of Zoology* 280: 1-7
- Legreneur, P., Thévenet F.-R., Libourel, P.-A., Monteil, K., Montuelle, S., Pouydebat, E. and Bels, V. 2013. Hindlimb interarticular coordinations in *Microcebus murinus* in maximal leaping. *Journal of Experimental Biology* 213:1320-1327
- Leutenegger, W. 1974. Functional aspects of pelvic morphology in simian primates *Journal of Human Evolution* 3: 207-222
- Leutenegger, W. 1977. Functional interpretation of sacrum of *Australopithecus africanus*. *Journal of South African Science* 73: 308-310
- Leutenegger, W., and Larson, S. 1985. Sexual dimorphism in the postcranial skeleton of New World primates. *Folia Primatology* 44: 82-95
- Lewton, K.L. 2010. *Locomotor Function and the Evolution of the Primate Pelvis*. Unpublished PhD thesis. Arizona: Arizona State University
- Lewton, K.L. 2012. Evolvability of the primate pelvic girdle. *Evolutionary Biology* 39: 126-139
- Lewton, K.L. 2015. Pelvic Form and Locomotor Adaptation in Strepsirrhini Primates. *The Anatomical Record* 298: 230-248
- Lieberman, D.E., Ross, C.F., and Ravosa, M.J. 2010. The primate cranial base: ontogeny, function, and integration. *American Journal of Physical Anthropology* S31: 117-169
- Lovejoy, C.O. 1988. Evolution of Human Walking. *Scientific American* 259(5): 118-125

- Lovejoy, C.O. 2005. The natural history of human gait and posture. Part 1. Spine and pelvis. *Gait Posture* 21: 95-112
- Lovejoy, C.O. 2009. Reexamining Human Origins in light of *Ardipithecus ramidus*. *Science* 326(5949): 74-74e8
- Lovejoy, C.O., Kingsbury, G.H., and Burstein, A.H. 1973. The gait of Australopithecus. *American Journal of Physical Anthropology* 38(3): 757-779
- Lovejoy, C.O., and McCollum, M.A. 2010. Spinopelvic pathways to bipedality: why no hominids ever relied on a bent-hip–bent-knee gait. *Philosophical Transactions of the Royal Society B* 365: 3289-3299
- Lovejoy, C.O., Suwa, G. Spurlock, L., Asfaw, B. and White, T.D. 2009. The pelvis and femur of *Ardipithecus ramidus*: the emergence of upright walking. *Science* 326(5949): 71-71e6
- Lycett, S.J., and von Cramon-Taubel, N. 2013. Understanding the comparative catarrhine context of human pelvic form: a 3D geometric morphometric analysis. *Journal of Human Evolution* 64: 300-310
- Lynch, M. and Walsh B. 1998. *Genetics and analysis of quantitative traits*. Oxford: Oxford University Press (8th ed.)
- Macchiarelli, R., Bergeret-Medina, A., Machi, D., and Wood, B. 2020. Nature and relationships of Sahelanthropus tchadensis. *Journal of Human Evolution* 149: 102898
- Machado, F.A., Zahn, T.M.G., and Marroig, G. 2018. Evolution of morphological integration in the skull of Carnivora (Mammalia): changes in Canidae lead to increased evolutionary potential of facial traits. *Evolution* 72: 1399-1419
- Magwene, P.M. 2001. New tools for studying integration and modularity. *Evolution* 55(9): 1734- 1745
- Malashichev, Y., Borkhardt, V., Christ, B., and Scaal, M. 2005. Differential regulation of avian pelvic girdle development by the limb field ectoderm. *Anatomy and Embryology* 210: 187-197
- Malashichev, Y., Christ, B., and Prols, F. 2008. Avian pelvis originates from lateral plate mesoderm and its development requires signals from both ectoderm and paraxial mesoderm. *Cell and Tissue Research* 331(3): 595-604
- Marchal, F. 2003. Size and shape of the australopithecine pelvic bone. *Human Evolution* 18: 161-176
- Marroig, G., Shirai, L., Porto, A., de Oliveira, F., and De Conto, V. 2009. The evolution of modularity in the mammalian skull II: evolutionary consequences. *Evolutionary Biology* 36: 136-148

- Marshall, A. F., Bardua, C., Gower, D. J., Wilkinson, M., Sherratt, E., and Goswami, A. 2019. High-density three-dimensional morphometric analyses support conserved static (intraspecific) modularity in caecilian (Amphibia: Gymnophiona) crania. *Biological Journal of the Linnean Society* 126(4): 721-742
- Martin, R. 1928. *Lehrbuch der Anthropologie in Systematischer Darstellung mit Besonderer Berücksichtigung der Anthropologischen Methoden für Studierende, Ärzte und Forschungsreisende*. Second Edition. Jena: Gustav Fischer.
- Martín-Serra, A., Figueirido, B., and Palmqvist, P. 2018. Changing modular patterns in the carnivoran pelvic girdle. *Journal of Mammalian Evolution* doi.org/10.1007/s10914-018-9454-9
- Maynard Smith, J., Burian, R., Kauffman, S., Alberch, P., Campbell, J., Goodwin, B., Lande, R., Raup, D., and Wolpert, L. 1985. Developmental constraints and evolution. *Quarterly Review of Biology* 60: 65-287
- McHenry, H.M., and Corruccini, R.S., 1978. Analysis of the hominoid os coxa by Cartesian coordinates. *American Journal of Physical Anthropology* 48: 215-226
- Melo, D. and Marroig, G. 2015. Directional selection can drive the evolution of modularity in complex traits. *Proceedings of the National Academy of Sciences of the United States of America (PNAS)* 112: 470-475
- Merila, J. and Bjorklund, M. 2004. Integration as a constraint and adaptation. In M. Pigliucci and K. Preston (eds.): *Phenotypic integration: studying the ecology and evolution of complex phenotypes*. Oxford: Oxford University Press. Pp. 107-129
- Middleton, E.R., Winkler, Z.J., Hammond, A.S., Plavcan, J.M., Ward, C.V. 2017. Determinants of iliac blade orientation in anthropoid primates. *Anatomical Record* 300:810–827
- Miller, R.A. 1945. The ischial callosities of primates. *American Journal of Anatomy* 76: 67-91
- Mitteroecker, P., and Bookstein, F. L. 2007. The conceptual and statistical relationship between modularity and morphological integration. *Systematic Biology* 56: 818-836
- Mitteroecker, P., and Bookstein, F. L. 2008. The Evolutionary Role of Modularity and Integration in the Hominoid Cranium. *Evolution* 62: 943-958
- Mitteroecker, P., and Gunz, P. 2009. Advances in Geometric Morphometrics. *Evolutionary Biology* 36(2): 235-247
- Mitteroecker, P., Gunstra, N.D.S., Stansfield, E., Waltenberger, L., and Fisher, B. 2021. Did population differences in human pelvic form evolve by drift or selection? *Bulletins et Mémoires de la Société d'Anthropologie de Paris* 3(1): 7460
- Moffett, E.A. 2017. Dimorphism in the Size and Shape of the Birth Canal Across Anthropoid 898 Primates. *Anatomical record* 300(5): 870-889

- Muller, G.B. 2007. Evo-devo: extending the evolutionary synthesis. *Nature Review Genetics* 8: 943-949
- Napier, J.R, and Napier, P.H. 1967. *A handbook of living primates*. New York: Academic Press
- Navalón, G., Marugán-Lobón, J., Bright, J.A., Cooney, C.C., and Rayfield E.J. 2020. The consequences of craniofacial integration for the adaptive radiations of Darwin's finches and Hawaiian honeycreepers. *Nature Ecology and Evolution* 4: 270–278
- Neaux, D. 2017. Morphological integration of the cranium in Homo, Pan, and Hylobates and the evolution of hominoid facial structures. *American Journal of Physical Anthropology* 162(4): 732-746
- Neaux, D., Sansalone, G., Ledogar, J.A, Heins Ledogar, S., Luk, T.H.Y., and Wroe, S. 2018. Basicranium and face: Assessing the impact of morphological integration on primate evolution. *Journal of Human Evolution* 118: 43-55
- Needham, J. 1933. On the dissociability of the fundamental processes in ontogenesis. *Biological Reviews* 8: 180-223
- Olson, E.C., and Miller, R.L. 1958. *Morphological Integration*. University of Chicago Press, Chicago.
- Pavclan, J.M. 2001. Sexual dimorphism in primate evolution. *American Journal of Physical Anthropology* 116(33): 25-53
- Pavlicev, M., Cheverud, J. M., and Wagner, G. P. 2009. Measuring morphological integration using eigenvalue variance. *Evolutionary Biology* 36(1): 157-170
- Pavlicev, M., Romero, R., and Mitteroecker, P. 2020. Evolution of the human pelvis and obstructed labor: new explanations of an old obstetrical dilemma. *American journal of obstetrics and gynaecology*, 222(1): 3-16
- Petter, J-J., and Desbordes, F. 2010. *Primates of the world*. Oxford and Princeton: Princeton University Press
- Pickford, M., Senut, B. Gommery, D, and Treil, J. 2002. Bipedalism in *Orrorin tugenensis* revealed by its femora. *Comptes Rendus Palevol* 1(4): 191-203
- Pigliucci, M. 2003. Phenotypic integration: studying the ecology and evolution of complex phenotypes. *Ecology Letters* 6: 265-272
- Pigliucci, M. 2008. Is evolvability evolvable? *Nature Reviews* 9(1): 75-82.

- Polly, P.D. 2016. Quantitative genetics provides predictive power for paleontological studies of morphological evolution. *Proceedings of the National Academy of Sciences of the United States of America (PNAS)* 113(33): 9142-9144
- Porto, A., de Oliveira, F., Shirai, L., De Conto, V., and Marroig, G.. 2009. The evolution of modularity in the mammalian skull I: morphological integration patterns and magnitudes. *Evolutionary Biology* 36: 118-135
- Pomikal, C., and Streicher, J. 2010. 4D-analysis of early pelvic girdle development in the mouse (*Mus musculus*). *Journal of Morphology* 271(1): 116-126
- Pomikal, C., Blumer, R., and Streicher, J. 2011. Four-dimensional analysis of early pelvic girdle development in *Rana temporaria*. *Journal of Morphology* 272: 287-301
- Porto, A., Shirai, L.T., de Oliveira, F.B., and Marroig, G. 2013. Size variation, growth strategies, and the evolution of modularity in the mammalian skull. *Evolution* 67: 3305-3322
- R Core Team 2017. R: a language and environment for statistical computing. Vienna: R Foundation for Statistical Computing
- Rak, Y. 1991. Lucy's pelvic anatomy: its role in bipedal gait. *Journal of Human Evolution* 20(4):283-290
- Randau, M., and Goswami, A. 2017. Unravelling intravertebral integration, modularity and disparity in Felidae (Mammalia). *Evolution and Development* 19(2): 85-95
- Ridley, M. 1995. Brief communication: pelvic sexual dimorphism and relative neonatal brain size really are related. *American journal of physical anthropology* 97(2): 197-200
- Roff, D.A. 1995. The estimation of genetic correlations from phenotypic correlations: a test of Cheverud's conjecture. *Heredity* 74: 481-490.
- Roff, D.A. 1996. The evolution of genetic correlations of patterns. *Evolution* 50: 1392-1403
- Rohlf, F.J. 2000. On the use of shape spaces to compare morphometric methods. *Hystrix, the Italian Journal of Mammalogy* 11(1): 9-25
- Rohlf, F.J., and Marcus, F.L. 1993. A revolution in morphometrics. *Trends in Ecology & Evolution* 8: 129-132
- Rohlf, F.J., and Slice, D. 1990. Extensions of the Procrustes method for the optimal superimposition of landmarks. *Systematics Biology* 39(1): 40-59
- Rolian C.C. 2009. Integration and evolvability in primate hands and feet. *Evolutionary Biology* 36: 100-111

- Rolian, C.C. 2014. Genes, development, and evolvability in primate evolution. *Evolutionary Anthropology* 23: 93-104
- Rolian C.C. 2019. Ecomorphological specialisation leads to loss of evolvability in primate limbs. *Evolution* 74-4: 702-715
- Rolian, C. and Willmore, K.E. 2009. Morphological Integration at 50: Patterns and processes of integration in biological anthropology. *Evolutionary Biology* 36: 1-4
- Rose, M.D. 1974. Ischial tuberosities and ischial callosities. *American Journal of Physical Anthropology* 40: 375-384
- Roseman, C.C., Capellini, T.D., Jagoda, E., Williams, S. A., Grabowski, M., O'Connor, C., Polk, J.D., and Cheverud, A.M. 2020. Variation in mouse pelvic morphology maps to locations enriched in Sox9 Class II and Pitx1 regulatory features. *Journal of Evolutionary Zoology B* 33(2): 100-112
- Rosenberg, K. 1992. The evolution of modern human childbirth. *Yearbook Physical Anthropology* 35: 89-124
- Rosenberg, K., and DeSilva, J.M. 2017. Evolution of the human pelvis. *Anatomical Record* 300(5):789-797
- Rosenberg, K., and Trevathan, W. 1996. Bipedalism and human birth: the obstetrical dilemma revisited. *Evolutionary Anthropology* 4: 161-168
- Rosenberg, K., and Threvathan, W. 2002. Birth, obstetrics and human evolution. *International Journal of Obstetrics and gynaecology* 109(11): 1199-1206
- Rosenberg, K., and Threvathan, W. 2005. Bipedalism and human birth: the obstetric dilemma revisited. *Evolutionary Anthropology* 161:4(5): 161-168
- Ruff, C.B. 1995. Biomechanics of the hip and birth in early Homo. *American Journal of Physical Anthropology* 98: 527-574
- Ruff, C.B. 2010. Body size and body shape in early hominins – implications of the Gona pelvis. *Journal of Human Evolution* 58: 166-178
- Ruff, C.B., Holt, B., and Trinkaus, E. 2006. Who's afraid of the big bad Wolff? Wolff's law and bone functional adaptation *American Journal of Physical Anthropology* 129: 484-498
- Sanger, T.J., Mahler, D.L., Abzhanov, A., and Losos, J.B. 2012. Roles for modularity and constraint in the evolution of cranial diversity among Anolis lizards. *Evolution* 66: 1525-1542
- Scheurer, L. and Black, S. 2004. *The Juvenile Skeleton*. London: Elsevier Academic Press.

- Schlager S. 2016. Morpho: Calculations and visualisations related to geometric morphometrics. R package version 2.3.1.1. <http://sourceforge.net/projects/morpho-rpackage/>
- Schultz, A.H. 1936. Characters common to higher primates and characters specific for man. *Quarterly Review of Biology* 11: 425-455
- Schultz, A.H. 1930. The skeleton of the trunk and limbs of higher primates. *Human Biology* 2: 303-438
- Schultz, A.H. 1949. Sex differences in the pelves of primates. *American Journal of Physical Anthropology* 7: 401-424
- Schultz, A.H. 1969. *The Life of Primates*. Universe Books, New York
- Sears, K.E., Capellini, T.D., and Diogo, R. 2015. On the serial homology of the pectoral and pelvic girdles of tetrapods. *Evolution* 69: 2543-2555
- Seilacher, A. 1970. Arbeitskonzept zur Konstruktions-Morphologie. *Lethaia* 3: 393-306
- Senuta, B., Pickford, M., Gommery, D., Meind, P., Cheboie, K., Coppens, Y. 2001. First hominid from the Miocene (Lukeino Formation, Kenya). *Palaeontology* 332: 137-144
- Singh, N., Harvati, K., Hublin, J.-J, and Klingenberg, C.P. 2012. Morphological evolution through integration: A quantitative study of cranial integration in Homo, Pan, Gorilla and Pongo. *Journal of Human Evolution* 62: 155-164
- Sharma, K. 2002. Genetic basis of human female pelvic morphology: A twin study. *American Journal of Physical Anthropology* 117(4): 327-333
- Shirai, L.T. and Marroig, G. 2010. Skull modularity in neotropical marsupials and monkeys: size variation and evolutionary constraint and flexibility. *Journal of Evolutionary Zoology* 314B: 663-683
- Showalter, H.G. 2018. *Sacral morphology of prehensile-tailed primates in relation to biomechanical loading*. Unpublished MA thesis. Arkansas: University of Arkansas
- Slice, D.E. 2005. *Modern morphometrics in physical anthropology*. New York: Kluwer Academic
- Slice, D.E. 2007. Geometric Morphometrics. *Annual Review Anthropology* 36: 261-281
- Small, C.G. 1996. *The statistical theory of shape*. New York: Springer-Verlag
- Smith, J. M., Burian, R., Kauman, S., Alberch, P., Campbell, J., Goodwin, B., Lande, R., Raup, D. and Wolpert, L. 1985. Developmental constraints and evolution: A perspective from the mountain lake conference on development and evolution. *The Quarterly Review of Biology* 60: 265-287

- Srivastava, A., and Klassen, E.P. 2016. *Functional and shape data analysis*. New York: Springer-Verlag.
- Stern, J.T. 2000. Climbing to the top: a personal memoir of *Australopithecus afarensis*. *Evolutionary Anthropology* 9: 113-133
- Stern, J.T., and Susman, R.L. 1983. The locomotor anatomy of *Australopithecus afarensis*. *American Journal of Physical Anthropology* 60: 279-317
- Straus, W.L. 1929. Studies on primate ilia. *American Journal of Anatomy* 43: 403-460
- Susman, R.L., and Stern, J.T. 1991. Locomotor behavior of early hominids: epistemology and fossil evidence. In Coppens, Y. and Senut, B. Paris (eds.) *Origine(s) de la bipédie chez les hominidés*. France: CNRS. Pp. 121-131
- Susman, R.L., Stern, J.T., and Jungers, W.L. 1984. Arboreality and bipedality in the Hadar hominids. *Folia Primatology* 43: 113-156
- Tague, R.G. 1995. Variation in pelvic size between males and females in nonhuman anthropoids. *American Journal of Physical Anthropology* 97: 213-233
- Tague, R.G. 2000. Do big females have big pelves? *American Journal of Physical Anthropology* 112: 377-393
- Tague, R.G. 2016. Pelvic sexual dimorphism among species monomorphic in body size: relationship to relative newborn body mass. *Journal of mammalogy*, 97(2): 503-517
- Travathan, W. 2015. Primate pelvic anatomy and implications for birth. *Philosophical Transactions of the Royal Society B* 5(370): 20140065
- Tuttle, R. 2014. *Apes and human evolution*. Cambridge, MA: Harvard University Press
- Vleeming, A., Scheuenke, M.D, Matsi, A.T., Carreiro, J.E., Danneels, L., and Willard, F.H. 2012. The sacroiliac joint: an overview of its anatomy, function and potential clinical implications. *Journal of Anatomy* 221(6): 537-567
- Vos, R.A. 2006. *Inferring large phylogenies: the big tree problem*. PhD thesis. Burnaby, Canada: Simon Fraser University
- Wagner G.P. 1995. Adaptation and the modular design of organisms. In F. Moran, A. Moreno, J.J. Merelo and P. Chacon (eds.): *Advances in Artificial Life*. Springer, Berlin. Pp. 317–328
- Wagner, G.P. 1996. Homologues, natural kinds and the evolution of modularity. *American Zoologist* 36: 36-43
- Wagner, G.P., and Altenberg, L. 1996. Complex adaptations and the evolution of evolvability. *Evolution* 50(3): 967-976

- Wagner, H., Liebetrau, A., Schinowski, D., Wulf, T., and de Lussanet, M.H.E 2012. Spinal lordosis optimizes the requirement for a stable erect posture. *Theoretical Biology and Medical Modelling* 9: 1-13
- Wagner, G.P., Pavlicev, M., and Cheverud, J. M. 2007. The road to modularity. *Nature Reviews Genetics* 8: 921-931
- Wagner, G.P., and Schenk, K., 2000. Evolutionarily stable configurations: functional integration and the evolution of phenotypic stability. *Evolutionary Biology* 31: 155-217
- Wagner, G.P., and Zhang 2011. The pleiotropic structure of the genotype–phenotype map: the evolvability of complex organisms. *Nature Reviews Genetics* 12: 204-213
- Wall-Scheffler, C., Kurki, H., and Auerbach, B. 2020. *The Evolutionary Biology of the Human Pelvis: An Integrative Approach* (Cambridge Studies in Biological and Evolutionary Anthropology). Cambridge: Cambridge University Press
- Ward, C.V., Maddux, S.D., and Middleton, E.R. 2018. Three-dimensional anatomy of the anthropoid bony pelvis. *American Journal of Physical Anthropology* 166: 3-25
- Warrener, A. 2011. Relating pelvic shape to hip abductor mechanics and locomotor cost. *American Journal of Physical Anthropology* 144(S52):306
- Washburn, S.L. 1960. Tools and Human Evolution. *Scientific American* 203: 63-75
- Watanabe A. 2018. How many landmarks are enough to characterize shape and size variation? *PLoS One* 13:e0198341
- Waterman, H.C. 1929. Studies on the evolution of the pelvis of man and other primates. *Bulletin of the American Museum of Natural History* 58: 585-642
- Weaver, T.D. and Hublin, J.J. 2009. Neandertal birth canal shape and the evolution of human childbirth. *Proceedings of the National Academy of Sciences of the United States of America* 106(20): 8151-8156
- Wells, J.C.K., DeSilva, J.M., and Stock, J.T. 2012. The obstetric dilemma: an ancient game of Russian roulette, or a variable dilemma sensitive to ecology? *American Journal of Physical Anthropology* 149(55): 40-71
- West-Eberhard, M.J. 2005. Developmental plasticity and the origin of species differences. *Proceedings of the National Academy of Sciences of the United States of America (PNAS)* 102(S1): 6543-6549
- Wiley, D.F. 2005. Landmark v 3.0. Institute for Data Analysis and Visualization. University of California Davis
- Wiley, D.F., Amenta, N., Alcantara, D. A., Ghosh, D., Kil, Y. J., Delson, E., and Hamann, B. 2005. *Evolutionary Morphing*. Paper presented at the Proceeding of IEEE Visualization 2005

- Willis, J. H., Coyne, J. A., & Kirkpatrick, M. (1991). Can one predict the evolution of quantitative characters without genetics? *Evolution* 45: 441-444
- Wilson, D.E. and Reeder, D.M 1993. *Mammal Species of the World: Taxonomic and Geographic Reference*. Washington: Smithsonian Institution Press. Second Edition
White, T.D., Black M.T. and Folkens, P.A. 2012. *Human Osteology*. San Diego: Academic Press. Third Edition
- Wittman, A.B. and Wall, L.L 2007. The evolutionary origins of obstructed labor: Bipedalism, encephalization, and the human obstetric dilemma. *Obstetrical & Gynecological Survey* 62(11): 739-748
- White, T.D., Black, M.T., and Folkens, P.A. 2012. *Human osteology*. London: Academic Press
- Wolpoff, M.H., Hawks, J., Pickfors, M., and Ahern, J. 2006. An ape or *the* ape: Is the Toumaï cranium TM 266 a hominin? *PaleoAnthropology* 2006: 36-50
- Wood, B.A., and Chamberlain, A.T. 1986. The primate pelvis: allometry or sexual dimorphism. *Journal of Human Evolution* 15: 257-263
- Young, N.M., and Hallgrímsson B. 2005. Serial homology and the evolution of mammalian limb covariation structure. *Evolution* 59: 2691-2704
- Young, N.M., Selleri L., and Capellini, T. 2019. Genetics of Scapula and Pelvis Development: An Evolutionary Perspective. *Current Topics in Developmental Biology* 132: 311-349
- Young, N.M., Wagner G. P., and Hallgrímsson B. 2010. Development and the evolvability of human limbs. *Proceedings of the National Academy of Sciences of the United States of America* 107: 3400-3405
- Zelditch, M.L, and Goswami, A. 2021. What does modularity mean? *Evolution & Development* 23(5): 377-403
- Zelditch, M.L., Swiderski, D.L., Sheets, H.D. 2012. *Geometric Morphometrics for Biologists: A Primer*. Amsterdam, The Netherlands: Elsevier. Second Edition
- Zollikofer, C.P.E., Ponce de León, M.S., Lieberman, D.E., and Guy, F. 2005. Virtual reconstruction of *Sahelanthropus tchadensis*. *Nature* 434(7034): 755-759

Appendix: primate pelvis shapes

Strepsirrhini



Daubentonia: Daubentonia madagascariensis - Aye-aye



Galagidea: Otolemur crassicaudatus - Brown greater galago



Indriidae: Indris indris - Bakakoto



Loridae: Nycticebus coucang - Great slowloris

Strepsirrhini



Lemuridae : Eulemur fulvus



Lemuridae : Lemur catta



Lemuridae : Varecia Variegata

Platyrrhini

Atelidae



Atelidae: Alouetta semniculus - Venezuelan red howler



Atelidae: Ateles geoffroy - Geoffroy's spider monkey



Atelidae: Ateles paniscus - Black spider monkey



Atelidae: Lagothrix lagothricha - Woolly monkey

Platyrrhini

Cebidae



Cebidae: Cebus apella - Tufted capuchin



Cebidae: Cebus capucinus - White-headed capuchin

Catarrhini

Cercopithecidae



Cercopithecidae: Cercocebus galeritus - Tana river mangabey



Cercopithecidae: Cercopithecus ascanius - Red-tailed monkey



Cercopithecidae: Cercopithecus cephus - Moustached guenon



Cercopithecidae: Cercopithecus hamlyni - Owl-faced monkey

Catarrhini

Cercopithecidae



Cercopithecidae: Cercopithecus lhoesti - Mountain mangabey



Cercopithecidae: Cercopithecus mitis - Blue monkey



Cercopithecidae: Cercopithecus mona - Mona monkey



Cercopithecidae: Cercopithecus neglectus - De Brazza's monkey

Catarrhini

Cercopithecidae



Cercopithecidae: Cercopithecus nictitans - Greater spot-nose monkey



Cercopithecidae: Cercopithecus petaurista - Lesser spot-nosed monkey



Cercopithecidae: Chlorocebus aetiops - Grivet

Catarrhini

Cercopithecidae



Cercopithecidae: Colobus guereza - Manteld guereza



Cercopithecidae: Colobus polykomas - King colobus



Cercopithecidae: Erythrocebus patas - Patas monkey



Cercopithecidae: Lophocebus albigena - grey-cheeked mangabey

Catarrhini

Cercopithecidae



Cercopithecidae: Colobus guereza - Manteld guereza



Cercopithecidae: Colobus polykomas - King colobus



Cercopithecidae: Erythrocebus patas - Patas monkey



Cercopithecidae: Lophocebus albigena - grey-cheeked mangabey

Catarrhini

Cercopithecidae



Cercopithecidae: Lophocebus aterrimus - Black crested mangabey - Manteld guereza



Cercopithecidae: Macaca fascicularis - Crab-eating macaque



Cercopithecidae: Macaca maura - Moor macaque



Cercopithecidae: Macaca mulatta - Rhesus macaque

Catarrhini

Cercopithecidae



Cercopithecidae: Macaca nemestrina - Southern pig-tailed macaca



Cercopithecidae: Mandrillus sphinx - Mandril



Cercopithecidae: Papio anubis - Olive baboon



Cercopithecidae: Papio cynocephalus - Yellow baboon

Catarrhini

Cercopithecoidea



Cercopithecoidea: Papio hamadryas - Hamadryas baboon



Cercopithecoidea: Pilocolobus badius - Western red colobus



Cercopithecoidea: Pilocolobus kirkii - Zanzibar red colobus



Cercopithecoidea: Presbytis comata - Surili

Catarrhini

Cercopithecoidea



Cercopithecoidea: Pygathrix nemaeus - Red-shanked douc



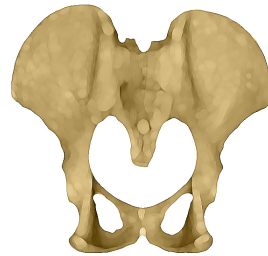
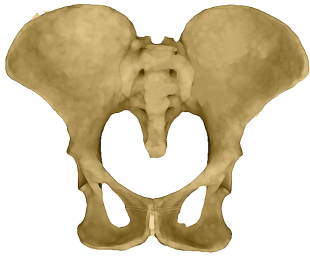
Cercopithecoidea: Semnopithecus entellus - Northern plains gray langur



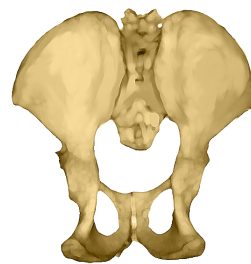
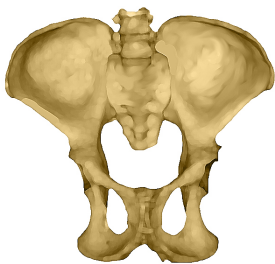
Cercopithecoidea: Theropithecus gelada - Bleeding-heart monkey

Catarrhini

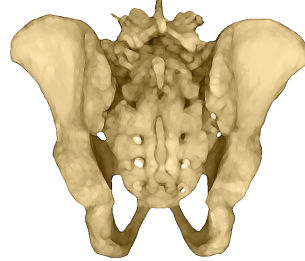
Hominidae



Hominidae: Gorilla beringei graueri - Eastern gorilla



Hominidae: Gorilla gorilla - Western lowland gorilla



Hominidae: Homo sapiens - Human



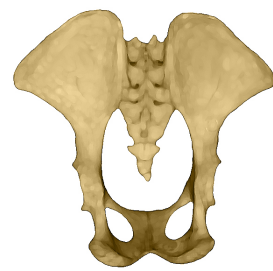
Hominidae: Pan paniscus - Bonobo

Catarrhini

Hominidae and Hylobatidae



Hominidae: Pan troglodytes - Chimpanzee



Hominidae: Pongo pygmaeus - Bornean orangutan



Hylobatidae: Hylobates lar - Common gibbon



Hylobatidae: Symphalangus syndactus - Siamang